



**A potential Role of Calcium in the Regulation of
Nitrogen Fixation in *Medicago truncatula* and *Vicia faba***

Dissertation

zur Erlangung des
Doktorgrades der Agrarwissenschaften (Dr. agr.)

der

Naturwissenschaftlichen Fakultät III
Agrar- und Ernährungswissenschaften,
Geowissenschaften und Informatik

der Martin-Luther-Universität Halle-Wittenberg,

vorgelegt von

M.Sc. Lisa Bischoff
geb. am 31.12.1983 in Berlin

Halle (Saale), 15.05.2023

Gutachter:

1. Professor Dr. Edgar Peiter
2. Professor Dr. Uwe Ludewig



Table of contents

List of abbreviations	i
1. Introduction.....	1
1.1 The symbiosis of legumes and rhizobia.....	1
1.1.1 The development of nodules.....	1
1.1.2 The structure and function of nodules.....	4
1.2 The fixation of N ₂	6
1.2.1 Mechanism of biological and industrial N ₂ fixation.....	6
1.2.2 The relevance of N ₂ fixation for agriculture	8
1.2.3 Regulation of N ₂ fixation in legumes	9
1.2.3.1 Factors which induce the down-regulation of N ₂ fixation.....	9
1.2.3.2 Regulation by carbon supply	9
1.2.3.3 Regulation by oxygen supply.....	10
1.2.3.4 N-feedback regulation.....	11
1.2.3.5 Further substances with potential to regulate N ₂ fixation.....	14
1.2.3.5.1 Regulation of N ₂ fixation by phytohormones.....	14
1.2.3.5.2 Regulation of the N ₂ fixation by calcium.....	14
1.3 Calcium - the most important signal ion in plants	15
1.3.1 The mechanism of calcium signaling.....	15
1.3.2 Calcium-permeable transport proteins involved in calcium signaling.....	16
1.3.2.1 Ca ²⁺ -permeable ion channels	16
1.3.2.2 Transporters	18
1.3.2.3 Calcium pumps: ATPases.....	18
1.4 Aims of the project.....	20
2. Materials and Methods	22
2.1 Bioinformatic and <i>in silico</i> analyses.....	22
2.2 Organisms.....	23
2.2.1 Plant cultivation.....	23
2.2.1.1 <i>Medicago truncatula</i>	23
2.2.1.2 <i>Vicia faba</i>	25
2.2.2 Bacteria cultivation.....	26
2.2.3 Yeast cultivation	28
2.3 Nucleic acid isolation and PCR.....	28

2.3.1 DNA isolation.....	28
2.3.2 RNA isolation and cDNA synthesis	29
2.3.3 qRT-PCR	30
2.3.4 PCR for verification of the UTRs	30
2.4 USER cloning.....	30
2.5 Transformation of the organisms.....	31
2.5.1 Generation of competent <i>Agrobacterium rhizogenes</i> cells	31
2.5.2 Transformation of <i>Agrobacterium rhizogenes</i>	31
2.5.3 Transformation of <i>Medicago truncatula</i>	31
2.5.4 Generation of competent <i>Escherichia coli</i> cells	32
2.5.5 Transformation of <i>Escherichia coli</i>	32
2.5.6 Transformation of <i>Saccharomyces cerevisiae</i>	32
2.6 Investigation of promoter activity by histochemical GUS staining	32
2.7 Localization of Ca ²⁺ -ATPases.....	33
2.8 Preparation of thin sections of nodules	34
2.9 Isolation of symbiosomes.....	34
2.10 Yeast complementation assay.....	35
2.11 Detection of calcium signals in roots and nodules.....	35
2.11.1 Measurements using aequorin.....	35
2.11.2 Measurements using R-GECO	36
2.12 Stable and transient mutations for the functional characterization of candidate genes	36
2.13 Calcium fertilization experiments with <i>Vicia faba</i>	37
2.12.1 Experiment with quartz sand	37
2.12.2 Experiment with soil/vermiculite mixture.....	38
2.12.3 Experiments with hydroponic culture	38
2.12.4 Mineral element analyses	38
2.12.5 Chlorophyll measurements	39
3. Results	40
3.1 Calcium measurements in nodules of <i>Medicago truncatula</i>	40
3.1.1 Measurements of changes in [Ca ²⁺] _{cyt} using aequorin.....	40
3.1.2 Measurements of changes in [Ca ²⁺] _{cyt} using R-GECO.....	41
3.2 The inventory of putatively Ca ²⁺ -permeable proteins of <i>Medicago truncatula</i>	41
3.3 Investigation of putative Ca ²⁺ -ATPases of <i>Medicago truncatula</i>	44
3.3.1 <i>In silico</i> analysis of genes encoding putative Ca ²⁺ -ATPases.....	44
3.3.2 Transport activity of selected Ca ²⁺ -ATPases.....	53

3.3.3 Expression of genes encoding selected Ca ²⁺ -ATPases	56
3.3.4 Subcellular localization of selected Ca ²⁺ -ATPases	60
3.3.5 Preparations for functional characterization of a candidate gene	67
3.4 Calcium fertilization experiments with <i>Vicia faba</i>	69
3.4.1 Experiment with quartz sand	69
3.4.2 Experiment with soil/vermiculite mixture.....	70
3.4.3 Experiments with hydroponic culture	70
4. Discussion	74
4.1 Measurement of [Ca ²⁺] _{cyt} in nodules of <i>Medicago truncatula</i>	74
4.2 Resources to investigate gene expression in root nodules.....	74
4.3 Investigation of Ca ²⁺ -ATPases.....	77
4.3.1 Expression of genes encoding Ca ²⁺ -ATPases	77
4.3.1.1 <i>In silico</i> analysis	77
4.3.1.2 Investigation of gene expression by RT-PCR	79
4.3.1.3 Investigation of gene expression by GUS assay	80
4.3.1.4 Investigations of gene expression - nodule specific problems.....	81
4.3.2 Localization of the candidate genes	82
4.3.3 Possible functions of the investigated Ca ²⁺ -ATPases.....	84
4.4 Modulation of N ₂ fixation by calcium fertilization	87
4.5 The pros and cons of current hypotheses on the regulation of N ₂ fixation	88
4.5.1 N feedback.....	88
4.5.2 Regulation by oxygen	89
4.6 Considerations on the regulation of N ₂ fixation.....	90
Outlook.....	92
References.....	93
List of tables	101
List of figures	102
Summary	104
Appendix.....	I
Acknowledgements	XVIII
Publications	XIX
Curriculum vitae	XX
Declaration under Oath.....	XXI

List of abbreviations

µg	Microgram
µM	Micromolar
µmol	Micromole
Å	Ångström
ABA	abscisic acid
ACA	autoinhibited Ca ²⁺ ATPase
aeq	aequorin
ANN	annexins
Asn	asparagine
ATP	adenosine triphosphate
BSA	bovine serum albumin
Ca ²⁺	calcium
CaM	calmodulin
CaMBS	calmodulin binding site
CAX	cation exchanger
cDNA	complementary desoxyribonucleic acid
CDS	coding sequence
CNGC	cyclic nucleotide-gated channel
dai	days after infection
dsDNA	double-stranded desoxyribonucleic acid
DNA	desoxyribonucleic acid
DSMZ	Deutsche Sammlung von Mikroorganismen und Zellkulturen (German collection of microorganisms and cell cultures)
DW	dry weight
ECA	ER-type Ca ²⁺ ATPase
EGFP	Enhanced Green Fluorescent Protein
EGTA	ethyleneglycol diamine tetraacetic acid
ER	endoplasmic reticulum
gDNA	genomic DNA

I List of abbreviations

GDT1	Gcr1 dependent translation factor 1
GLR	glutamate receptor
GUS	β -glucoronidase activity
h	hour
ICP-AES	inductively coupled plasma - atomic emission spectrometry
LB	Luria-Bertani (medium)
Lb	leghemoglobin
LbNO	nitrosyl-leghemoglobin
min	minutes
M-MuLV/M-MLV	<i>Moloney Murine Leukemia Virus</i>
mRFP	monomericRed Fluorescent Protein
N	nitrogen
N ₂	dinitrogen
NAD(H)	nicotinamide adenine dinucleotide
NH ₃	ammonia
NH ₄ ⁺	ammonium
NO ₃ ⁻	nitrate
O ₂	oxygen
OD	optical density
PCR	polymerase chain reaction
qRT-PCR	quantitative reverse-transcriptase polymerase chain reaction
RNA	ribonucleic acid
rpm	rotations per minute
RT	room temperature
SM	symbiosome membrane
SOC	Super Optimal broth with Catabolite repression (medium)
TPC	two pore channel
TSS	transformation and storage solution
TY	tryptone yeast (medium)
UTR	untranslated region
x-Gluc	5-bromo-4-chloro-3-indolyl- β -D-glucuronic acid
YEM	yeast extract mannitol (medium)

1. Introduction

1.1 The symbiosis of legumes and rhizobia

1.1.1 The development of nodules

The symbiosis between the plant family Leguminosae (legumes) and bacteria of the genera *Azorhizobium*, *Bradyrhizobium*, *Photorhizobium*, *Rhizobium*, and *Sinorhizobium* (collectively called rhizobia) is the most common N₂-fixing symbiosis and distinguishes oneself by the closest relation between both partners. The plants allow the access of the bacteria into their organism, separated by just one membrane. This intimate, highly specific relationship requires a polished communication between the legumes and the rhizobia. Rhizobia identify their symbiotic partner by plant-specific flavonoids (flavones, chalcones, isoflavones, and flavanones), like luteolin or 4,4' dihydroxy-2'methoxychalcone, which induces the expression of bacterial Nod factors (Fig.1). Nod factors are lipochitooligosaccharides with a β -1,4-linked *N*-acetyl-D-glucosamine chitin backbone and a fatty acid chain of 16 or 18 carbons, which are specific for each bacterium and act as signal molecules recognized by the plant. Nod factors of different rhizobial species can further vary in the number of *N*-acetyl-D-glucosamine monomers (3 to 5) and different substitutions for hydrogen (Cullimore et al., 2001).

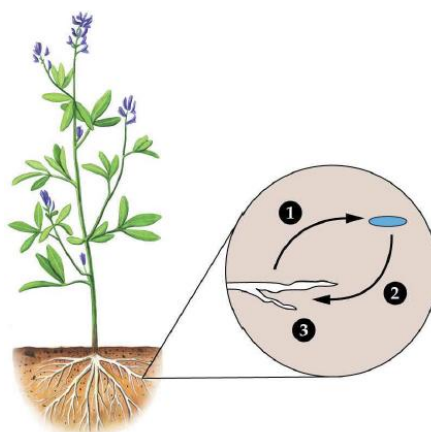


Fig. 1 Communication between legumes and rhizobia for initiation of the nodulation.

Plant flavonoids trigger the synthesis of bacterial Nod factors (1), which are specific signal molecules released by bacteria (2) and recognized by the plant root (3) (Buchanan et al., 2000).

1. Introduction

Nod factor perception by plant receptor-like kinases triggers a nuclear calcium (Ca^{2+}) spiking within the root hair (Ehrhardt et al., 1996), as shown in Figure 2. This is followed by the expression of early nodulin genes (ENODs) (Zipfel and Oldroyd, 2017). The Ca^{2+} spiking involves DMI1, a potassium (K^+) channel localized in the inner nuclear membrane (Riely et al., 2007). It is hypothesized that the release of K^+ into the perinuclear space drives membrane hyperpolarization resulting in the activation of Ca^{2+} -permeable cyclic nucleotide-gated channels (CNGCs) (Charpentier et al., 2016). Ca^{2+} activates a calcium- and calcium/calmodulin-dependent protein kinase (CCaMK; DMI3) within the nucleus and is transported back to the perinuclear space by Ca^{2+} -ATPases. Capoen et al. (2011) identified the Ca^{2+} -ATPase MCA8, which is required for this part of the Ca^{2+} oscillation.

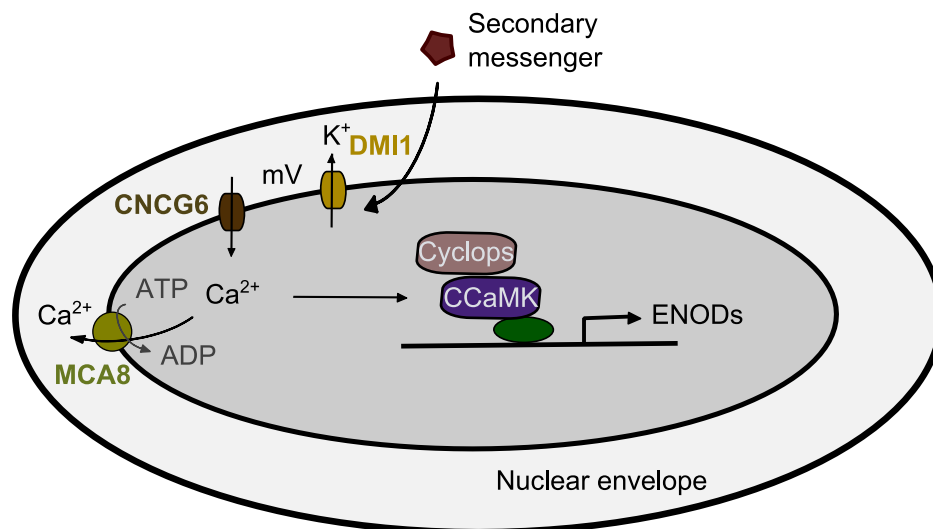


Fig. 2 Signal transduction at the beginning of the nodulation process.

After perception of bacterial Nod factors, an unknown secondary messenger triggers the nuclear Ca^{2+} oscillation which activates the expression of early nodulin genes (ENODs). The Ca^{2+} oscillation is generated by the potassium channel DMI1, the putatively voltage-gated Ca^{2+} channels CNGC6a,b,c, and the Ca^{2+} -ATPase MCA8.

During the attachment of the bacteria to the root hair, the microtubular cytoskeleton of the pericycle reorganizes, and cells of the inner cortex start to divide (Timmers et al., 1999). In this way, a nodule primordium forms. In the root hair, above the developing nodule primordium, the reorganisation of microtubular cytoskeleton is also activated, resulting in a deformation of the root hair tip, which forms a curl around the attached rhizobia. In the centre of this curl the plasma membrane extends internally and lines an infection thread, which grows within the root hair down to the inner part of the root. In the infection thread the bacteria travel into the root towards the nodule primordium. Upon reaching the inner

1. Introduction

cells of the nodule primordium, the rhizobia are released into the host cell cytosol by an endocytosis-type mechanism and remain surrounded by the plant membrane, which is now called symbiosome membrane (SM) or peribacteroid membrane (PBM). Together with this membrane the rhizobia form a new cell organelle-like structure, the symbiosome (Fig. 3).

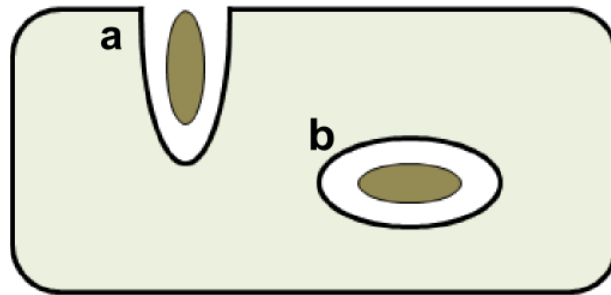


Fig. 3 Entrance of rhizobia into the plant cell by an endocytosis-like process.

(a) The plant plasma membrane deforms and encloses the bacteroid (brown) and separates it from the plant cytosol (green). (b) This process leads to a new cell organelle-like structure, the symbiosome, which contains the bacteroid, the surrounding membrane (now called symbiosome membrane) and the space between the symbiosome membrane and the bacteroid, known as symbiosome space.

Now, as a compartment of the symbiosome the bacteria are called bacteroids. During the differentiation to bacteroids, bacteria become bigger and take a longitudinal shape. Also their gene expression is modified. Becker et al. (2004) identified 982 genes with changed expression in symbiotic living bacteroids. For example, the expression of *sma0677*, encoding a putative glutamate or aspartate transporter, is induced (Becker et al., 2004). Furthermore, the ammonium uptake of free-living bacteria is much higher compared to symbiotic bacteroids (Howitt et al., 1986), suggesting the down-regulation of the expression of ammonium uptake transporters. Taté et al. (1998) showed that the ammonium transporter *amtB* of *Rhizobium etli* is indeed down-regulated during bacteroid differentiation. The most important difference between bacteria and bacteroids is the ability to fix atmospheric nitrogen (N_2). Rhizobia lack the ability to synthesize homocitrate, an essential part of the FeMo cofactor of the N_2 -fixing enzyme complex, nitrogenase (Hakoyama et al., 2009). Also, in contrast to free-living rhizobia, bacteroids are protected against oxygen, which inactivates the nitrogenase. This protection is realized by the complex structure of plant nodules.

1. Introduction

1.1.2 The structure and function of nodules

With regard to the plant species, two types of nodules can be distinguished. Tropical plants form determinate nodules with limited growth and a characteristic spherical shape. In contrast, temperate legumes have indeterminate nodules with a meristematic zone at the top, which allows an unlimited growth. Therefore, the shape of this nodule type is longitudinal (Fig. 4). Beside the meristematic zone, the indeterminate nodule contains the infection zone differentiated in a proximal and a distal part, the nitrogen fixation zone and the senescence zone. All zones are surrounded by two cortex layers (inner and outer cortex) with an endodermis in between.

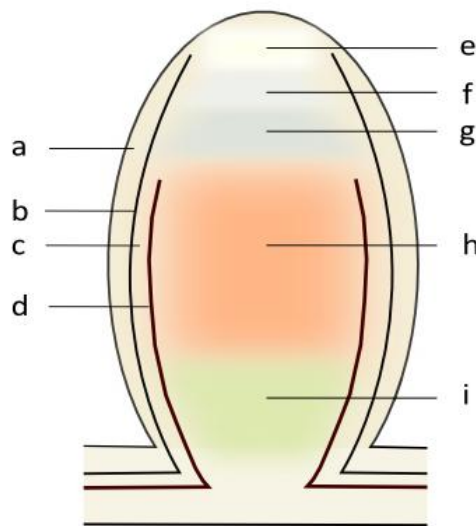


Fig. 4 Structure of an indeterminate nodule.

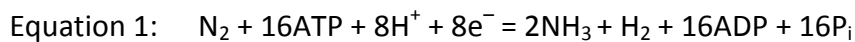
The nodule is protected by the cortex separated by an endodermis (b) into the inner (c) and the outer cortex (a). The inner part of the nodule contains the meristematic zone (e), the distal infection zone (f), the proximal infection zone (g), the nitrogen fixation zone (h) and the senescence zone (i). The nitrogen fixation zone and the senescence zone are surrounded by vascular bundles (d).

The apical meristematic zone is bacteria-free and contains undifferentiated dividing plant cells. In the adjacent distal infection zone, these cells start to differentiate and form infection threads for the bacterial invasion as described above for the infection of the nodule primordium. The bacteria, still able to divide, enter the infection threads within the proximal infection zone. Here, the cells are penetrated by the infection thread, enabling the endocytosis of the bacteria into the plant cell, followed by differentiation to bacteroids. This differentiation is completed in the red-colored nitrogen fixation zone. This zone occupies a large part of a mature nodule. By its complex structure, the nitrogen fixation zone ensures

1. Introduction

three functions: the production of plant-available nitrogen compounds, the exchange of these compounds with carbon sources for the bacteroids, and the transfer of nitrogen and carbon compounds to and from the vascular bundle.

Enlarged infected cells of the nitrogen fixation zone host hundreds of bacteroids which convert atmospheric N_2 into ammonia by an O_2 -sensitive enzyme complex, the nitrogenase. To avoid the inactivation of the nitrogenase by O_2 , the infected and uninfected cells of the nitrogen fixation zone produce O_2 -binding leghemoglobin (VandenBosch and Newcomb, 1988). Besides the protection against O_2 , the infected cells facilitate nitrogenase activity by providing the bacteroids with malate and homocitrate. Malate serves as a energy source and contributes to the synthesis of NADH in the citrate cycle. As electron donor in the respiratory process, NADH is used for the synthesis of ATP, which is required for the N_2 fixation. The nitrogenase uses 16 ATP to generate 2 NH_3 molecules (Equation 1). Thus, the N_2 fixation requires a large investment of energy. To obtain 1 g fixed nitrogen, legumes consume 8 to 12 g of organic carbon (Heytler and Hardy, 1984).



Homocitrate is an essential co-factor of the nitrogenase enzyme complex. Interestingly, the gene *NifV*, which encodes the homocitrate synthase in most diazotrophs, is not present in many rhizobia. However, legumes are able to generate homocitrate by the nodule-specific homocitrate synthase FEN1 (Hakoyama et al., 2009). Some *Aeschynomene* species synthesize NifV (Nouwen et al., 2017). Thus, the N_2 fixation is, inter alia, dependent on the homocitrate supply of the bacteroids by the host plant.

To supply the bacteroids, malate and homocitrate have to be transported across the SM. This membrane functions as a barrier between bacteroids and the plant cytosol. It enables a selective exchange between both organisms by channels, transporters, and pumps. So far, transporters for iron (GmDMT1), zinc (GmZIP1), and sulfate (LjSST1) have been identified in the symbiosome membrane (summarized by Clarke et al. (2014). Furthermore, H^+ -ATPases are localized in the symbiosome membrane (Fedorova et al., 1999) and enable the conversion of ammonia to ammonium by acidification of the symbiosome space. So far, transport proteins for ammonium have not been identified in the symbiosome membrane, but analysis of ion currents by the patch clamp technique detected a voltage-

1. Introduction

gated monovalent cation channel capable to transport NH_4^+ (Tyerman et al., 1995). Another protein responsible for nitrogen transport across the symbiosome membrane is nodulin 26 (nod26), a member of the major intrinsic protein (MIP)/ aquaporin superfamily. It constitutes more than 10% of the symbiosome membrane proteins (Rivers et al., 1997) and is able to permeate ammonia (Hwang et al., 2010; Niemi et al., 2000).

The nitrogenous compounds ammonia and ammonium are released by the symbiosome into the plant cytosol of the infected cells, where ammonia is incorporated into glutamate by glutamine synthetase to produce glutamine. By transfer of the amino group of glutamine to aspartate, asparagine is synthesized. In which way the amino acids, mainly asparagine, are exported from infected cells to the vascular bundle of the nodule is not known, but the track-like arrangement of the uninfected cells and their high plasmodesmatal frequency indicate a symplastic transport from infected cells via uninfected cells to the peripheral vascular system (Abd-Alla et al., 2000; Peiter et al., 2004). There, the amino acids are transferred to the xylem, which enables the amino acid transport into the shoot.

The vascular system is dichotomously branched and contains vascular bundles enclosed by a vascular endodermis. This endodermis contains a Casparian band, which blocks the apoplastic pathway. Another endodermis, the nodule endodermis, is located between the inner and outer cortex. Almost all cells of this endodermis are enveloped by suberin lamellae forming an apoplastic barrier (Hartmann et al., 2002). The only cells of the nodule endodermis which remain without suberin lamellae are directly adjacent to the vascular bundles (Hartmann et al., 2002).

1.2 The fixation of N_2

1.2.1 Mechanism of biological and industrial N_2 fixation

Biological N_2 fixation is realized by the enzyme complex nitrogenase. This complex consists of two enzymes, the $\alpha_2\beta_2$ heterotetramer dinitrogenase and the homodimer dinitrogenase reductase. As mentioned above, NADH serves as electron donor for ATP synthesis, but electrons from NADH are also needed for the N_2 fixation itself. Via ferredoxin electrons are transferred from NADH to the iron-sulfur (4Fe-4S) cluster of the dinitrogenase reductase (Fig. 5). By binding and hydrolysis of MgATP, the 4Fe-4S cluster shifts outwards (Schindelin et al., 1997), and thereby electrons are transferred to the P-cluster, and further to the FeMo

1. Introduction

cofactor, of the dinitrogenase. This process has to be repeated eight times until the dinitrogenase reduces two N_2 molecules to two NH_3 and one H_2 molecule.

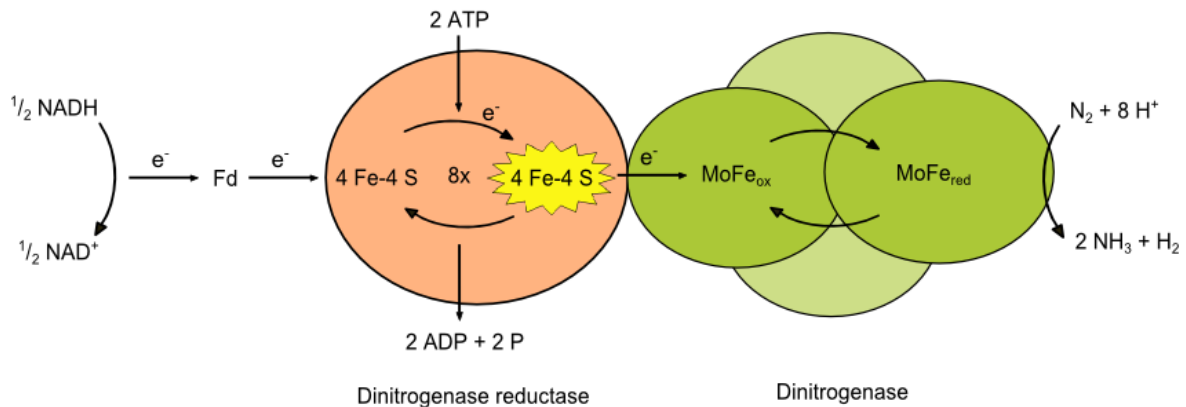
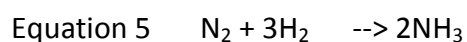
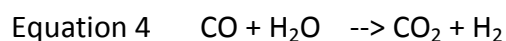
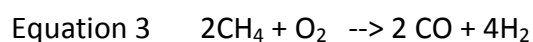
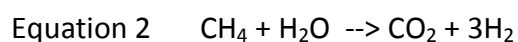


Fig. 5 Nitrogen fixation by the enzyme complex nitrogenase.

Nitrogenase consists of dinitrogenase reductase and dinitrogenase. Electrons of NADH are transferred via ferredoxin (Fd) to the dinitrogenase reductase, which reduces the dinitrogenase by hydrolysis of ATP. Two N_2 molecules are reduced by the dinitrogenase to two NH_3 .

As in plants, the industrial N_2 fixation requires a large energy input. The energy is needed to break the triple bond of the two N atoms, which here is realized by high temperature and pressure. The reaction, known as Haber-Bosch process, was developed at the beginning of the 20th century and has since been modified several times. Mainly natural gas provides the energy for N_2 fixation, but also coal or mineral oil are used as energy source. In general, industrial N_2 fixation is based on two steps: the generation of the synthesis gas and the synthesis of ammonia. There are two methods to generate the synthesis gas, the steam-reforming process and the partial oxidation process. The steam-reforming process involves three steps, in which methane (CH_4), the main component of natural gas, is converted into carbon dioxide (CO_2) and hydrogen (H_2) at temperatures of 800 to 1000°C and pressure of 0.25 to 0.35 MPa (Equation 2-4). At 400 to 500°C and 10 MPa, H_2 and N_2 react to ammonia (Equation 5). This process consumes 27 MJ/kg ammonia (Schilling, 2000).



1. Introduction

In contrast to the partial oxidation, the steam-reforming process is an allothermic process consuming thermal energy by combustion of natural gas. As autothermic non-catalytic process, the partial oxidation includes the supply of oxygen for the partial combustion of the used substance.

Furthermore, it should be mentioned that the industrial N_2 fixation generates the greenhouse gas CO_2 . According to the Institute for Prospective Technological Studies (IPTS) 1.15-1.4 t CO_2 are produced per t NH_3 in the steam-reforming process and 2-2.6 t CO_2 per t NH_3 in the partial oxidation. Only in case of further processing of NH_3 to urea, generated CO_2 is consumed again.

Due to the high energy consumption of the Haber-Bosch process, scientists feel compelled to search for alternative methods of industrial N_2 fixation. One alternative method is the Schrock cycle, which imitates the work flow of nitrogenase (Yandulov and Schrock, 2003).

1.2.2 The relevance of N_2 fixation for agriculture

As macronutrient, nitrogen (N) is needed in high amounts for plant growth. In agricultural systems, soils have to be supplemented with N fertilizers to offer sufficient amounts of N for growth and high yields. Depending on the crop species, the demand for N ranges from 100 and 400 kg N/ha (Amberger, 1996). Under favourable conditions, the N_2 fixation capacity of legumes amounts to 100 to 200 kg N/ha. Thus, the cultivation of legumes can be an important measure to save industrial fertilizers. Legumes used in agriculture, like broad bean (*Vicia faba*), pea (*Pisum sativum*), alfalfa (*Medicago sativa*), and soybean (*Glycine max*), leave N to the subsequently planted crops, which is indeed able to partially substitute industrial fertilizers. Results of the projects LeguAN (2012-2015) and DemoNetErBo (2016-2017), conducted by the FH Südwestfalen (Soest) and the HfWU Nürtingen-Geislingen, respectively, showed that the cultivation of legumes enables N fertilizer savings of around 30 kg/ha. Conventional agricultural enterprises partaking in these projects saved 32 kg/ha N fertilizer by the cultivation of broad beans. The cultivation of peas resulted in N fertilizer savings of 28 kg/ha. Thus, the integration of legumes in the crop rotation seems to be an appropriate intervention for reduction of industrial N fertilizer requirements.

1. Introduction

Symbiotic N₂ fixation is highly sensitive to environmental factors and therefore, the N amounts available for subsequently planted crops can vary widely. Drought stress, unfavourable temperatures, and the availability of mineral N decrease the N₂-fixing capacity of legumes (Marino et al., 2007; Montanez et al., 1995; Streeter, 1985). Furthermore, the activity of nitrogenase is determined by the N demand of the plant. For example, defoliation decreases the N demand of the plant and triggers a down-regulation of N₂ fixation (Hartwig et al., 1994). Thus, the N amount for following crops is highly dependent on growth conditions beneficial for N₂ fixation. Therefore, the down-regulation of N₂ fixation is one of the main reasons for the low usage of legumes in agriculture. Understanding that mechanism is an important step to solve this problem, but little is known about it.

1.2.3 Regulation of N₂ fixation in legumes

1.2.3.1 Factors which induce the down-regulation of N₂ fixation

As mentioned above, several environmental factors affect the N₂ fixation, but also developmental processes of the host plant, like defoliation or pod-filling, have an effect on the activity of nitrogenase. Thus, the plant itself controls the process of N₂ fixation. How the regulation is realized by the plant is not known, but three modes have been suggested: a) the regulation by carbon supply, b) the regulation by O₂ supply and c) the N-feedback regulation (discussed by Schulze (2004) and Schwember et al. (2019)).

1.2.3.2 Regulation by carbon supply

This hypothesis implies that the plant regulates the supply of bacteroids with carbon and thereby the energy needed for N₂ fixation. The carbon provided by the host plant originates from photosynthesis in which carbon dioxide (CO₂) is assimilated. Sucrose is translocated from leaves to nodules where it is converted to malate. The bacteroids use malate for the generation of NADH via the citrate cycle. During respiration NADH is used for the generation of ATP necessary for N₂ fixation.

The theory is based on the correlation between photosynthetic activity and nodule activity, which was detected, inter alia, by Lawn and Brun (1974). Soybean plants with

1. Introduction

decreased photosynthetic activity, caused by shading the shoots or defoliation, showed less nodule activity, while plants treated with supplemental light maintained increased nodule activity (Lawn and Brun, 1974). Furthermore, N accumulation, increased nodule number and increased N_2 fixation are observed, if legumes are exposed to enhanced CO_2 concentrations, as summarized by Vance and Heichel (1991). However, a comparison of several studies shows that long-term CO_2 fertilization of different legumes results in an increased nodule mass, but just in 1 of 12 experiments a stimulation of nitrogenase activity was observed (Vance and Heichel, 1991).

In soybean plants subjected to a moderate water stress, the sucrose synthase activity decreased rapidly, and sucrose was accumulated in the nodules (González et al., 1995). Not only during water stress, but also after treatment with nitrate (NO_3^-) and during salt stress, the expression of the sucrose synthase is down-regulated in soybean nodules (Gordon et al., 1997). The authors proposed that the N_2 fixation is regulated via the sucrose metabolism.

Inducing the decline of nitrogenase activity by interrupting the phloem supply (by stem girdling, stem chilling, or leaf removal) triggers a decline in nodule starch and soluble sugar (Walsh et al., 1987). The authors interpreted the decline of nodule starch as an indicator of carbohydrate limitation of nodule function.

1.2.3.3 Regulation by oxygen supply

Oxygen is needed for the generation of ATP by bacteroid respiration. Thus, a continuous supply of O_2 to infected cells is important for nitrogenase activity by securing the supply of ATP. The elevation of the O_2 concentration up to 15 nM in the nitrogen fixing zone even caused an increase in nitrogenase activity (Denison et al., 1992). The O_2 supply regulation hypothesis implies that a reduced respiration decreases the generation of ATP and therefore the energy supply of bacteroids and nitrogenase.

Furthermore, it has been shown that O_2 is involved in the transcriptional and post-transcriptional regulation of N_2 fixation genes (*nif*) in bacteroids. In *S. meliloti*, O_2 regulates both the expression of *nifA* (the main regulator of N_2 fixation) and the activity of its protein. NifA belongs to the enhancer-binding protein (EBP) family with a central AAA^+ ATPase domain and a DNA-binding domain at the C-terminus. Three further proteins which regulate N_2 fixation are oxygen/redox sensors: the anti-activator NifL and the histidine kinases FixL

1. Introduction

and RegB [summarized by Dixon and Kahn (2004)]. Oxidized NifL inhibits NifA activity (Hill et al., 1996). FixL is negatively regulated by O₂. In the absence of O₂, FixL phosphorylates FixJ, which subsequently activates the expression of *nifA* (de Philip et al., 1990; Tuckerman et al., 2002). RegB (also known as PrrB, RegS, or ActS) controls *nifA2* expression by phosphorylation of RegA (Elsen et al., 2000) and is regulated by a redox-active cysteine (Swem et al., 2003).

There is also evidence for the involvement of O₂ and leghemoglobin in the regulation of N₂ fixation within nodules. For instance, the O₂ concentration in soybean nodules treated with NO₃⁻ decreases within 48 h from 20-34 nM to 7 nM (Layzell et al., 1990). Furthermore, Cabeza et al. (2014) detected the down-regulation of all genes encoding leghemoglobins in *M. truncatula* after treating the plants with NO₃⁻.

1.2.3.4 N-feedback regulation

This hypothesis suggests that N compounds act as signal molecules sensing the N status of the plant and thereby inducing the down-regulation of nitrogenase activity. There are different suggestions of which N compound could act as N sensor and from which part of the plant the compound could come from.

Bacanamwo and Harper (1996) found a correlation between shoot N concentration and nitrogenase activity of soybeans after NO₃⁻ treatment. After treating the plants with 15 mM NO₃⁻, the N concentration in the shoot was increased and nitrogenase activity was inhibited. The extent of nitrogenase inhibition correlated with the shoot N concentration. Later, Bacanamwo and Harper identified the N compound which mainly causes the elevation of the N concentration in soybean shoots: the concentration of free asparagine (Asn) was increased 35 times 24h after treatment with 15 mM NO₃⁻ (Bacanamwo and Harper, 1997). The authors suggested that Asn is translocated from the shoot to the nodule and acts as signal molecule involved in the regulation of nitrogenase activity by sensing of N status. However, in nodules no significant increase in Asn concentration was detected. Instead, the concentration of aspartate and glutamate was increased in nodules after NO₃⁻ treatment. The authors concluded that asparagine is converted into aspartate (Asp) and glutamate (Glu), which subsequently could be transported through the symbiosome membrane and sensed by the bacteroid.

1. Introduction

However, after exposure to other factors that decrease nitrogenase activity, soybeans accumulate Asn in nodules. For instance, Vadez et al. (2000) measured a more than 25-fold increase of Asn concentration in nodules of soybeans treated with polyethylene glycol (PEG) to induce water deficit. In contrast, the nodule Asp concentration remained unchanged. In response to different treatments inhibiting nitrogenase activity, Vadez et al. (2000) also detected an elevation of the concentration of ureides (the export products of N_2 fixation in determinate nodules) in soybean nodules. The authors hence proposed two feedback mechanisms for the decrease of nitrogenase activity: One inside the nodule, based on the accumulation of N_2 fixation products, and a second mechanism outside the nodule, which includes the transport of nitrogenous compounds from the shoot.

Whitehead et al. (2001) investigated the effect of cytoplasmic polyamines on transport processes across the symbiosome membrane of soybean nodules. Thereby they found an inhibition of the unknown NH_4^+ channel by spermine. Putrescine and spermine also reduced the activity of an H^+ -ATPase. Depending on the concentration, spermidine, cadaverine, and putrescine increased or decreased the malate transport across the SM. The transport was reduced at concentrations in the milli-molar range and enhanced in the micro-molar range. According to these results, the authors suggest that ammonium and malate transport may be affected directly or via a decreased voltage and pH gradient caused by the inhibition of H^+ -ATPase. Furthermore, the concentrations of polyamines and ureides are similar in nodules, and both compounds may compete with each other for N (Whitehead et al., 2001). The authors hence suggest that instead of ureides, polyamines are synthesized if glutamate accumulates (Fig. 6), which may provide the basis of an N feedback regulation of N_2 fixation by polyamines.

1. Introduction

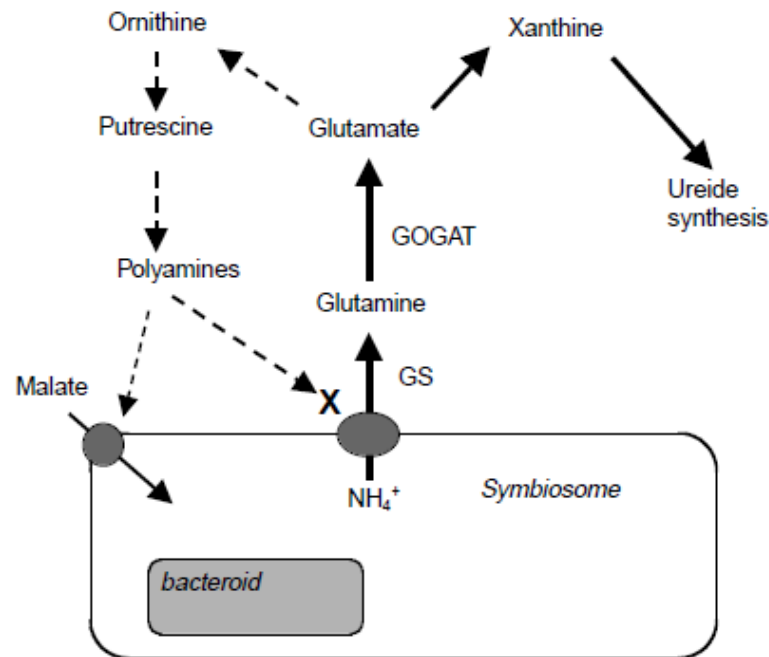


Fig. 6 Proposed N-feedback regulation of N₂ fixation by polyamines.

Glutamate accumulation triggers synthesis of polyamines, which inhibit the transport of ammonium and malate (Whitehead et al., 2001).

In indeterminate nodules, not ureides, but Asn is the main export product. Similar to determinate nodules, Asn appears to be involved in the down-regulation of N₂ fixation. In nodules and phloem sap of *M. truncatula* plants treated with ammonium nitrate (NH₄NO₃), the concentration of amino acids, primarily Asn, was increased (Suliman et al., 2010). Furthermore, under P-deficiency, which also induces the down-regulation of nitrogenase activity, an increased Asn concentration in roots and nodules of clover was measured (Almeida et al., 2000).

An N feedback mechanism by translocation of N compounds from shoot to roots was also suggested for temperate legumes forming indeterminate nodules (Schulze, 2003). However, the systemic regulatory activity of re-translocated N compounds has also been questioned. Marino et al. (2007) investigated nitrogenase activity in nodules of pea (*P. sativum*) plants growing in a split-root system. While in the half of the root system that suffered drought stress the nitrogenase activity was reduced to 70%, it remained unaffected in the irrigated half. In case of drought stress, the authors suggest rather a local than a systemic control of the nitrogenase activity.

Studies investigating the regulation of the N₂ fixation have delivered just indirect evidence for the involvement of amino acids, O₂, and carbon. Schwember et al. (2019)

1. Introduction

concluded that no specific mechanism has been identified yet. Furthermore, a potential involvement of other substances has been shown.

1.2.3.5 Further substances with potential to regulate N₂ fixation

1.2.3.5.1 Regulation of N₂ fixation by phytohormones

Abscisic acid (ABA) is a sesquiterpene signaling molecule acting as phytohormone with inhibitory effects in plants. It is involved in several developmental processes, like seed dormancy, plant growth, fruit ripening, and defoliation, as well as stress responses to abiotic stress inflicted by drought, salt, heat, or cold, and to biotic stress. Furthermore, ABA was shown to affect the N₂ fixation in legumes. For instance, pea plants supplied with exogenous ABA exhibited a reduced N₂ fixation rate by 70% within 5 days after the beginning of the treatment (González et al., 2001). *Lotus japonicus enhanced nitrogen fixation 1 (enf1)* mutants with decreased endogenous ABA concentration exhibited enhanced N₂ fixation activity, similar to wild type plants in which the ABA concentration was reduced by abamine (Tominaga et al., 2010). Abamine-treated plants and *enf1* mutants also contain less nitric oxide (NO), a strong inhibitor of N₂ fixation activity. Hence, Tominaga et al. (2010) proposed that low ABA concentration causes a decrease in NO production, which is responsible for the increased N₂ fixation activity.

1.2.3.5.2 Regulation of the N₂ fixation by calcium

Ca²⁺ was shown to influence different proteins involved in N transport across the SM. For instance, in soybeans, the elevation of the Ca²⁺ concentration within the symbiosome space inhibits a NH₄⁺ channel (Tyerman et al., 1995). Furthermore, the aquaporin Nodulin-26, which is permeable for NH₃ (Hwang et al., 2010), is activated by a Ca²⁺-dependent protein kinase (Weaver et al., 1991). The regulation of the N transport by Ca²⁺ implied the involvement of this ion in the regulation of the N₂ fixation. Despite these indications, no studies investigating the importance of Ca²⁺ for the nodule activity exist.

1. Introduction

1.3 Calcium - the most important signal ion in plants

1.3.1 The mechanism of calcium signaling

As second messenger Ca^{2+} is involved in cellular signal transduction triggered by various environmental stimuli such as cold, drought, and pathogen attack. After the recognition of an abiotic or biotic stimulus, Ca^{2+} is translocated from internal stores (e.g. vacuole, ER, mitochondria) or the cell wall into the cytosol. Subsequently, Ca^{2+} is transported back to internal or external stores. This Ca^{2+} in- and efflux occurs once or in repetition and is described as Ca^{2+} transient or Ca^{2+} oscillation, respectively. The amplitude, frequency, and duration of the Ca^{2+} spikes are believed to be characteristic for the stimulus and to activate the appropriate response. In the cytosol, Ca^{2+} activates enzymes directly or indirectly by activating Ca^{2+} -binding proteins (Fig. 7).

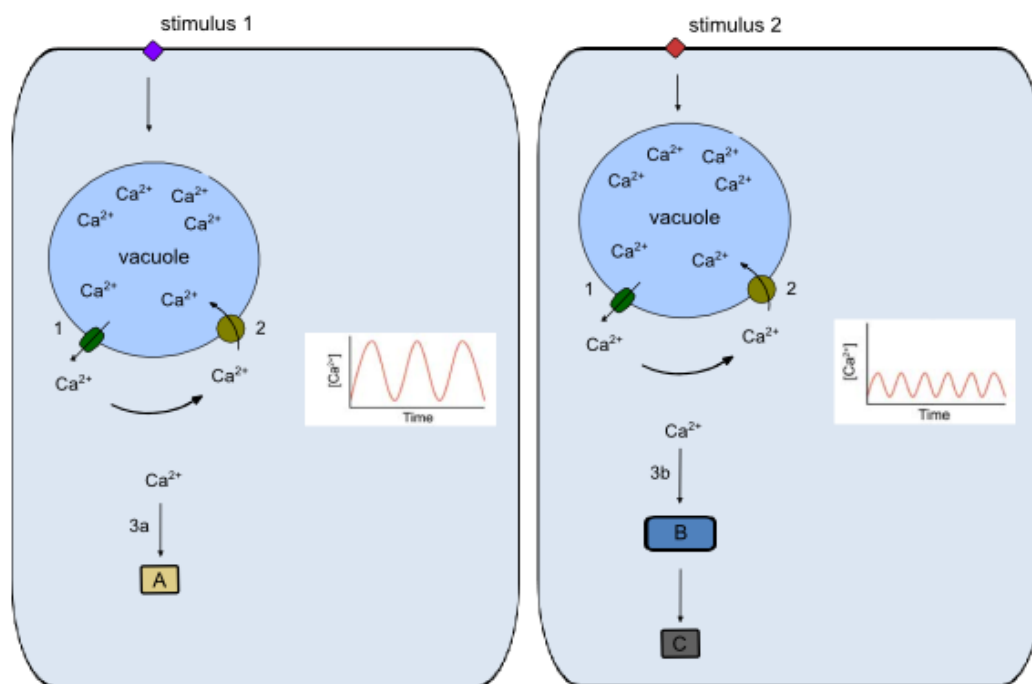


Fig. 7 Ca^{2+} signatures triggered by different stimuli.

The Ca^{2+} influx into the cytosol (1) and the following Ca^{2+} efflux out of the cytosol (2) generate Ca^{2+} spikes or oscillations with different amplitude, frequency, and duration, depending on the stimulus. In the cytosol, Ca^{2+} activates responsive proteins (A, C) directly (3a) or indirectly (3b) by activating Ca^{2+} -binding proteins (B). Inset diagrams taken from McAinsh and Pittman (2009).

1. Introduction

Due to the low Ca^{2+} concentration in the cytosol (100 to 200 nM), Ca^{2+} is transported passively along its electrochemical gradient from Ca^{2+} stores into the plant cytosol. This passive transport is realized by channel proteins, such as cyclic nucleotide-gated channels (CNGCs), glutamate receptor-like channels (GLRs), or two-pore channel 1 (TPC1). For instance, MtCNGC15a/b/c are involved in the generation of Ca^{2+} oscillations during nodulation (Charpentier et al., 2016); AtGLR3.3 and AtGLR3.6, as well as TPC1 are related to a systemic Ca^{2+} signal after wounding (Kiep et al., 2015; Salvador-Recatalà, 2016; Toyota et al., 2018). The efflux out of the cytosol is an active transport against the concentration gradient. It is realized by Ca^{2+} -ATPases and calcium/ H^+ exchangers (CAX).

In the cytosol Ca^{2+} ions bind to proteins, which activate further target proteins or directly trigger the response to the stimulus. Calmodulin (CaM) and calmodulin-like proteins (CMLs) are Ca^{2+} -binding proteins able to activate pumps (e.g. Ca^{2+} -ATPases), transcription factors (e.g., CAMTAs), or close channels (CNGCs) (DeFalco et al., 2016; Galon et al., 2008; Tidow et al., 2012). Further Ca^{2+} -binding proteins, calcineurin B-like proteins (CBLs), activate CBL-interacting kinases (CIPKs), which phosphorylate antiporters (e.g., SOS1), symporters (e.g., NRT1.1), or channels (e.g., AKT1) (Halfter et al., 2000; Ho and Frommer, 2014; Li et al., 2014; Qiu et al., 2002). Calcium- and calmodulin-dependent kinases (CCamKs) are also activated by calmodulin. They regulate the expression of early nodulation genes (ENODs) (Hayashi et al., 2010). Calcium-dependent protein kinases (CDPKs) are directly activated by Ca^{2+} ions and phosphorylate for example anion channels (e.g., SLAC1) or transcription factors (Geiger et al., 2010).

1.3.2 Calcium-permeable transport proteins involved in calcium signaling

1.3.2.1 Ca^{2+} -permeable ion channels

Ca^{2+} -permeable channels form pore-like structures in membranes and mediate the passive influx of Ca^{2+} ions into the cytosol. The central pore region is surrounded by helices with a negative charge at the inner site, which enable the selection of cations. A further selection is realized by the pore size. Ca^{2+} -permeable channels can be opened or closed by membrane potential (e.g., TPC1) or binding of ligands (e.g., CNGC, GLR).

In *A. thaliana* the CNGC family comprises 20 members and is divided into five subgroups (I, II, III, IV-A, and IV-B). Group I, II, and III are closely related to each other, while

1. Introduction

Group IV-A and IV-B show greater distance to every other group. Most characterized members are located in the plasma membrane. As exception, AtCNGC15 is localized in the nuclear envelope (Leitão et al., 2019). CNGCs contain six transmembrane domains and a cyclic nucleotide-binding domain at the C-terminus. They are regulated by cyclic nucleotides, like 3',5'-cyclic adenosine monophosphate (cAMP) and 3',5'-cyclic guanosine monophosphate (cGMP) as well as Ca^{2+} -CaM, as summarized by Cukkemane et al. (2011).

The GLR family comprises 20 members in *A. thaliana* and is divided into three phylogenetic clades. While animal GLRs occur as tetramers containing two types of subunits for glutamate and glycine binding (Colquhoun and Sivilotti, 2004), plant GLRs are activated by glutamate, glycine and other amino acids like alanine, serine, asparagine, and cysteine (Qi et al., 2006; Tapken et al., 2013). Once activated by their ligand, GLRs enable the translocation of cations and trigger a membrane depolarization. Due to their permeability to Na^+ , K^+ and Ca^{2+} , GLRs may act as non-selective channels (Tapken and Hollmann, 2008).

The two-pore channel1 (TPC1) is a singleton in *A. thaliana*. It is the basis of the slow vacuolar channel activity, selective for cations (K^+ , Ca^{2+} , Mg^{2+}) and activated by membrane voltage and $[\text{Ca}^{2+}]_{\text{cyt}}$. It functions as dimer, each with six transmembrane domains, forming a pore of 8-9 Å (Guo et al., 2016). TPC1 is involved in stomatal closure, seed germination (Peiter et al., 2005), and systemic responses to herbivores (Kiep et al., 2015) and salt stress (Choi et al., 2014).

Annexins are ubiquitous soluble proteins able to interact with other proteins and to associate with membranes by binding to phospholipids. Annexins are in association with different membranes including the plasma membrane, tonoplast, and outer chloroplast membrane, maybe also the nuclear envelope (Kovács et al., 1998; Seals et al., 1994; Seigneurin-Berny et al., 2000; Thonat et al., 1997). Bound to membranes, annexins act as cation channels. For instance, AnnAt1 exhibits pH-dependent channel activity (Gorecka et al., 2007) and is responsible for Ca^{2+} transport (Laohavisit et al., 2013). The eight annexin-encoding genes in *A. thaliana* show changes in gene expression in response to salt, drought, high and low temperature conditions, and thus are proposed to be involved in stress responses (Cantero et al., 2006).

1. Introduction

1.3.2.2 Transporters

Calcium/H⁺ exchangers (CAX) belong to the Ca²⁺/cation antiporter (Ca/CA) superfamily and are divided in three phylogenetic groups (Shigaki et al., 2006). They enable the transport of Ca²⁺ against the electrochemical gradient from the cytosol into cell compartments or out of the cell. CAXs transport Ca²⁺ in exchange to protons, and some are also able to transport Mn²⁺ and Cd²⁺ (Han and Kim, 2008). In *Arabidopsis thaliana* 11 CAXs were identified, but AtCAX7 to 11 show more sequence similarity to the mammalian Na⁺/Ca²⁺ antiporter NCKX6 (Shigaki et al., 2006).

Bivalent cation transporters (BICATs) are a family of five members in Arabidopsis. The characterized members function as organellar Ca²⁺ and Mn²⁺ transporters (He et al., 2021). In *A. thaliana*, BICAT2 moves Mn²⁺ into chloroplasts and BICAT1 further into the thylakoid lumen. Both transporters also shape Ca²⁺ signals in the chloroplast stroma (Frank et al., 2019).

1.3.2.3 Calcium pumps: ATPases

ATPases are membrane-bound transport proteins, which enable the active transport of ions and molecules against their electrochemical gradient by cleavage of ATP or the synthesis of ATP by utilization of the proton-motive-force. Regarding to their main structure, ATPases are divided in P-type ATPases, F- and V-type ATPases, and ABC (ATP-binding cassette) transporters, which are localized in different compartments of the cell (e.g. mitochondria, chloroplasts, Golgi apparatus or vacuole), and the plasma membrane. Ca²⁺-ATPases belong to the P-type ATPase family, which is composed of five subgroups (P₁ to P₅). In plants, ATPases of the groups P_{2A}, P_{2B}, and P₅ are suggested as Ca²⁺ pumps.

P_{2A}-type ATPases are also known as ECAs (ER-type Ca²⁺-ATPases) and show a high similarity to animal sarco-endoplasmic reticulum Ca²⁺ pumps (SERCA). P_{2B}-type ATPases are closely related to animal CaM-stimulated Ca²⁺ pumps (PMCA), which are localized in the plasma membrane. The main structural difference between both types is the N-terminal CaM-binding site in P_{2B}-type ATPases, which acts as an autoinhibitory domain. Therefore, this type is also named autoinhibited Ca²⁺-ATPases (ACAs). Tidow et al. (2012) proposed a two-step, Ca²⁺-mediated CaM activation mechanism for ACAs because two CaM-binding sites

1. Introduction

(CaMBS1 and CaMBS2) were found at the N-terminus of AtACA8. The authors suggested that with increasing Ca^{2+} concentration, Ca^{2+} -CaM first binds to the high-affinity CaMBS1 and thereby displaces this domain. With further increase of the Ca^{2+} concentration, Ca^{2+} -CaM binds and displaces CaMBS2, resulting in a displacement of the whole N-terminus (Fig. 8).

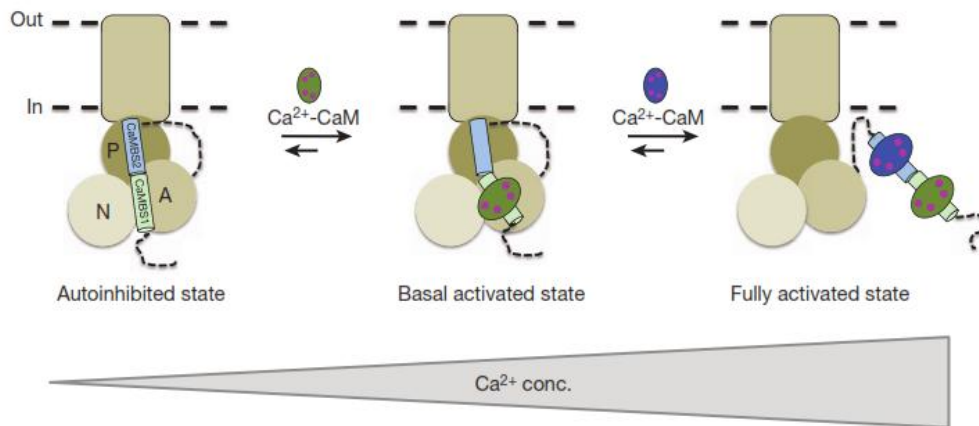


Fig. 8 Proposed two-step activation mechanism of ACAs.

With increasing Ca^{2+} concentration the ACA is basally activated by Ca^{2+} -CaM binding to CaMBS1 and fully activated by a second Ca^{2+} -CaM binding to CaMBS2 (Tidow et al., 2012).

Except for the autoinhibitory domain, the structure of ACAs and ECAs is very similar. Both types contain 10 transmembrane domains, forming the transport domain (TM1 - TM6) and the support domain (TM7 - TM10) of the protein. Further domains are located in the cytosol. The loop between TM2 and TM3 contains the actuator domain (A) with the highly conserved TGES motif that accounts for a phosphatase. The nucleotide-binding domain (N) and the phosphorylation domain (P) lie in the loop between TM4 and TM5 (Fig. 9).

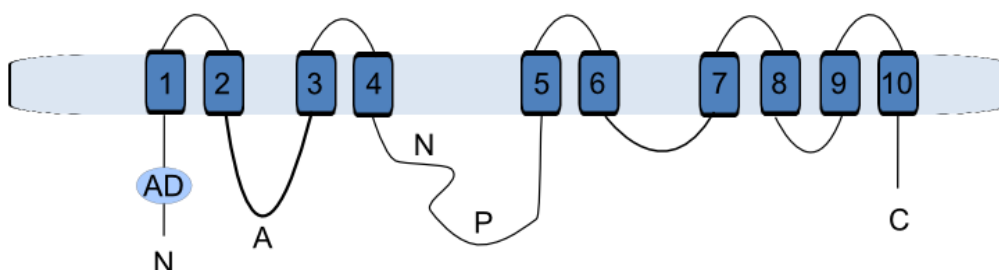


Fig. 9 Topology of autoinhibitory Ca^{2+} -ATPase (ACA).

The protein contains ten transmembrane domains (1-10), an actuator domain (A), nucleotide-binding domain (N), phosphorylation domain (P) and an autoinhibitory domain (AD), which is not present in ER-type Ca^{2+} -ATPases (ECAs).

1. Introduction

For the translocation of Ca^{2+} ions, ATPases undergo a conformational change from E1 to E2 state (reviewed by Demidchik et al. (2018)). In the E1 state the enzyme has a high affinity to Ca^{2+} and binds a Ca^{2+} ion. Subsequently, γ -phosphate of ATP binds to the Asp residue within the highly conserved DKTGT motif of the P-domain and triggers the shift to the E2 status. In this state the affinity to Ca^{2+} is reduced and Ca^{2+} is released to the other side of the membrane. In general, ACAs and ECAs differ in selectivity and affinity for Ca^{2+} . While ACAs are highly selective, ECAs (AtECA1, AtECA3, LCA1) were shown to be also involved in the transport of Mn^{2+} (Johnson et al., 2009; Mills et al., 2008; Wu et al., 2002).

In *Arabidopsis thaliana* 10 ACAs and 4 ECAs were found. ACAs are divided into four clusters. Cluster 1 contains AtACA1, AtACA2, and AtACA7; cluster 2 is formed by AtACA4 and AtACA11; cluster 3 consists of AtACA12 and AtACA13; and the remaining proteins (AtACA8, AtACA9, AtACA10) belong to cluster 4. Most ACAs are localized in the plasma membrane (AtACA7, AtACA8, AtACA9, AtACA10, AtACA12, and AtACA13). However, there are also ACAs localized in other membranes, like ER membrane (AtACA1 and AtACA2) and tonoplast (AtACA4 and AtACA11), as summarized by Yu et al. (2018). In general, ECAs are localized in compartments of the secretory pathway. For AtECA1 a localization in the ER membrane was shown (Liang et al., 1997), whereas AtECA3 was shown to be localized in the Golgi (Mills et al., 2008).

1.4 Aims of the project

The supply of crops with N is necessary for optimal plant growth and high yields. However, the synthesis of N fertilizers requires a lot of energy, and the usage of mineral and organic fertilizers leads to increasing nitrate concentrations in the ground water. An alternative, often used in organic farming, is the cultivation of legumes to elevate the N supply of following crops. However, during drought stress and in presence of N, legumes down-regulate the N_2 fixation. Unfortunately, little is known about the regulation of the N_2 fixation. Besides the currently existing hypotheses, there is evidence for the involvement of Ca^{2+} in the regulation of N_2 fixation. Ca^{2+} is an important signal ion involved in many different regulatory processes in plants. This work aims to identify the role of Ca^{2+} in the regulation of the N_2 fixation in legumes.

1. Introduction

One aim of this work is to elucidate if stimuli generating a down-regulation of N₂ fixation trigger Ca²⁺ signals in nodules. Therefore, *M. truncatula* plants will be transformed with Ca²⁺ sensors. To get insight into the Ca²⁺ signaling machinery of the nodule, the expression of genes encoding Ca²⁺-permeable proteins (channels, transporters, and pumps) will be investigated in nodules. Selected Ca²⁺-permeable proteins shall be characterized regarding to their expression pattern, subcellular localization, and function. In order to optimize Ca²⁺ fertilization of an agronomically relevant legume, the effect of enhanced Ca²⁺ supply on growth of N₂-fixing *V. faba* plants will be investigated.

2. Materials and Methods

2.1 Bioinformatic and *in silico* analyses

For identification of Ca²⁺-permeable transporters, pumps, and channels of the legume model plant *Medicago truncatula*, amino acid sequences of *Arabidopsis thaliana* were used for a BLASTp search. The search was performed using three databases, one for *M. truncatula* (<http://blast.jcvi.org/Medicago-Blast/index.cgi>), one for *A. thaliana* (<https://www.arabidopsis.org/>), and the Protein Data Bank (PDB) protein database containing data of several organisms (<https://blast.ncbi.nlm.nih.gov/Blast.cgi>). First, the *M. truncatula* database was used for the BLASTp-search with following parameters: max target sequence 10, word-size Default, and E-value 10. Subsequently, the amino acid sequences of the suggested *M. truncatula* genes were blasted using the *A. thaliana* database and the NCBI PDB database. This second BLAST-search served to validate the results of the first search using the *M. truncatula* database.

To identify Ca²⁺-permeable transporters, pumps, and channels of *M. truncatula* which are specifically expressed in nodules, published and unpublished expression studies were queried. Most of the published expression data were based on Affymetrix microarray studies (Heath et al., 2012; Limpens et al., 2013; Seabra et al., 2012; Sinharoy et al., 2013). Studies of Roux et al. (2014) and unpublished data of Schulze and Cabeza (University of Göttingen) were based on RNA sequencing (RNA-seq) experiments. Furthermore, a database for Affimatrix GeneChip data (GENEVESTIGATOR; <https://geneinvestigator.com>) and the eFP Browser of a *M. truncatula* database (<http://bar.utoronto.ca>) were used.

The phylogenetic relationships between proteins of *M. truncatula* and *A. thaliana* were represented by creating phylogenetic trees using the programme TreeViewX (<https://treeview-x.en.softonic.com>). The topology of proteins was predicted using TMHMM (www.cbs.dtu.dk/services/TMHMM/).

2. Materials and Methods

2.2 Organisms

This thesis focuses on legumes with indeterminate nodules, which are common for temperate climate zones. While the model plant *M. truncatula* was used for molecular work, agronomically relevant experiments were conducted with *V. faba*. As symbiotic partners, *Sinorhizobium meliloti* and *Rhizobium leguminosarum* *bv. viciae* were used for *M. truncatula* and *V. faba*, respectively. *Agrobacterium rhizogenes* served for transient plant transformation, and *Escherichia coli* was used for cloning work. For complementation assays, *Saccharomyces cerevisiae* was used. The utilized organisms are listed in Table 1.

Tab. 1 List of Organisms used in this work

Organisms	Cultivar / Strain	Source
<i>Medicago truncatula</i>	Jemalong A17	Bettina Hause, Leibniz Institute for Plant Biochemistry, Halle (Germany)
<i>Vicia faba</i>	Taifun, Fuego	Norddeutsche Pflanzenzucht Hans-Georg Lembke KG (Germany)
<i>Sinorhizobium meliloti</i>	102F51 2011 (mRFP)	Georg August University Göttingen (Germany) Leibniz University Hannover (Germany)
<i>Rhizobium leguminosarum</i>	6044	Leibniz Institute, German Collection of Microorganisms and Cell Cultures GmbH (Germany)
<i>Agrobacterium Rhizogenes</i>	ARqua1	Bettina Hause, Leibniz Institute of Plant Biochemistry, Halle (Germany)
<i>Echerischia coli</i>	TOP 10 XL-Blue	Thermo Fisher No C4040-xx
<i>Saccharomyces Cerevisiae</i>	K601 K616	Kyle Cunningham, Johns Hopkins University, Baltimore (USA)

2.2.1 Plant cultivation

2.2.1.1 *Medicago truncatula*

For plant reproduction, *M. truncatula* seeds were sterilized with sulfuric acid for 10 minutes, washed four times with sterile tap water (4°C), and germinated on filter paper for four days (two days at 4°C, one day at room temperature in darkness and one day in light). Subsequently, the seedlings were transferred to pots containing soil (Einheitserde ED73 or

2. Materials and Methods

GS90) mixed with quartz sand (3:1) and grew for approximately nine weeks under greenhouse conditions until seed ripeness.

For plant transformation, *M. truncatula* seeds were sterilized with sulfuric acid for 10 minutes, washed four times with sterile ultrapure water (4°C), sown on agar (0.8%) and stored in darkness (12°C) for two to three days until a radicle length of approximately 1 cm was reached. Subsequently, seedlings were transferred to Fahraeus medium plates. Plates were stored one day in darkness at 20°C (arranged at an angle of 45°), two days in a growth chamber (16h light at 20°C, 8h darkness at 17°C, 70% RH and 90 $\mu\text{mol m}^{-2} \text{s}^{-1}$) at an angle of 45°, and three days at an angle of 90°. The growth conditions were changed to 16h light at 24°C, 8h darkness at 19°C, and 45 $\mu\text{mol m}^{-2} \text{s}^{-1}$ light intensity at the beginning of the second week. Under these conditions the plants grew for another three weeks. For nodulation, the light intensity was increased to 350 $\mu\text{mol m}^{-2} \text{s}^{-1}$, and the plants were transferred to N-free Fahraeus medium, Lecaton, Seramis, or hydroponic culture medium. Plants growing in Lecaton (LamstedtTon) or Seramis were fertilized with 10 mL Long Ashton Fertilizer per plant at the day of the transfer.

Long Ashton Fertilizer

The Long Ashton Fertilizer solution contained 40 mM KNO_3 , 40 mM $\text{CaNO}_3 \cdot 4\text{H}_2\text{O}$, 13.5 mM $\text{NaH}_2\text{PO}_4 \cdot \text{H}_2\text{O}$, 29 mM $\text{MgSO}_4 \cdot 7\text{H}_2\text{O}$, 1 mM NaCl, 100 μM $\text{MnSO}_4 \cdot \text{H}_2\text{O}$, 10 μM $\text{CuSO}_4 \cdot 5\text{H}_2\text{O}$, 11 μM $\text{ZnSO}_4 \cdot 7\text{H}_2\text{O}$, 501 μM H_3BO_3 , 0.7 μM $(\text{NH}_4)_6\text{Mo}_7\text{O}_{24} \cdot 4\text{H}_2\text{O}$, and 0.63 mM FeNa-EDTA.

Fahraeus medium

For 1L Fahraeus medium the following stock solutions (Tab. 2) were mixed with 200 mg MES and 11 g Phytigel. The pH was adjusted to 7.4 with 1M KOH, and the medium was autoclaved at 121°C for 20 min. Antibiotics and CaCl_2 solution were added at 50°C.

2. Materials and Methods

Tab. 2 Stock solutions of Fahraeus medium

stock solution	final concentration
MgSO ₂ *7H ₂ O	0.5 mM
KH ₂ PO ₄	20.3 µM
Na ₂ HPO ₄ *2H ₂ O	10 µM
Ferric citrate	20 µM
NH ₄ NO ₃	1 mM
CaCl ₂	0.9 mM
MnCl ₂	0.26 µM
CuSO ₄ *5H ₂ O	0.13 µM
ZnCl ₂	0.05 µM
H ₃ BO ₃	1.61 µM
Na ₂ MoO ₄ *2H ₂ O	0.13 µM

Hydroponic culture

The *M. truncatula* plants grew in 4.5 L aerated nutrient solution containing 0.25 mM MES. The pH was adjusted to 6.5. The concentrations of the nutrients are listed in Tab.3.

Tab. 3 Nutrient solution of hydroponic culture for *M. truncatula*

Nutrient solution	Final concentration
KH ₂ PO ₄	12 µM
MgSO ₂ *7H ₂ O	0.5 mM
K ₂ SO ₄	0.7 mM
CaCl ₂ *2H ₂ O	0.8 mM
FeNaEDTA	3.3 µM
MnCl ₂	0.7 µM
CuCl ₂	0.3 µM
ZnSO ₄	0.3 µM
H ₃ BO ₃	1.3 µM
Na ₂ MoO ₄	0.03 µM
CoCl ₂	0.07 µM

2.2.1.2 *Vicia faba*

V. faba seeds were imbibed overnight in CaSO₄ solution (2 mM) and germinated in filter paper rolls soaked with 2 mM CaSO₄ solution at 25°C in darkness for four days. In initial test experiments, the seedlings were transferred to pots containing quartz sand and nutrient

2. Materials and Methods

solution or soil/vermiculite mixture (2:1). Later they were transferred to hydroponic culture (4.5 and 50 L). The aerated nutrient solution (Tab. 4), adjusted to pH 6.5 (KOH), was renewed twice a week. The plants were inoculated with *R. leguminosarum* *bv. viciae* ($OD_{600} = 1$) and grown under greenhouse conditions.

Tab. 4 Nutrient solution for *Vicia faba*

Nutrient solution	Final concentration
NH ₄ NO ₃	0.5 mM
KH ₂ PO ₄	0.1 mM
K ₂ HPO ₄	0.1 mM
KCl	0.2 mM
MgSO ₂ *7H ₂ O	0.5 mM
K ₂ SO ₄	1 mM
CaCl ₂ *2H ₂ O	1 mM
FeNaEDTA	30 μM
MnSO ₄ *H ₂ O	0.5 μM
CuSO ₄ *5 H ₂ O	0.2 μM
ZnSO ₄ *7H ₂ O	0.5 μM
H ₃ BO ₃	10 μM
(NH ₄) ₆ Mo ₇ O ₂₄ *4 H ₂ O	0.05 μM
CoCl ₂ *6 H ₂ O	0.5 μM

2.2.2 Bacteria cultivation

S. meliloti (102F51) was cultivated in YEM medium at 28°C for 2-4 days. *S. meliloti* (2011-mRFP) was cultivated in LB medium (5μgmL⁻¹ Tetracycline) at 30°C for 3-4 days. For plant inoculation the bacteria grew on solid medium and were suspended in sterile ultrapure water to avoid plant contact with Tetracycline.

R. leguminosarum (6044) was cultivated on soil medium (Rhizobium Medium 98, DSMZ) at 26°C for two days. For plant inoculation the bacteria were suspended in sterile ultrapure water.

E. coli (TOP 10, XL1-Blue) grew on solid or in liquid LB medium containing a corresponding antibiotic for plasmid selection at 37°C over night (12-15 hours).

A. rhizogenes (ARqua1) was cultivated on solid TY medium containing Streptomycin (25μgmL⁻¹) for bacterial selection and 2 mM CaCl₂. Successfully transformed bacteria were

2. Materials and Methods

selected by Kanamycin ($20 \mu\text{g mL}^{-1}$). To improve the plant transformation the TY medium was covered with $200 \mu\text{L}$ 1 mM acetosyringone solution before bacteria were plated. For long-term storage, bacteria were grown in the appropriate liquid medium and were frozen at -80°C after addition of 25% glycerol.

LB medium

For 1 L Luria-Bertani (LB) medium 5 g yeast extract, 10 g BactoTrypton, and 7 g NaCl were dissolved in ultrapure water and autoclaved at 121°C for 20 min. Antibiotics were added after the medium had cooled to 50°C .

Medium with soil extract

Soil (Einheitserde ED73) was dried at room temperature over night. For 200 mL soil extract, 80 g dry soil, 0.2 g Na_2CO_3 , and 400 ml ultrapure water were autoclaved for one hour at 121°C . For 1 L medium, 1 g yeast extract, 10 g mannitol, 15 g agar, 200 mL soil extract, and 800 mL ultrapure water were mixed and autoclaved at 121°C for 20 min.

SOC medium

For 1L SOC medium 20 g tryptone, 5 g yeast extract, 0.58 g NaCl, and 0.18 g KCl were mixed with ultrapure water and autoclaved at 121°C for 20 min. Subsequently, 2 M MgSO_4 and 1 M glucose solution were added to a final concentration of 20 mM each.

TY medium

For 1L TY (tryptone yeast extract) medium 5 g tryptone and 3 g yeast extract were mixed with ultrapure water and autoclaved at 121°C for 20 min. Subsequently, 0.9 M CaCl_2 solution was added to a final concentration of 2 mM at 50°C . Antibiotics were also added after the medium had cooled to 50°C .

YEM medium

For 1L YEM (yeast extract mannitol) medium 5 g mannitol, 0.5 g yeast extract, 0.2 g $\text{MgSO}_4 \cdot 7\text{H}_2\text{O}$, 0.1 g NaCl, 0.5 g K_2HPO_4 , 5g Na-gluconate were mixed with ultrapure water and autoclaved at 121°C for 20 min. CaCl_2 solution was added to a final concentration of

2. Materials and Methods

16.6% after the medium had cooled to 50°C. For solid media 15 g agar per 1L medium were added.

2.2.3 Yeast cultivation

The yeast strains K601 and K616 were initially propagated in YPD medium. The mutant K616 was subsequently selected on SC-TRP/HIS/LEU medium containing 20 mM CaCl₂. Both strains were grown at 30°C.

SC medium

For 1L SC medium 1.9 g Yeast Nitrogen Base Without Amino Acids and (NH₄)₂SO₄, 0.77 g Complete Supplement Mixture (CSM) without URA (for complementation assay) or without TRP/HIS/LEU/ADE (for selection of K616), 5 g (NH₄)₂SO₄, and 20 g glucose were mixed with ultrapure water and autoclaved at 121°C for 20 min. Finally, sterile adenine (20 mgL⁻¹ final concentration) and CaCl₂ (20 mM final concentration) were added. For solid media 20 g agar per 1L medium were added.

YPD

For 1L YPD medium 20 g yeast extract, 10 g peptone and 20 g glucose were mixed with ultrapure water and autoclaved at 121°C for 20 min. For solid medium 20 g agar per 1 L medium were added.

2.3 Nucleic acid isolation and PCR

2.3.1 DNA isolation

Plant genomic DNA was isolated by mashing leaf material in an extraction buffer [200 mM Tris-HCL (pH 7.5), 250 mM NaCl, 25 mM EDTA, 0.5% SDS]. Subsequently, the DNA was precipitated with isopropanol and finally washed with ethanol (70%). After removing ethanol the pellet was air-dried and dissolved in 10 mM Tris-HCL (pH 8.5).

Plasmids were isolated from *E. coli* using the "Wizard®Plus SV Minipreps DNA Purification System" (Promega, Madison, USA). Cells from 2 mL overnight culture were

2. Materials and Methods

pelleted by centrifugation for 2 min at 10 000 rpm (MiniSpin, Eppendorf, Hamburg, Germany) and resuspended in resuspension solution. After adding lysis solution and alkaline protease the mixture was neutralized and subsequently DNA was separated by column and washed two times with ethanol-containing wash solution. Finally, the DNA was diluted in ultrapure water.

For the purification of DNA fragments from agarose gels, the "Wizard®SV Gel and PCR Clean-Up System" (Promega) was used. After excising a gel piece containing the desired fragment, the gel piece was dissolved in membrane-binding solution at 65°C in a heat block (biostep, Jahnsdorf, Germany). The DNA was separated by SV Minicolumn and washed two times with ethanol-containing membrane wash solution. Finally, the DNA was diluted in ultrapure water.

DNA concentrations were measured using a NanoDrop2000c spectrophotometer (Peqlab, Erlangen, Germany).

2.3.2 RNA isolation and cDNA synthesis

For RNA isolation, nodules, roots, and shoots of *M. truncatula* (Jemalong A17) were harvested from nine-week-old plants and immediately transferred to liquid nitrogen. The plant material was powdered using an ice-cold pestle and mortar. Total RNA of was isolated using the "Spectrum Plant Total RNA Kit" (Sigma Aldrich, St Louis, USA) according to the manufacturer's protocol and frozen at -80°C before use.

For qRT-PCR cDNA was synthesized using a (dN)₆ primer and M-MLV reverse transcriptase. The primer was mixed with 1 µg RNA and incubated for 5 min at 65°C before 5x M-MLV buffer, M-MLV reverse transcriptase (Promega), and dNTPs were added. For the RT reaction samples were incubated for 5 min at 25°C, 1 h at 42°C, and 5 min at 75°C. In a final step RNase A (MBI Fermentas) was added at 37°C, and samples were incubated further for 20 min.

For verification of UTRs cDNA was synthesized with (dT)₃₇ primer and a recombinant M-MuLV reverse transcriptase with reduced RNase H activity (ProtoScript II, New England Biolabs). Reverse transcription was performed with 1 µg RNA, 1.3 mM (dT)₃₇ primer and 1.3 mM dNTPs. Samples were heated to 65°C for 5 min. Subsequently, ProtoScript reaction buffer, 10x DTT (100 mM) and ProtoScriptII MMuLV reverse transcriptase were added at

2. Materials and Methods

42°C. After 1h samples were heated to 80°C for 5 min and subsequently cooled down to 37°C. Finally, RNase A was added, and samples were incubated further for 20 min.

2.3.3 qRT-PCR

For quantification of dsDNA synthesis in realtime PCR reactions, SYBR® Green was used. Each reaction (7.5 µl total volume) contained 6.26 µl 2 x MasterMix reagent, 100 ng cDNA, and 1.6 µM of each gene-specific primer. The amplification was carried out by the following PCR protocol: 10 min for 95°C; 60 cycles of 95°C for 15 sec and 60°C for 1 min. The primers used are listed in Tab. A11 (Appendix).

2.3.4 PCR for verification of the UTRs

UTRs of the candidate genes were amplified using primers binding at the start of the 5'UTR and at the first or second exon of the CDS (for 5'UTR amplification) or at the last exon of the CDS and the end of the 3'UTR (for 3'UTR amplification). Used primers are listed in Tab. A12 (Appendix). The PCR products were sequenced by Eurofins, and the received sequences were aligned against the predicted sequences using Multalign (JCVI). The predicted start and stop codons were verified.

2.4 USER cloning

The fragment of interest was amplified using primers with an Uracil (U)-containing overhang of 8 nt (Tab. A13). The PCR was performed with Phusion U Hot Start DNA Polymerase (F-555, ThermoFisher Scientific, Waltham, United States) and 5x HF buffer (F-518, Thermo Fisher Scientific). The size of the PCR products was controlled by gel electrophoresis, and products were purified from the agarose gel using the "Wizard® SV Gel and PCR Clean-Up System" purification kit (Promega).

Recipient vectors containing the PacI USER cassette were digested with PacI and Nt.BbvCI to generate 8 nt single-stranded 3' overhangs. For digestion, 15 µg recipient vector was incubated with 0.4 units PacI for 6h at 37°C, followed by an overnight incubation with 1 unit Nt.BbvCI at 37°C in CutSmart buffer (B7204, New England Biolabs, Ipswich, United

2. Materials and Methods

States). For ligation, 10 ng of the digested vector was incubated with the PCR product and USER enzyme mix (M5508, New England Biolabs) in a buffer (50mM KCl, 1.5 mM MgCl₂, 10 mM Tris-HCl, pH 8.3) for 30 min at 37°C and 1h at 25°C.

2.5 Transformation of the organisms

2.5.1 Generation of competent *Agrobacterium rhizogenes* cells

Competent *A. rhizogenes* (Arqua1) cells were generated by the CaCl₂ method. To this end, bacteria were cultivated in Trypton Yeast (TY) medium until they reached an OD₆₀₀ of 0.5. The bacteria were centrifuged (5000 rpm, 4°C, 20 min) in a swing-out rotor (5804 R, Eppendorf), and the pellet was resuspended in 500 µL CaCl₂ (20 mM) or 500 µL TSS (1 mM MgSO₄, 10% DMSO, 20%PEG 8000 in TY). Competent cells were aliquoted and stored at -80°C.

2.5.2 Transformation of *Agrobacterium rhizogenes*

For transformation of *A. rhizogenes* (Arqua1) 100 µl competent cells were incubated with 1 µg plasmid on ice (5 min), frozen in liquid nitrogen (5 min), and incubated at 37°C (5 min). Finally 1 mL TY medium was added, and the bacteria were incubated for three hours at 28°C (180 rpm) in a shaking incubator (Certomat BS-I, Sartorius, Göttingen, Germany).

2.5.3 Transformation of *Medicago truncatula*

M. truncatula plants were transformed by root transformation according to Boisson-Dernier et al. (2001). To this end, seeds were germinated at 12°C for 2-3 days. After the radicle had reached a length of approximately 1 cm, the radicle tip was cut, and the wounded surface was covered with transformed *A. rhizogenes* (ARqua1). Subsequently, the plants grew on Fahraeus medium for three weeks and were transferred to hydroponic culture or Lecaton for nodulation, as described in 2.2.1.1.

2. Materials and Methods

2.5.4 Generation of competent *Escherichia coli* cells

E. coli cells were cultivated in LB medium at 37°C until they had reached an OD₆₀₀ of 0.3. Subsequently, cells were centrifuged (1000 g, 4°C, 10 min) in a swing-out rotor (5804 R, Eppendorf). The pellet was resuspended in TSS [20 mM MgCl₂, 20 mM MgSO₄, 10% (w/v) PEG 4000, 5% (v/v) DMSO in LB, pH 6.5] and incubated on ice for 5 min.

2.5.5 Transformation of *Escherichia coli*

For the transformation of *E. coli* chemical or electrocompetent cells were used. Chemical competent cells were incubated with plasmid (1-10 µl) on ice for 20 min, heat-shocked for 90 sec at 42°C and incubated again on ice for 2 min. Depending on the used antibiotics, cells were subsequently incubated in SOC medium at 37°C for 1 h (200 rpm) in a shaking incubator (KS 4000 ic control, IKA, Staufen, Germany) and plated on selective LB medium. In case of ampicillin, cells were directly plated on selective LB medium and incubated over night at 37°C. For the transformation of electrocompetent cells 0.5-1 µl plasmid and 60 µl cells were electrically shocked with 2500 V in an electroporator (2510, Eppendorf).

2.5.6 Transformation of *Saccharomyces cerevisiae*

The yeast was precultured on solid SC medium (30°C) for 2-3 days and subsequently resuspended in transformation buffer [100 mM Liacetate, 10 mM Tris-HCl (pH 7.5), 1 mM EDTA]. After centrifugation and removing the supernatant, salmon testes DNA, 1 µg of the plasmid and PLATE buffer [100 mM Liacetate, 10 mM Tris-HCl (pH 7.5), 1 mM EDTA, 40% PEG 3350] were added, followed by an overnight (16 h) incubation. For heat shock the yeast was subsequently incubated for 15 min at 42°C and finally washed with sterile water. The cell suspension was plated on selective SC medium and incubated for 2-3 days at 30°C.

2.6 Investigation of promoter activity by histochemical GUS staining

The genomic sequences around 3 kb upstream of the start codon of *MA1*, *MA3*, *MA4*, and *MA5* were amplified by PCR with primers containing the XbaI and SmaI restriction sites (Tab. A14). The purified PCR products were digested with XbaI and SmaI and ligated into the plasmid pBI101.3 containing *uidA* (Jefferson et al., 1987). Due to the large introns in the 5'UTR

2. Materials and Methods

of *MA2*, the region upstream the start codon was amplified by two separate PCR reactions. The 5'UTR was amplified using cDNA as template and a U-containing reverse primer. The region upstream of the 5'UTR was amplified using gDNA and a U-containing forward primer. The reverse primer for amplification of the upstream region and the forward primer for amplification of the 5'UTR contained overlapping regions. In this way, by linking both fragments the original sequence was reconstituted seamlessly. The PCR products were finally inserted into a USER-compatible version of pBI101.3 as described in 2.4. All constructs were validated by sequencing the amplified sequence before they were used for plant transformation. The sequencing reactions were performed by MicroSynth AG (Switzerland).

The constructs were transformed into *A. rhizogenes* (see 2.5.2) and subsequently into *M. truncatula* (Jemalong A17, see 2.5.3). As positive control plants were transformed with the pBI121 plasmid, which contains a CaMV 35S promoter. Three weeks after transformation plant roots were inoculated with *S. meliloti* (strain 102F51). Six weeks after transformation nodules were harvested, cut in 100 µm sections (see 2.8) and stained with GUS staining solution [100 mM sodium phosphate (pH 7.0), 10 mM EDTA, 3 mM $K_4[Fe_2(CN)_6]$ (II), 0.1% Triton X-100, 0.5 mM $K_3[Fe_2(CN)_6]$ (III), 2 mM x-Gluc in DMSO] for 30 min or two hours at 37°C. Subsequently, the thin sections were observed with a SteREO Discovery V.20 stereomicroscope (Carl Zeiss, Jena, Germany). Images were taken with an AxioCam HRC digital camera (Carl Zeiss).

2.7 Localization of Ca^{2+} -ATPases

For localization, the candidate proteins were fused to Enhanced Green Fluorescent Protein (EGFP). To this end, four fragments (CsVMV promoter, gene-of-interest, EGFP (without stop codon), and nos terminator) were amplified by PCR and inserted into the USER-compatible vector pCAMBIA2300u (kindly provided by Hassam H. Nour-Eldin, Department of Plants and Environmental Sciences, University of Copenhagen, DK) in one step. The PCR was performed with 0.02 Units PhusionU Hot Start DNA Polymerase (F-555, ThermoFisher Scientific) and 1 x Phusion HF Buffer (F-518, Thermo Fisher Scientific) in a total volume of 50µL. As DNA template for the CsVMV promoter the plasmid pILTAB (kindly provided by Debora Samac, USDA Agricultural Research Service, Minnesota, USA) was used. For the USER reaction 100 ng vector were mixed with 60 ng of each fragment in 5x HF buffer and USER enzyme mix.

2. Materials and Methods

The USER reaction was performed at 37°C for 30 min followed by 60 min at 25°C. The resulting constructs were sequenced (Microsynth, primers listed in Tab. A16) and transformed into *A. rhizogenes* (see 2.5.2) and subsequently into *M. truncatula* (Jemalong A17, see 2.5.3). As positive control plants were transformed with pCAMBIA2300u containing CsVMV-EGFP-nos. Three weeks after transformation plant roots were inoculated with *S. meliloti* (2011) labeled with mRFP. Three weeks later nodules were harvested and sectioned in 100 µm sections. Thin sections of nodules and isolated symbiosomes were investigated with a Zeiss LSM 880 META confocal laser-scanning microscope (Carl Zeiss). Samples were excited with an argon laser (excitation wavelength of 488 nm for GFP and 512 nm for mRFP). To distinguish the EGFP signal from autofluorescence of nodules, untransformed nodules were analyzed by using the same settings. The untransformed nodules emitted light at a wavelength of 520-600 nm with a maximum intensity at 560 nm. The EGFP signal was detected using a band pass filter with 505-530 nm to exclude detection of autofluorescence.

2.8 Preparation of thin sections of nodules

Root nodules were embedded in 3% (w/v) low-melting agarose (840101, Biozym, Hessisch Oldendorf, Germany), stored at 4°C for 2 h, and subsequently cut with a Hyrax V 50 vibrating microtome (Carl Zeiss). The following settings were used: frequency 30, trim 100, amp 1.2 and V 32.

2.9 Isolation of symbiosomes

Nodules were pestled in ice-cold extraction buffer [250 mM mannitol, 0.1% glycerol, 10 mM EGTA (pH 7.0), 10 mM MgSO₄, 5 mM DTT, 1% BSA, 1% PVP-40, 2 mM ascorbate, and 25 mM HEPES (pH 7.0)] and centrifuged (10 sec) in a Minispin centrifuge. The supernatant was filtered through pre-rinsed Miracloth (Calbiochem, Darmstadt, Germany) and centrifuged for 10 minutes in a swing-out rotor (Eppendorf 5804 G) at 200 *g* and 4°C. The pellet was resuspended in extraction buffer, transferred to a Percoll step gradient (30%, 60%, 80%) and centrifuged at 1,000 *g* and 4°C for 30 minutes. Symbiosomes accumulated in the interface between the 60% and 80% Percoll layers.

2. Materials and Methods

2.10 Yeast complementation assay

The autoinhibitory domain of ACAs was truncated by amplifying the CDS using a forward primer binding downstream the CaMBS2 motif (Tidow et al., 2012). For *MA4* and *MA5* the full-length CDS was amplified (primers listed in Tab. A15). The CDS of the candidate genes was cloned into the vector pFL61 (Minet et al., 1992) modified for USER cloning compatibility. The constructs were transformed into yeast strains K601 (WT) and K616 (*MAT α pmr1::HIS3 pmc1::TRP1 cnb1::LEU2*, Cunningham and Fink (1994)) as described in 2.5.6. For the complementation assay, the yeast strains were grown in SC medium lacking uracil at 30°C and 180 rpm in a shaking incubator (Certomat SI, Sartorius). For the mutant, 10 mM CaCl₂ was added to the medium. When log phase was reached, the yeast strains were washed with sterile ultrapure water and dropped onto SC medium containing 10 mM EGTA in a tenfold dilution series starting with a concentration of 1×10^7 cells mL⁻¹. Yeast cells were counted with a Neubauer-Improved counting chamber. As control, yeast strains were dropped onto SC medium containing 10 mM CaCl₂. Subsequently, the yeast strains were incubated for three days at 30°C.

2.11 Detection of calcium signals in roots and nodules

2.11.1 Measurements using aequorin

A. rhizogenes cells were transformed with the plasmid pGPTVhyg-pUBQ10-Aeq. These were used to transform *M. truncatula* plants. For nodulation, plants were transferred to N-free Fahraeus medium and inoculated with *S. meliloti* (102F51) one week after transfer. Three weeks later plant roots were sprayed with coelenterazine solution (10 μ M coelenterazine, 0.01% Tween20). Plants were stored overnight at room temperature in darkness. The next morning plants were investigated with a photon-counting camera (HRPCS-4, Photek, St. Leonards-on-Sea, UK) equipped with a Peltier temperature controller (PTC5.0, Photek). Aequorin luminescence was triggered by 0.5 M NaCl and cold stimuli. Therefore, the Peltier plate was cooled down to 0°C.

2. Materials and Methods

2.11.2 Measurements using R-GECO

CsVMV promoter, R-GECO, and nos terminator were amplified using primers creating linkers between the amplicons (Tab. A18) and inserted into pCAMBIA2300u in a one-step USER cloning reaction. *A. rhizogenes* and *M. truncatula* were transformed as described above (2.5.2 and 2.5.3). Plants were inoculated with *S. meliloti* (102F51) three weeks after transformation. Three to four weeks later nodules were harvested and observed with an Axio Observer Z1 microscope. Samples were investigated using the filter set FS31 (Carl Zeiss) with an excitation band pass filter 565/30 nm and an emission band pass filter 620/60 nm. For excitation aHXP120 lamp (Carl Zeiss) was used. Pictures were taken with an AxioCam MRm camera (Carl Zeiss).

2.12 Stable and transient mutations for the functional characterization of candidate genes

M. truncatula mutant lines of the *MA4* gene (NF11817_high 4 and NF4429-Insertion-3), obtained from Noble Research Institute (Ardmore, Oklahoma, USA), were screened by PCR using gDNA and primers (F_AAAAAACCCGGGATGTCTAATAATCATAATCTACAATATGATGG and R_AAAAAACCCGGGTGCAAAGCATTCTTAATCTTGAAG) used previously for cloning the CDS of *MA4*.

For the generation of mutants by CRISPR/Cas9, sgRNAs were designed using CRISPR-P v2.0 (<http://crispr.hzau.edu.cn/CRISPR2/>) and custom-synthesized. Sequences without off targets (sgRNA1) and with off targets in introns or intergenic regions (sgRNA2) were chosen (Tab. A17). For hybridization, the oligonucleotides (100 μ M) were mixed, diluted to a concentration of 10 μ M, heated to 98°C for 5 min and slowly cooled down at RT. Finally, they were diluted with ultrapure water to a final concentration of 50 fmol μ L⁻¹. Hybridized sgRNAs were cloned into the shuttle vectors pUC-M1E, pUC-M1, and pUC-M2E (Tab. 5) in one step. To this end, 60 ng vector was mixed with 50 fmol sgRNA, BsiI/BbsI, 10x ligation buffer, T4 DNA Ligase (1 U μ L⁻¹), and 10x BSA (1 mgmL⁻¹). The mixture was incubated at 37°C for 2 min and 16°C for 5 min (15 cycles), followed by an incubation for 10 min at 50°C and 10 min at 80°C. This cloning step linked the sgRNA with the AtU6 promoter and a scaffold placed between two BsaI restriction sites for the ligation into the recipient vector. This was pursued by mixing 320 ng of the recipient vector with 40 ng sgRNA TU shuttle vectors, 10x ligation

2. Materials and Methods

buffer, 10x BSA (1mgmL⁻¹), Bsal, and T4 DNA Ligase (1-5 U μL⁻¹). The mixture was incubated at 37°C for 2 min and 16°C for 5 min (15 cycles), followed by an incubation at 50°C for 10 min and 80°C for 10 min. The recipient vector contained Cas9-, GFP-, and GUS-encoding genes. The vectors used for CRISPR/Cas9 were designed and kindly provided by Johannes Stuttmann (Institut für Biologie, MLU Halle-Wittenberg).

Tab. 5 Shuttle vectors for CRISPR/Cas9

shuttle vectors	Insertion
pUC M1	Bsal-TTGC-link-pAtU6-ATTG-Bpil_ccdB-Cm ^R _Bpil-GTTT-sgRNA scaff.-CCCT-Bsal
pUC M1E	Bsal-TTGC-link-pAtU6-ATTG-Bpil_ccdB-Cm ^R _Bpil-GTTT-sgRNA scaff.-GCTT-Bsal
pUC M2E	Bsal-CCCT-pAtU6-ATTG-Bpil_ccdB-Cm ^R _Bpil-GTTT-sgRNA scaff.-GCTT-Bsal

2.13 Calcium fertilization experiments with *Vicia faba*

To investigate the practically relevant question if Ca²⁺ supply has an effect on N₂ fixation, *V. faba*, which is, in contrast to *M. truncatula*, relevant for practical farming, was used. As the cultivation of this crop was not established in the laboratory, different systems of plant cultivation were tested.

2.12.1 Experiment with quartz sand

V. faba (Taifun) seeds were surface-sterilized with bleach (5% NaClO, 0,02% Triton X100) and imbibed in 1 mM CaSO₄ solution over night. The soaked seeds were transferred to quartz sand moistened with 1 mM CaSO₄ for two days. Subsequently, the plantlets were grown in pots containing 1.35 kg quartz sand supplied with nutrient solution (10 mM MgSO₄*7H₂O, 14 mM KH₂PO₄, 14 mM K₂SO₄, 4.2 mM NH₄NO₃, 3.4 μM MnCl₂*4H₂O, 17.2 μM H₃BO₃, 0.3 μM ZnSO₄*7H₂O, 0.4 μM CuSO₄*5H₂O, 0.03 μM (NH₄)₆Mo₇O₂₄*4H₂O and 0.5 mM Fe-EDTA) to a water holding capacity of 60%. Ca²⁺ was added as CaCl₂*2H₂O in three different amounts (15, 35, and 75 mM). Two days after transfer plants were inoculated with 5 mL of *R. leguminosarum* (6044) suspension (OD₆₀₀=1) per plant. The pots were irrigated daily with ultrapure water to maintain the water holding capacity of 60% at a constant level.

2. Materials and Methods

2.12.2 Experiment with soil/vermiculite mixture

V. faba (Fuego) seeds were imbibed in 1 mM CaSO₄ solution for 16 h and sown in pots containing 800 g soil (Einheitserde ED73)/vermiculite (2:1) mixed with 3.4 or 6.8 g CaSO₄. For control pots no CaSO₄ was added. Plants were inoculated with 5 mL of *R. leguminosarum* (6044) suspension (OD₆₀₀ = 0.4) directly on the seed and were grown for five weeks under greenhouse conditions. Nine days after sowing plants were thinned to two plants per pot. Pots were irrigated every third day with deionised water.

2.12.3 Experiments with hydroponic culture

Four experiments were performed with plants growing in hydroponic culture. For the first experiment, seeds of *V. faba* (Fuego) were surface-sterilized with bleach and imbibed in 1 mM CaSO₄ solution as described above. The soaked seeds were germinated in filter paper rolls moistened with 2 mM CaSO₄ solution for eight days. Subsequently, they were transferred to an aerated hydroponic solution (4.5 L), the composition is listed in Tab. 4. During the first three days the nutrient solution was half-concentrated. The plants were inoculated with 1 mL of *R. leguminosarum* (6044) suspension (OD₆₀₀=1) per vessel containing five plants. One day later the nutrient solution was replaced by N-free, full-concentrated nutrient solution, which was renewed twice a week. The pH was manually adjusted with KOH to 6.5. In later experiments the 4.5L vessels were replaced by 50L vessels and the pH was adjusted using a titrator. After nodules were visible, the nutrient solution contained 1 or 10 mM CaSO₄.

2.12.4 Mineral element analyses

The plants were separated into shoots (leaves and petioles), roots, and nodules and milled to a fine powder. For the estimation of Ca²⁺ the plant powder was digested by nitric acid and hydrogen peroxide (2:1) for 20 min at 180°C using a MARS 5 Xpress (CEM, Kamp-Lintfort, Germany) microwave oven. Subsequently, the Ca²⁺ concentration of the diluted solution was measured by ICP-AES using an Ultima 2 instrument (Horiba Scientific, Tenyamachi, Japan).

2. Materials and Methods

The N concentration of the plant powder was estimated by a C/N analyser (Elementar, Langenselbold, Germany).

2.12.5 Chlorophyll measurements

The relative chlorophyll content was measured using a SPAD meter (Konica Minolta). The lowest pinna of the youngest pinnate leaf was measured in six biological replications.

3. Results

3. Results

3.1 Calcium measurements in nodules of *Medicago truncatula*

3.1.1 Measurements of changes in $[Ca^{2+}]_{cyt}$ using aequorin

For detection of changes in $[Ca^{2+}]_{cyt}$ in root and nodule cells upon stimulation, *M. truncatula* root systems were transiently transformed with *APOAEQUORIN* and investigated using a photon-counting camera. Although transformed plants were selected by hygromycin, some roots of the root system remained untransformed, as apparent from absent luminescence. To identify the transformed roots of a root system, plants were treated with a cold shock. After a recovering period of 2 h, the plants were treated with 500 mM NaCl (Fig.10).

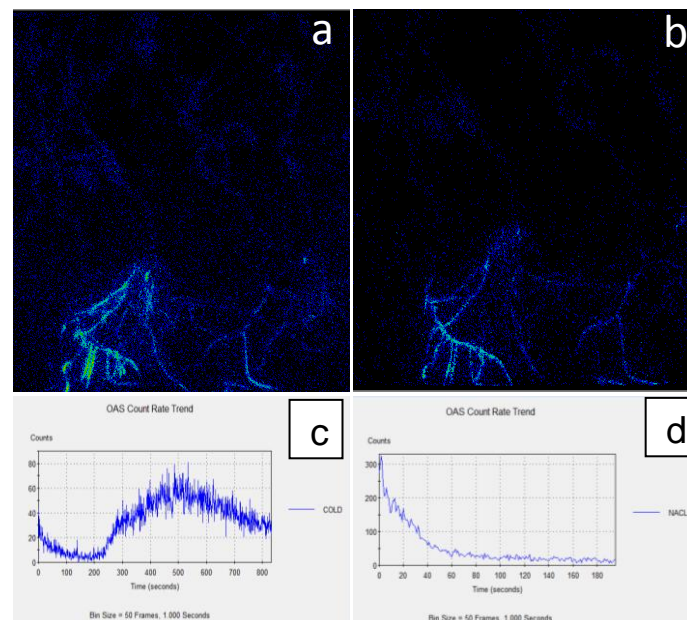


Fig. 10 Detection of $[Ca^{2+}]_{cyt}$ in *M. truncatula* roots transformed with *APOAEQUORIN*.

(a) Five-week-old plants were treated with cold stress by decreasing the temperature to 0°C. (b) After recovering from cold treatment, 500 mM NaCl was applied to the root system. (c) and (d) Rate of counted photons released by aequorin in (a) and (b), respectively.

This first test showed that the transformation of the plants was successful and that the selection of transformed roots by triggering a cold-induced Ca^{2+} signal does not impair the Ca^{2+} signal of a second stimulus. However, the photon signal was weak compared to signals previously measured in *A. thaliana* (T. Peiter-Volk, personal communication). While in roots a weak signal was detectable, the signal was absent in nodules (Fig. 11). For that reason, this approach was discontinued.

3. Results

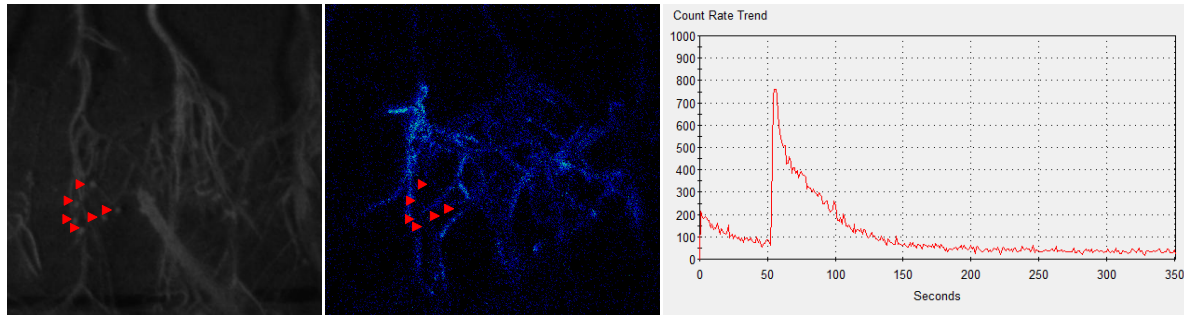


Fig. 11 Detection of $[Ca^{2+}]_{cyt}$ in nodulated roots of *M. truncatula* plants transformed with *APOAEQUORIN*.

Five-week-old plants were treated with 0.5 M NaCl. Nodules are highlighted with red arrowheads.

3.1.2 Measurements of changes in $[Ca^{2+}]_{cyt}$ using R-GECO

Besides aequorin, a further Ca^{2+} sensor (R-GECO) was tested to measure changes of $[Ca^{2+}]_{cyt}$ in nodules. R-GECO is a genetically encoded Ca^{2+} indicator containing a red-fluorescent protein fused to CaM as sensor domain. Fluorescence increases if Ca^{2+} binds to CaM. Nodules of *M. truncatula* plants transformed with *R-GECO* were investigated by fluorescence microscopy. Unfortunately, it was not possible to detect the fluorescence signal of R-GECO because autofluorescence of nodules was very strong.

3.2 The inventory of putatively Ca^{2+} -permeable proteins of *Medicago truncatula*

BLAST searches using amino acid sequences of Ca^{2+} -permeable transport proteins of *A. thaliana* revealed 22 CNGCs, 16 GLRs, 1 TPC1, 10 ANN, 12 CAXs, 3 BICATs, and 20 Ca^{2+} -ATPases, which are listed in Table 6.

3. Results

Tab. 6 Putative Ca²⁺-permeable channels, transporters, and pumps of *Medicago truncatula*

Ion channels

CNGC	GLR	TPC1	ANN
Medtr1g028370	Medtr2g015260.1	Medtr2g090380.1	Medtr3g018780
Medtr1g064240	Medtr2g015270.1		Medtr3g018790
Medtr2g081110	Medtr2g015280.1		Medtr3g018920
Medtr2g094810	Medtr2g015290.1		Medtr5g063670
Medtr2g094860	Medtr2g015310.1		Medtr8g038150
Medtr2g460590	Medtr2g088430.1		Medtr8g038170
Medtr3g088875	Medtr2g088450.18		Medtr8g038180
Medtr3g091080	Medtr3g105595.1		Medtr8g038210
Medtr3g109030	Medtr3g105610.1		Medtr8g038220
Medtr4g058730	Medtr3g115910.1		Medtr8g107640
Medtr4g130820	Medtr4g087925.1		
Medtr5g007630	Medtr5g024350.2		
Medtr6g075290	Medtr5g059900.1		
Medtr6g075410	Medtr5g059920.3		
Medtr6g075440	Medtr8g073210.1		
Medtr6g075460	Medtr8g073490.1		
Medtr6g477760			
Medtr7g012260			
Medtr7g034605			
Medtr7g117310			
Medtr8g027755			
Medtr8g464570			

3. Results

Transporters

Pumps

CAX	BICAT	ATPase
Medtr2g078240	Medtr1g046730.1	Medtr2g038310
Medtr2g078350	Medtr5g009810.1	Medtr2g105690
Medtr2g105640	Medtr7g079850.1	Medtr3g103070
Medtr3g082180		Medtr3g103270
Medtr4g016720		Medtr4g008170
Medtr5g070330		Medtr4g008650
Medtr6g027570		Medtr4g014480
Medtr6g027580		Medtr4g043690
Medtr7g068380		Medtr4g096990
Medtr7g113730		Medtr5g015590
Medtr8g021180		Medtr5g097270
Medtr8g033030		Medtr6g016470
		Medtr7g095710
		Medtr7g100110
		Medtr8g027160
		Medtr8g045070
		Medtr8g089870
		Medtr8g090125
		Medtr8g013780
		Medtr8g013810

The phylogenetic relationship between putative Ca²⁺ transport proteins of *A. thaliana* and *M. truncatula* was investigated by the creation of phylogenetic trees. These were examined for subgroups specific for *M. truncatula*. One such subgroup was found within the GLR family (Fig. 12), while this was not the case for the other gene families. The phylogenetic tree for putative Ca²⁺-ATPases is displayed in Fig. 13 those of the other families are shown in the appendix (Figs. A46 to A49).

3. Results

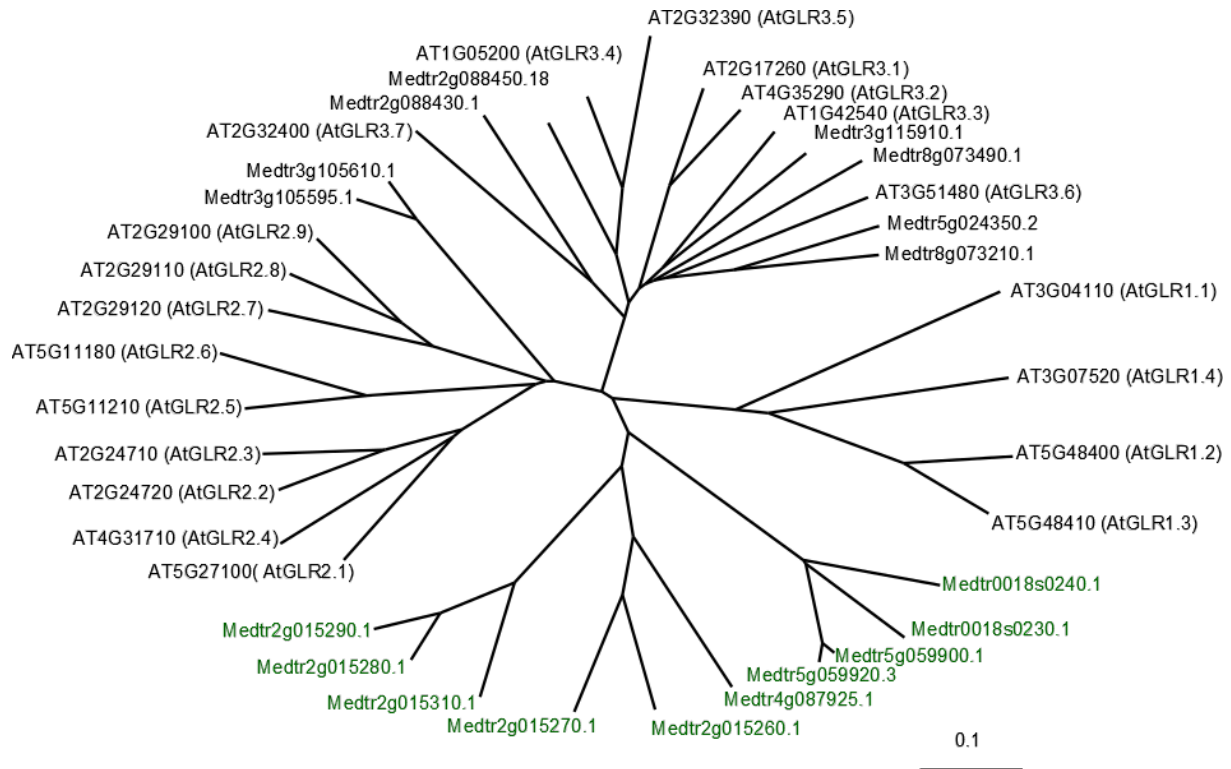


Fig. 12 Phylogenetic tree of GLRs.

Unrooted tree of GLR proteins of *A. thaliana* (AT) and *M. truncatula* (Medtr). The *M. truncatula*-specific group of GLRs is highlighted in green. In this tree also scaffolds (Medtr0018s0240 and Medtr0018s0230) are integrated.

To investigate which of these genes are expressed nodule-specifically, the results of several expression studies based on Affymetrix microarrays or RNA-seq data and different databases (Genevestigator, eFPBrowser (JCVI)) were used. Surprisingly, none of the genes encoding putatively Ca^{2+} -permeable transport proteins showed a nodule-specific expression. Heat maps for the expression of the members of each gene family are shown in the appendix (Fig. A50 to A55) and in the following section for genes encoding Ca^{2+} -ATPases.

3.3 Investigation of putative Ca^{2+} -ATPases of *Medicago truncatula*

3.3.1 *In silico* analysis of genes encoding putative Ca^{2+} -ATPases

According to the gene expression studies, more than half of the identified genes are expressed in nodules and may have an impact on the regulation of N_2 fixation. A screening of mutant lines for the characterization of all those genes was not feasible in this project due to time and cost reasons. Therefore, it was focused on a protein family predicted to regulate $[\text{Ca}^{2+}]$ in the symbiosome space. As mentioned above, the elevation of the Ca^{2+}

3. Results

concentration in the symbiosome space triggers the inhibition of an ammonium channel. The Ca^{2+} concentration in the symbiosome space may be raised by the action of Ca^{2+} -ATPases, which transport Ca^{2+} against the concentration gradient from the cytosol into the symbiosome space. As this may trigger the inhibition of the ammonium channel, Ca^{2+} -ATPases were chosen for further investigation. As mentioned above, *M. truncatula* contains 20 putative Ca^{2+} -ATPase genes that often, but not always, have close homologs in *A. thaliana* (Fig. 13).

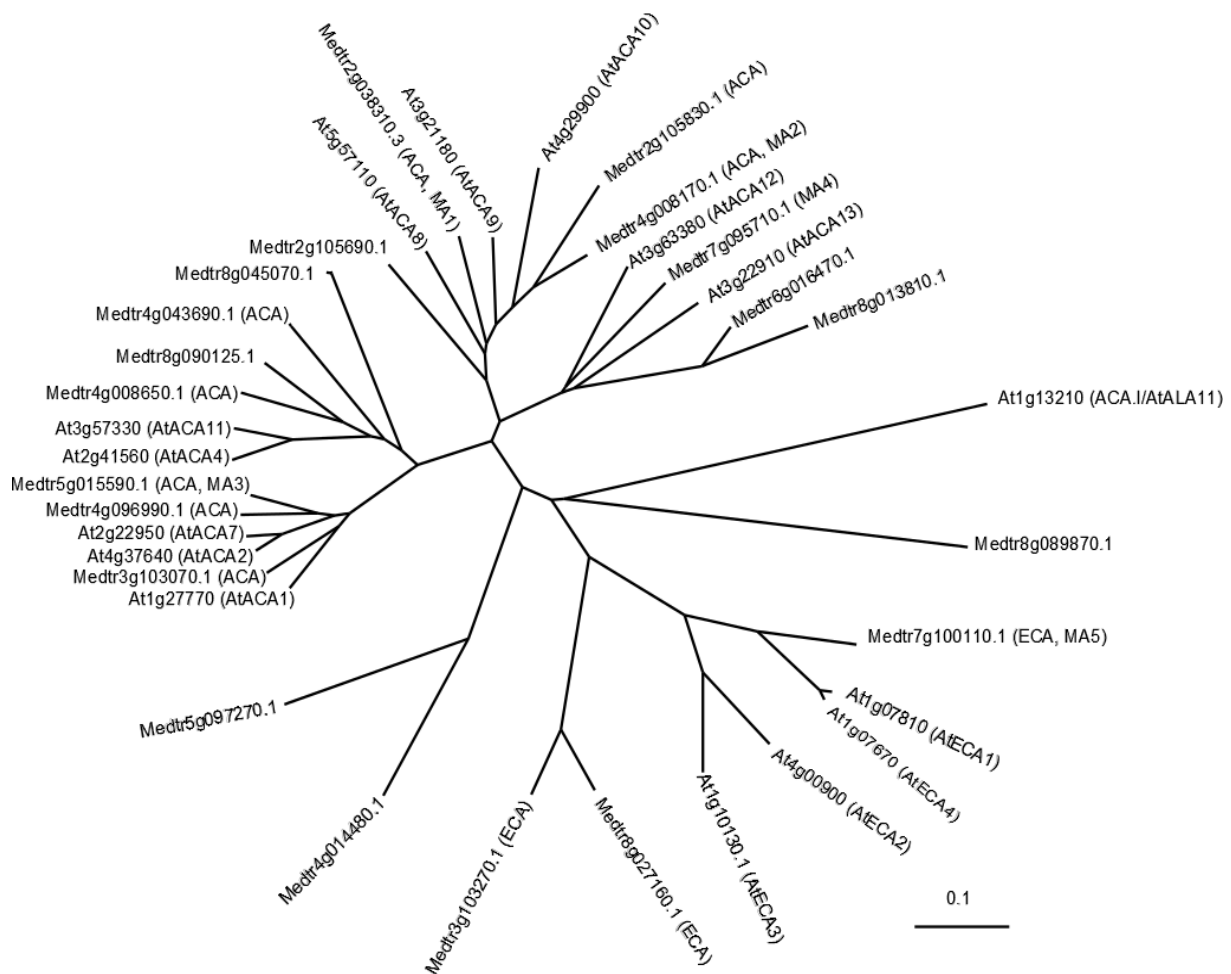


Fig. 13 Phylogenetic tree of Ca^{2+} -ATPases in *A. thaliana* (At) and *M. truncatula* (Medtr).

(ECA) Proteins annotated as SERCA ATPase by JCVI. (ACA) Proteins containing calmodulin-binding sites. (MA1-MA5) Proteins investigated in this thesis. Proteins without abbreviation in brackets are annotated as calcium-transporting ATPase by JCVI, but do not contain calmodulin-binding sites.

The expression of genes encoding the putative Ca^{2+} -ATPases represented on the Affymetrix Medicago GeneChip is shown as heat map in Fig. 14 and as diagram in Fig. 15. The heat map was created using Genevestigator, which combines the data of different gene

3. Results

expression studies and shows the gene expression in different plant organs and tissues. Interestingly, no gene is expressed specifically in nodules.

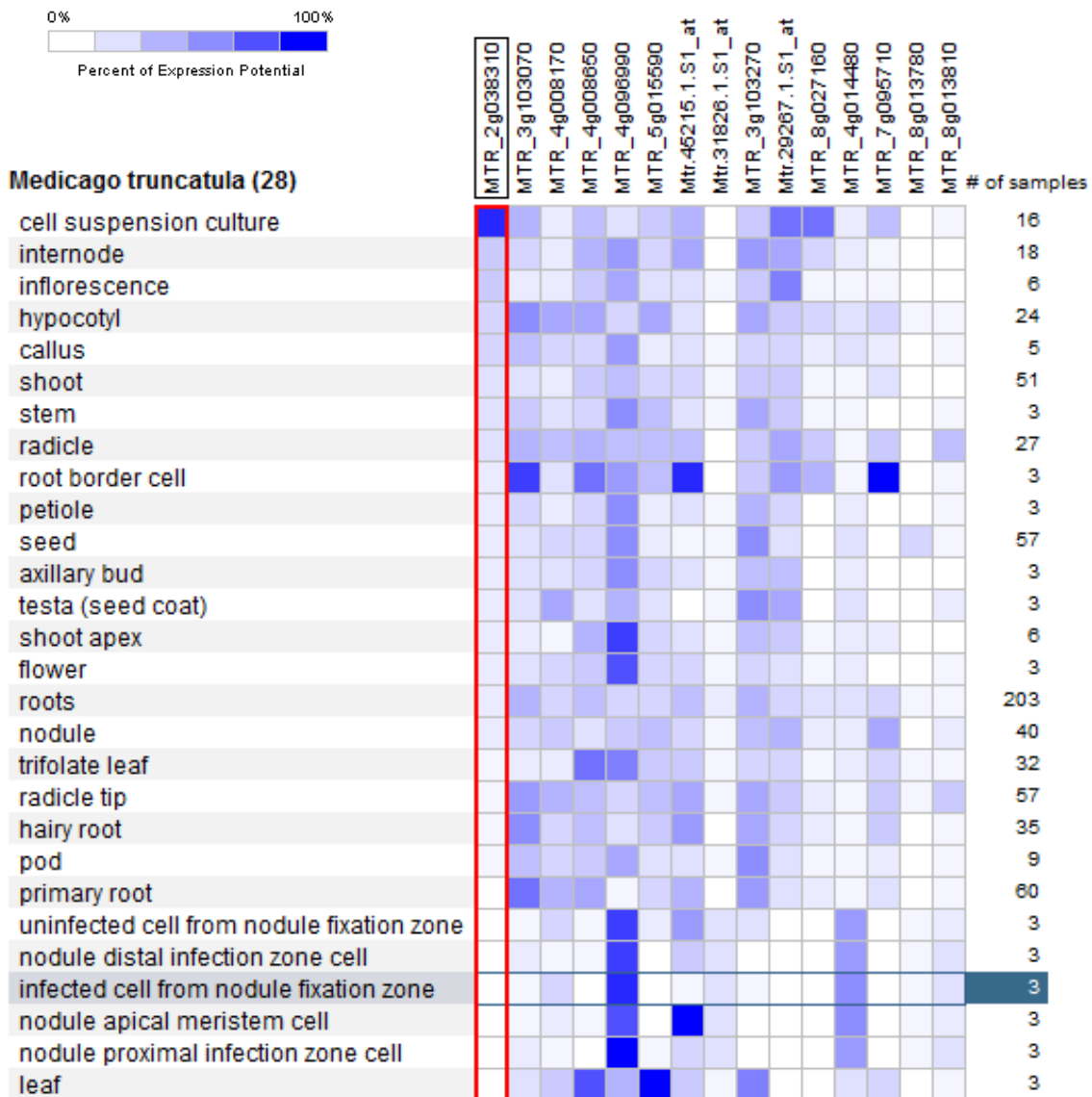


Fig. 14 Expression of genes encoding putative Ca²⁺-ATPases present on the Affymetrix GeneChip. The relative expression strength is indicated by blue color intensity. Data of different gene expression studies are summarized. (Mtr.45215.1.S1_at = Medtr8g090120, Medtr8g090125; Mtr.29267.1.S1_at = Medtr7g100110). The heat map was created using Genevestigator.

The diagram in Fig. 15 shows the expression data compiled by Limpens et al.(2013) which are available at the Gene Expression Omnibus (GEO) of NCBI (<https://www.ncbi.nlm.nih.gov/geo/>). Surprisingly, the signal values of Affymetrix probe

3. Results

numbers representing one gene differ strongly (Medtr2g038310, Medtr4g008170, Medtr5g015590 and Medtr7g100110).

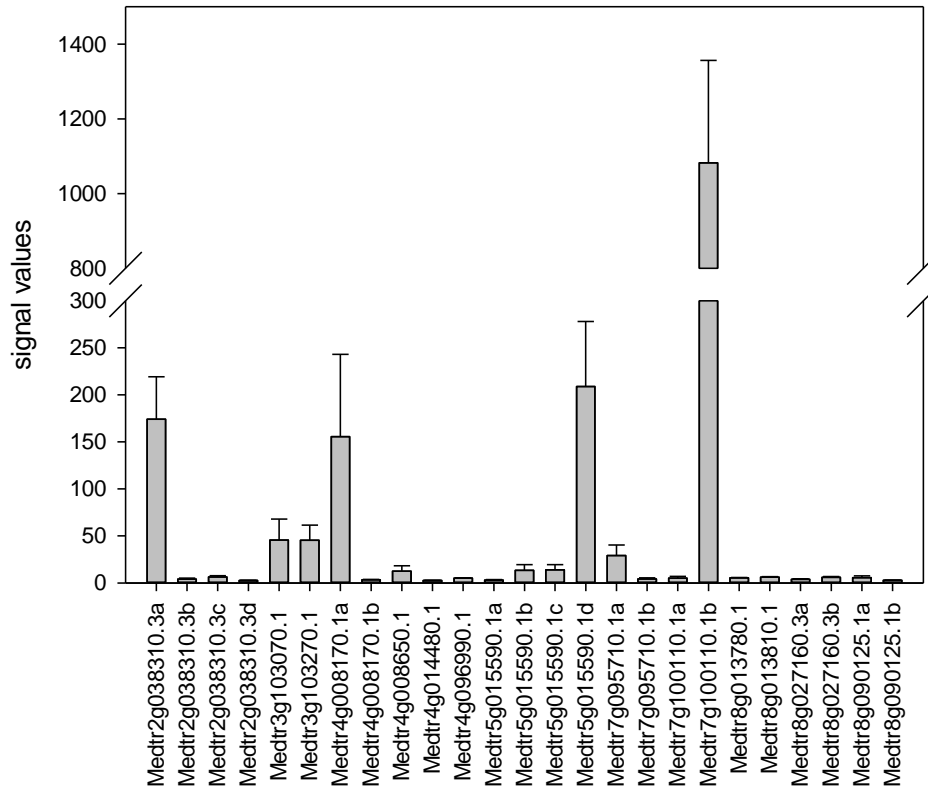


Fig. 15 Expression of genes encoding putative Ca^{2+} -ATPases in the infected cells of the N_2 fixation zone.

Genes represented by various Affymetrix probes are labeled with letters (Medtr2g038310a = Mtr.8909.1.S1_at, Medtr2g038310b = Mtr.30887.1.S1_s_at, Medtr2g038310c = Mtr.31084.1.S1_at, Medtr2g038310d = Mtr.4152.1.S1_at, Medtr4g008170.1a = Mtr.43923.1.S1_at, Medtr4g008170.1b = Mtr.8275.1.S1_at, Medtr5g015590.1a = Mtr.2046.1.S1_at, Medtr5g015590.1b = Mtr.21285.1.S1_at, Medtr5g015590.1c = Mtr.48837.1.S1_s_at, Medtr5g015590.1d = Mtr.40540.1.S1_at, Medtr7g095710.1a = Mtr.44516.1.S1_at, Medtr7g095710.1b = Mtr.13570.1.S1_at, Medtr7g100110.1a = Mtr.29267.1.S1_at, Medtr7g100110.1b = Mtr.40647.1.S1_at, Medtr8g027160.3a = Mtr.3073.1.S1_s_at, Medtr8g027160.3b = Mtr.42399.1.S1_at, Medtr8g090125.1a = Mtr.45215.1.S1_at, Medtr8g090125.1b = Mtr.4942.1.S1_at). Data from Limpens et al. (2013).

The heat map shown in Fig. 16 displays the expression of those genes in three individual samples of infected cells of the N_2 fixation zone. These three samples are repetitions of one experiment performed by Limpens et al. (2013). Especially for Medtr4g008170 the expression varies strongly in the replicate samples.

3. Results

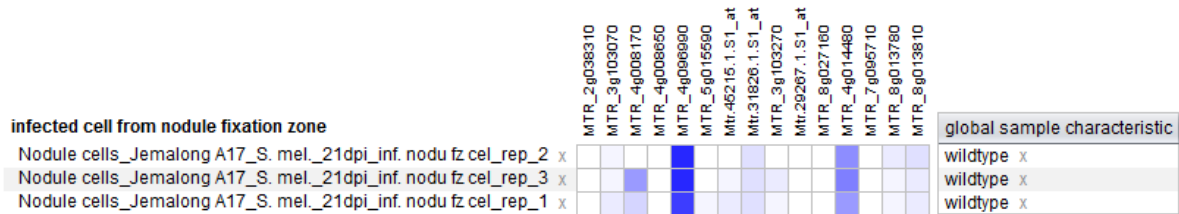


Fig. 16 Expression of genes encoding putative Ca^{2+} -ATPases in infected cells of the N_2 -fixation zone.

The data are three replicates of a study by Limpens et al.(2013). The heat map was created using Genevestigator. (Mtr.45215.1.S1_at = Medtr8g090120, Medtr8g090125;Mtr.29267.1.S1_at= Medtr7g100110). Color code is the same as in Fig. 14.

In Fig. 17 the expression of the Ca^{2+} -ATPase-encoding genes is shown as a scatterplot with log2 scaling, in which the expression level is marked as low, medium, or high. The scatter plot was created using Genevestigator and includes the data of five expression studies in which the gene expression in nodules was investigated (Benedito et al., 2008; Heath et al., 2012; Limpens et al., 2013; Seabra et al., 2012; Sinharoy et al., 2013). The expression level of almost every Ca^{2+} - ATPase-encoding gene is medium or high in nodules (Fig. 17).

3. Results

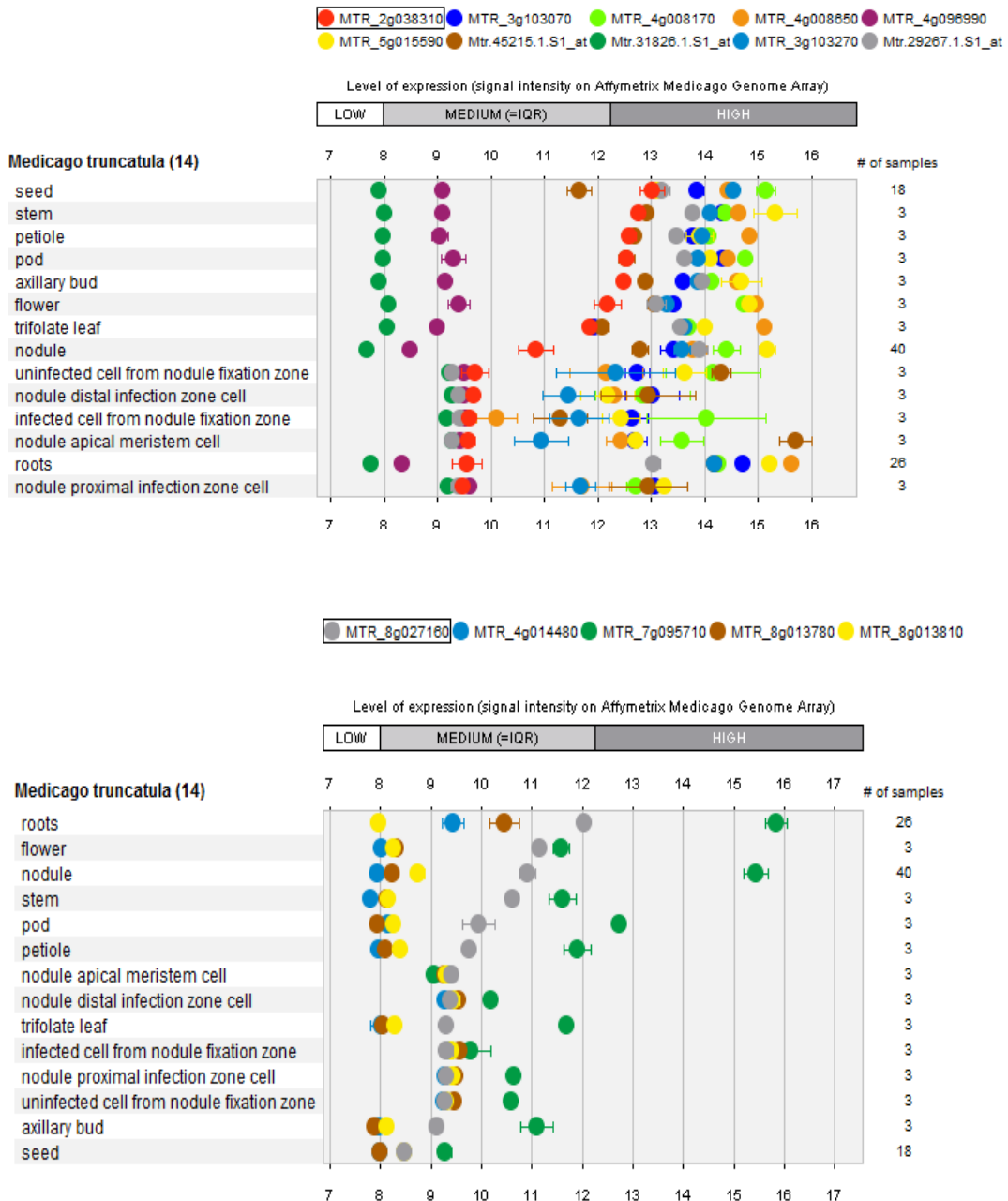


Fig. 17 Scatterplot of expression of genes encoding putative Ca^{2+} -ATPases present on the Affymetrix GeneChip.

Absolute expression level of the genes is differentiated in low, medium and high. The scatterplot was generated using Genevestigator. (Mtr.45215.1.S1_at = Medtr8g090120, Medtr8g090125; Mtr.29267.1.S1_at = Medtr7g100110).

According to RNA-seq data prepared by Roux et al.(2014) nearly all genes encoding putative Ca^{2+} -ATPases are expressed in nodules. Sixteen of those genes are expressed in the nitrogen fixation zone (Fig. 18). Compared to the other genes, Medtr4g008170 and Medtr7g095710 show the highest proportion of reads in this zone.

3. Results

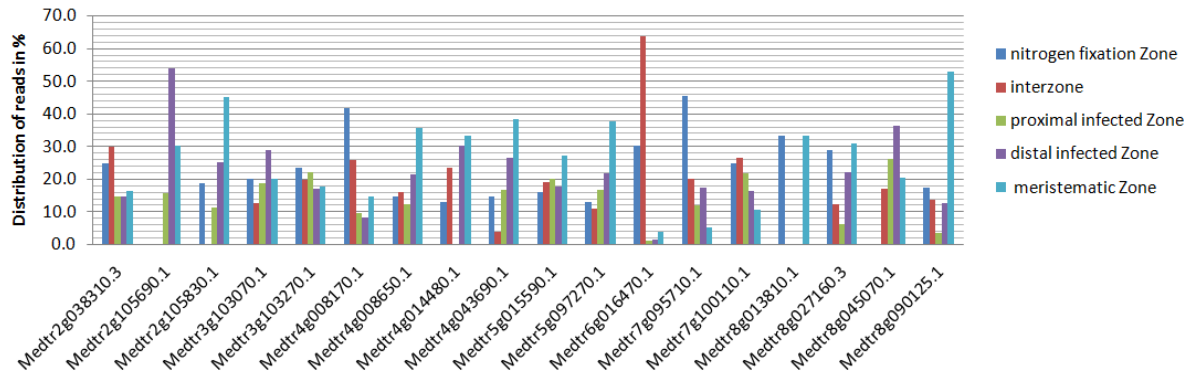


Fig. 18 Expression of genes encoding putative Ca^{2+} -ATPases based on RNA-seq data.

The distribution of reads over the nodule zones is shown. The data set was generated by Roux et al. (2014).

Amongst the putative Ca^{2+} -ATPases expressed in infected cells of the nodule, those localized in the symbiosome membrane were of particular interest, as discussed above. A proteomic analysis previously identified three putative Ca^{2+} -ATPases of *Glycine max* (Glyma09g06890, Glyma03g33240 and Glyma19g35960) with this localization (Clarke et al., 2015). Therefore, a BLAST search with amino acid sequences of those proteins was performed. With an identity of 88.7%, Medtr2g038310 is the closest homologue to Glyma09g06890. The putative Ca^{2+} -ATPase with the gene number Medtr7g100110.1 is the protein with the highest identity to Glyma03g33240 (88.3%) and Glyma19g35960 (88.8%). All proteins identified in this BLAST search with an E-value of 0.0 are listed in Tab.7.

3. Results

Tab. 7 Putative *M. truncatula* Ca²⁺-ATPases with high homology to those localized in the symbiosome membrane of *G. max*

Gm Ca ²⁺ -ATPases	Mt Ca ²⁺ -ATPases	Identity (%)	E-value
Glyma09g06890	Medtr2g038310.3	88.74	0.0
	Medtr2g038310.2	88.74	0.0
	Medtr2g038310.1	88.74	0.0
	Medtr2g038310.4	88.79	0.0
	Medtr4g008170.2	73.14	0.0
	Medtr2g105830.1	70.82	0.0
	Medtr6g016470.1	56.33	0.0
	Medtr7g095710.1	56.01	0.0
	Medtr4g008650.1	48.77	0.0
	Medtr8g090125.1	48.94	0.0
	Medtr3g103070.1	48.77	0.0
	Medtr4g096990.1	48.62	0.0
	Medtr5g015590.2	48.03	0.0
	Medtr5g015590.1	48.03	0.0
	Medtr4g043690.1	46.82	0.0
	Medtr3g103070.2	51.45	0.0
	Medtr5g015590.5	48.45	0.0
	Medtr5g015590.3	48.45	0.0
Glyma03g33240	Medtr7g100110.1	88.37	0.0
	Medtr8g027160.3	66.57	0.0
	Medtr8g027160.2	66.90	0.0
	Medtr8g027160.4	64.19	0.0
	Medtr8g027160.1	64.06	0.0
	Medtr3g103270.1	46.43	0.0
Glyma19g35960	Medtr7g100110.1	88.84	0.0
	Medtr8g027160.3	66.57	0.0
	Medtr8g027160.2	66.90	0.0
	Medtr8g027160.4	64.17	0.0
	Medtr8g027160.1	64.04	0.0
	Medtr3g103270.1	45.99	0.0

The putative Ca²⁺-ATPases of *M. truncatula* with homology to *G. max* proteins localized in the symbiosome membrane were further examined for the presence of a nuclear localization signal (NLS). This *in silico* analysis was performed using the cNLS mapper (nls-mapper.iab.keio.ac.jp/cgi-bin/NLS-Mapper_y.cgi). NLS were predicted for the genes Medtr2g015270.1, Medtr4g014480.1, and Medtr5g024350.2 (Fig. 19). Those were not analysed further.

3. Results

A	B	C
Predicted NLSs in query sequence	Predicted NLSs in query sequence	Predicted NLSs in query sequence
MEDTRGMHLYLSTFPQALARIWLFVLLVFPFALVYGRDETMSNDKRVIS I 50	MEDTRGMFPESDDGNNIELGATLLTTTRGVCNKKWQLWLYKPTTSRAN 50	MEDTRGMVVKVLLALMLLYNGFSSTVAGTHNSTRPDLVNI GALFSPNTS 50
GVILIDGSRIGKEQEVAMDIAAQSYNNTSRNKLALYFPNSTKDTLKAIK 100	YEESTSPILSSVELRVTNDIAGIVKEDLKSLLLEFGVGRVCDLVRGQIHH 100	GKIKIALRAAVNDVNSDPNII LGETKIKLSLQEDSKYRGLFSAEVLQVM 100
IAEENINPVQVQVILIQMCPQEAAMVAVRGSKQVVIISFVATITPFLM 150	SSARKITRNLSGSSFLMWTYIKDKNCRVSLLLLSALFSLAIGMEEGLK 150	ARHNVAII GPHSSVTHAVITHTANELQVPLISFSAIDPPLSSIQPFPPFIR 150
EAHWFPLRLANQYATYIKLEIEIQAYSRKRVVLYEEDQYGGYKLA 200	YGRHDGVALIAFSVLLMLAFSSITSPFRWRKMMNK RTTRKGRGKVKFNVRKG 200	TCHSDLYQMAALADIVYQWRVIAVTIDDMGRNIGIGALGDLAKRNC 200
LLAEALQVDVSMIEHRLVLPPISSIQDDEIVSEEMKLLKQTSRVFIVL 250	EVSQSDVLDLSASDVIYVGMFELSPHDEVPADGLVSHGILLVLAIKRNE 250	RI SYKAPVRRREATPEEITVNLVQVALAESRVIIVHMTIGGKPVFVAKN 250
KSSLEMAIHVFKASKVGVDKESAMMIPESIANLLSDVNSKSAISYMEGA 300	KVDEDNDNFLLIAGSSEVIACYQMVIVSVWRSEDFRSMNSSHFKKGL 300	LGMIGCVVVIATAFLSALDLESPLSDRDMDEIGVLTARVHPDSELK 300
LGIKTYYSERSREYKFEAQFRRTFMSKNPEEDNRYPGFYALQAYDSINI 350	LEKLEKPII SYLDKASLFIPTLVAFVVEIHQICEKDKDGDGLPMKVSIVG 350	RKFVSKQNLTHGNTDNGPLGSLFSLYAYDTIYALAHALDAFLKQGNQI 350
VTQALNRMTSRNSNPPFTLREILISCNPLGLSGHIQLSEGLMQKMLVLR 400	LMLELLENILLRPRGRISILACVPTAALLFVQHGMPMVFVSLHYHINDV 400	TFPNSKLSLTLRGDNLRLDALNIPDGGNLRRIIYEVNMTGVTGLFKYAP 400
IYVWAKGYSRELCFQWQKQFTTIIHRAQGGQNYVACNTGFRGVRWDRW 450	VPEEAIVNDLSACTTMLGLVTVICVDVSRGLSKPMVEVSEIWMGEGETE 450	DKNLVNPTEYIINNVCTGSRQICVNSHSLSSIIPELTHSKPQNNFRES 450
ARLPRGQMPTEKKNPLAIAVRSRFSRFRVYVYGGGEEDKYTCFIEI 500	CEVEGSETVVLDKLEKGVVLSISPELSLSPRSSALVSWARTKCEMDTNS 500	KRLSPVIVPQNTAQKPRGVVFPNNGRLRIIGVFI GVSYRQFVSQVPTDT 500
FVILVHNLGDLTPSYYPIDGTYNLDLQVLYNRYDAVVGDMFIEERLE 550	FIERFDIFGHKLNLSKGGSGVLVGVVLLHPQVWRVHDIMVVKENVM 550	FQGFCDVFLSAINMLFVAVPKFIPYGGKNNPNTLVRKIITGTEYG 550
TVDFVVPYASGLSMIVMCKPGEAMMPKPFTELEMLVGTALILYTMVL 600	PWEIKRIFVQKILIMEGSGIAPFAFRKRTVLQVLEJDLTLALIGFK 600	AVGDIATITTRTQWDPQYTESLGLVVAIVRETTESALAPLAPTFPM 600
VWLEREINPELSTALWPTFSSELPFAIRAMSHSNTRVVMVSWLFLVL 650	EKRSRISKSLGVQWVGIKIKLISDEDIDLVEEIAVELGIEVVGHLE 650	WFTVALFPIIVGVVWVLEHRVNDVFRGPKKQMTIIPWFSFMPFSHR 650
IYSSYFSLSSMLPVQLRPFVDEIQWJMNKIKICGQDGSVRFLEK 700	GKFKPLDEHAGRFDEVDKAIAMGSCFACEDKLCMVNYIQKGDVVAFIDQR 700	ENTVSTFGRVLLMLVFLVLIITSSYASLTSILVQQLSSPIKIESLV 700
VEKFPENIINIITDEYKNDAFNSNIAAFLLEFVYKRVYKCYKRYT 750	LITRHASEVLKADVIVISLNSLRKMDKSGCGITMTCFSALEPIVKAGR 750	IGKEPIGYTQGSFKNYLQEI GIDESRLALKTPEAAARALEKGGQNG 750
FTPRTRFGGFGMPFGKSDLVKDSKALHLESEKAEKRLKEKWLISSQ 800	RKYHNIQKFIQLQTVSISGLLTLITITPTGNSPLTAIQMIWINVLMCL 800	VAAIIDQRAYIDIFLASRCKFTIVGQPTNRNGVGFPRDSEPLAIDLSTA 800
CSNNTSNETNSLNLGSLWVLYMSGATSTICVLIQTIKWLSNQPHED 850	LGLLMMVMELSREELAKQCDNRQPIITMKIKLNIYVQVLYQAFLEML 850	ILQMVDGDLQRIBHDKWLSRACLQGALEVQRRLKLSFWGLVLCGSA 850
LPFREGNTTSDERVWKAITFAQIYSRKINSSRQVDVDCSSRSRGA 900	QFGGHIHSEKQVRKTIIFNTFLFCQFLNMLNNVYLLKQGLKMIVQNL 900	CLVALLIYFIRIIRQYTKRSEELDSDQNPSSGSGSFKFMSFADEKE 900
SIADYFESHELSLIPDVISIIGVIVYNSRIGREGLAETASQSYMYS 950	FVSALGSCVVMQVLYIQYARGLADCVINFAQWTLVLLVLSALSWVEWIL 950	TVGRSRKRRKMERIISTRGEGSSSIIINRQIDAQSRGIADSVPMGSE 950
KNKLVLYFNSKDTLKAIEAEMINQKQVVIIGMHTWFEAALMED 1000	KSLFVIMHTYATSSFACTELLFAPIMLQKLNRLNLFV 989	QVVFVKV 957
GSKAQVPIISFAAPTITPFIIMNHWFLVRLANNGTYYIKCAIEIVHAYC 1050		
WRKRVVVIC 1058		

Fig. 19 Protein sequences of ATPases containing NLS.

(A) Medtr2g015270.1, (B) Medtr4g014480.1 and (C) Medtr5g024350.2. NLS are highlighted in red.

According to the *in silico* expression analyses, the BLAST results, and the screen for NLS, five putative Ca²⁺-ATPases were chosen for further study (Tab. 8). Except for MtMCA8 (Medtr7g100110), none of these genes has been investigated before. These genes were named with MA abbreviations (Tab. 8), whereby M stands for Medicago and A for ATPase. The annotations proposed by JCVI are also listed in Tab. 8, but since Ca²⁺ transport activity of these ATPases has not been shown yet, this nomenclature is not adopted in this thesis.

Tab. 8 List of candidate genes

Abbreviation	Annotation(JCVI)	Gene number
MA1	MedtrACA1	Medtr2g038310
MA2	MedtrACA4	Medtr4g008170
MA3	MedtrACA8 /MCA5	Medtr5g015590
MA4	MedtrATPase4	Medtr7g095710
MA5	MCA8	Medtr7g100110

MA1 (Medtr2g038310) was chosen as candidate gene due to its high identity to Glyma09g06890. According to Genevestigator it shows a moderate expression in infected cells of the N₂ fixation zone (Fig. 17), and also RNA-seq data show an expression of MA1 in the N₂ fixation zone (Fig. 18). Furthermore, MA1 does not have an NLS. Based on these data MA1 may be located in the symbiosome membrane.

MA2 (Medtr4g008170) show also a high similarity (73%) to Glyma09g06890 and a high expression in the infected cells of the N₂ fixation zone (Fig. 17), albeit the heat map (Fig. 15) shows strong differences between the repetitions. According to RNA-seq data, MA2 is expressed in the N₂ fixation zone (Fig. 18).

3. Results

MA3 (Medtr5g015590) seems to be highly expressed in all zones of the nodule (Fig. 17). RNA-seq data show a homogenous expression through all nodule zones (Fig. 18). The similarity to Glyma09g06890 is only moderate (48%).

MA4 (Medtr7g095710) was chosen as candidate gene due to its expression pattern. According to the RNA-seq data, *MA4* is much more highly expressed in the N₂ fixation zone than in other nodule zones (Fig. 18). Similar to *MA3*, the identity to Glyma09g06890 is only moderate (56%).

MA5 (Medtr7g100110) was shown to be involved in the (peri-)nuclear Ca²⁺ oscillations in root hairs after Nod factor perception (Capoen et al., 2011) and therefore seems to be localized in the nuclear envelope. Despite this, it was chosen as candidate gene in this thesis because of its high similarity to the symbiosome membrane-localized *G. max* Ca²⁺-ATPases Glyma03g33240 (88.4%) and Glyma19g35960 (88.8%). According to the RNA-seq data, *MA5* is expressed in the N₂ fixation zone (Fig. 18).

3.3.2 Transport activity of selected Ca²⁺-ATPases

As mentioned above, four of the five candidate genes are gene predictions. Thus, it was necessary to test if these genes indeed encode Ca²⁺-ATPases. Therefore, a yeast complementation assay was performed. A commonly used yeast strain for the investigation of Ca²⁺-ATPases is the K616 mutant (*MATapmr1::HIS3 pmc1::TRP1 cnb1::LEU2,ura3*), which lacks the Ca²⁺-ATPases Pmr1 and Pmc1, as well as the Calcineurin B subunit Cnb1 (Cunningham and Fink, 1994). The yeast strain was transformed with the vector pFL61 containing the candidate genes. The wild type strain K601 transformed with a pFL61 empty vector served as positive control. For *MA1*, *MA2*, and *MA3* truncated versions were cloned because these genes are predicted to encode autoinhibited Ca²⁺-ATPases (ACAs) which show low or no activity at low Ca²⁺ concentrations (Tidow et al., 2012). In the presence of the Ca²⁺ chelator EGTA these ATPases remain in the autoinhibited state. *MA4* also encodes an ACA, but it has a high phylogenetic similarity to AtACA12, which was shown to be active in the presence of EGTA (Limonta et al., 2014). Therefore, *MA4* was cloned in full length as well as *MA5*, which encodes a non auto inhibited ECA.

The truncated versions of *MA1*, *MA2*, and *MA3* were able to rescue the mutant growing on EGTA-containing medium (Figs. 20, 21, and 22).

3. Results

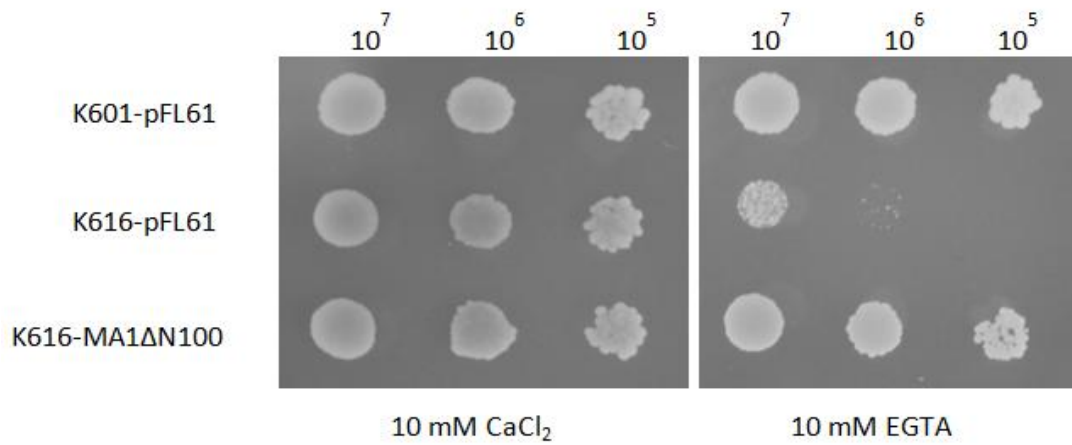


Fig. 20 Complementation of *S. cerevisiae* K616 by *M. truncatula* MA1.

K601 and K616 carry the vector pFL61 (empty vector), K616 contains the pFL61:MA1ΔN100 construct. Yeast strains were diluted as indicated, and 10 μ L aliquots were grown on Ca²⁺-deficient medium containing 10 mM EGTA and medium containing 10 mM Ca²⁺.

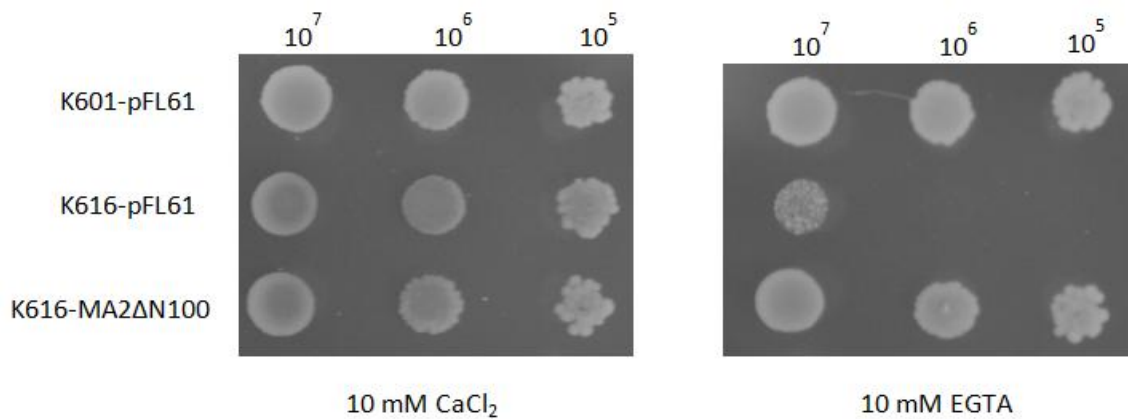


Fig. 21 Complementation of *S. cerevisiae* K616 by *M. truncatula* MA2.

K601 and K616 carry the vector pFL61 (empty vector), K616 contains the pFL61:MA2ΔN100 construct. Yeast strains were diluted as indicated, and 10 μ L aliquots were grown on Ca²⁺-deficient medium containing 10 mM EGTA and medium containing 10 mM Ca²⁺.

3. Results

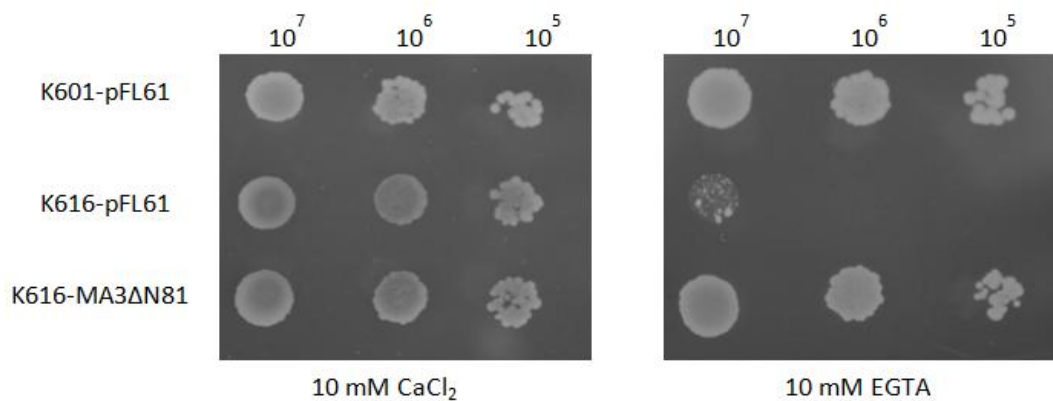


Fig. 22 Complementation of *S. cerevisiae* K616 by *M. truncatula* MA3.

K601 and K616 carry the vector pFL61 (empty vector), K616 contains the pFL61:MA3ΔN81 construct. Yeast strains were diluted as indicated, and 10 μ L aliquots were grown on Ca²⁺-deficient medium containing 10 mM EGTA and medium containing 10 mM Ca²⁺.

The Ca²⁺-ATPase MA4 (full length) also improved the growth of K616 on Ca²⁺-deficient medium, but to a lesser extent, while K616 complemented with MA5 (full length) grew similar to the wild type (Fig. 23).

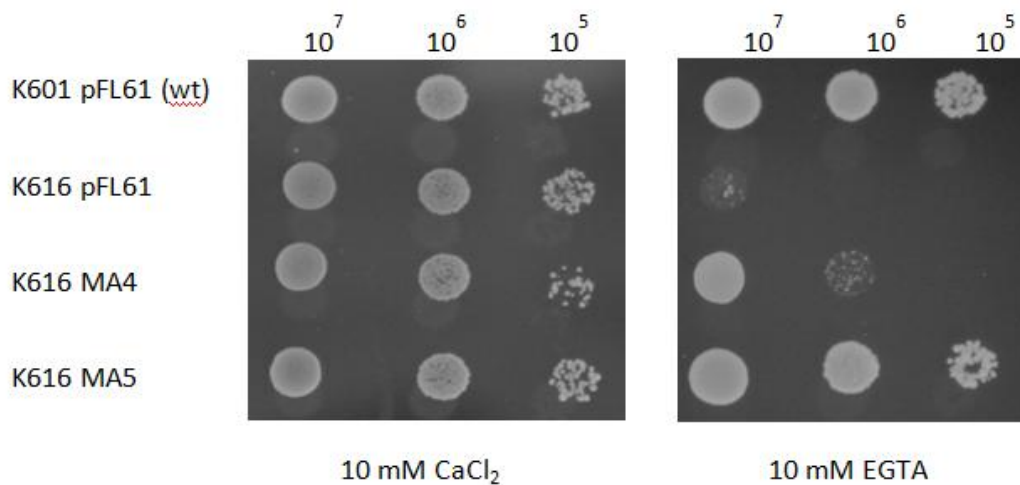


Fig. 23 Complementation of *S. cerevisiae* K616 by *M. truncatula* MA4 and MA5.

K601 and K616 carry the vector pFL61 (empty vector), K616 contains the pFL61:MA4 or pFL61:MA5 constructs. Yeast strains were diluted as indicated, and 10 μ L aliquots were grown on Ca²⁺-deficient medium containing 10 mM EGTA and medium containing 10 mM Ca²⁺.

3. Results

3.3.3 Expression of genes encoding selected Ca²⁺-ATPases

Due to the high variation of the data of the expression studies, the expression of the candidate genes in nodules was examined by RT-PCR. To this end, RNA of three-week-old nodules was extracted and transcribed into cDNA, which was used for the amplification of 100-250 bp of the genes with gene-specific primers by PCR. For each gene bands became visible (Fig. 24).

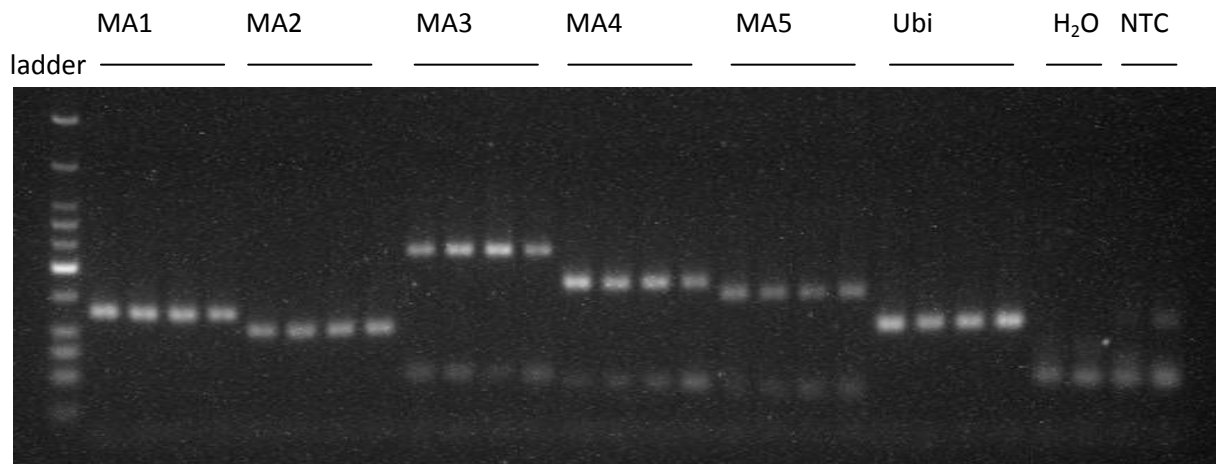


Fig. 24 Analysis of the expression of the selected genes in root nodules.

Gene expression was examined by RT-PCR. As positive control ubiquitin (Ubi) was used, as negative control cDNA was replaced by water (H₂O), and as no-template control (NTC) reverse transcriptase was omitted. For both negative controls ubiquitin primers were used. The size marker (ladder) ranges from 25 to 766 nucleotides. N=4 for MA1-MA5, N=2 for H₂O and NTC.

The promoter activity of the selected genes was investigated by fusing the promoter region (around 3 kb) of each candidate gene to the *uidA* gene encoding β -glucuronidase. Roots and sections of nodules transformed with this construct were incubated in staining solution containing x-Gluc, which is converted into blue-colored 5,5'-dibromo-4,4'-dichloroindigo by the β -glucuronidase. In this way, the expression pattern of the gene becomes visible by blue coloration.

The root system bearing the *ProMA1:uidA* construct shows a blue coloration in the root cap and possibly other cell types of the root apex, as well as in developing lateral roots and nodules (Fig. 25 a-c). In mature nodules only the vascular bundles stained blue, whereas promoter activity was not detectable in the central tissue of the nodule (Fig. 25 d).

3. Results

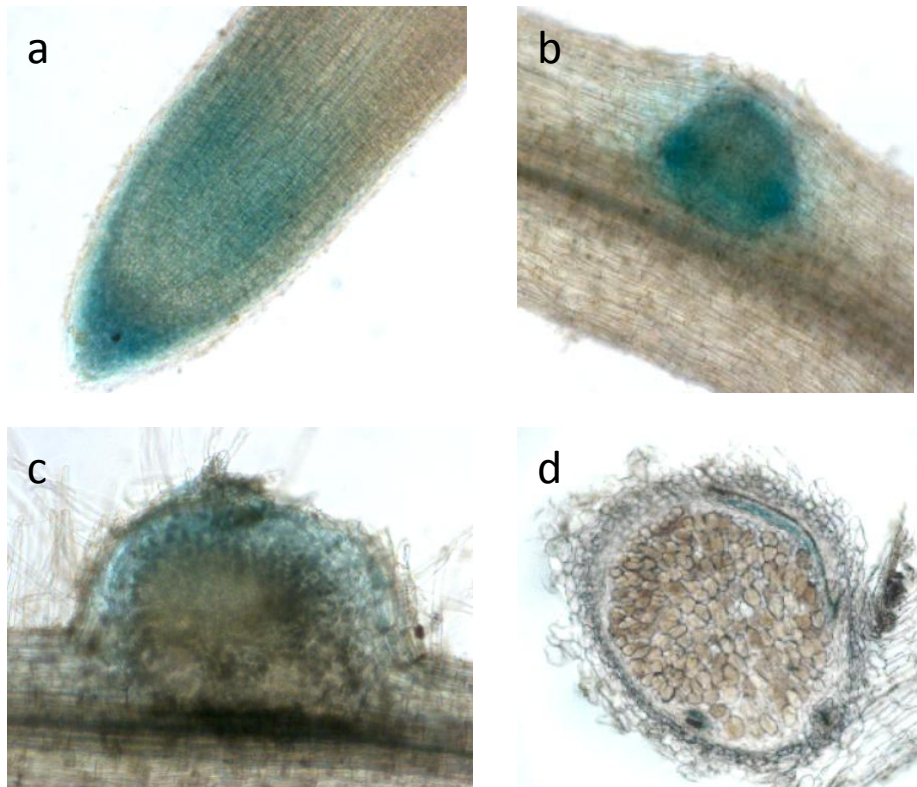


Fig. 25 GUS analysis of MA1 promoter activity.

Blue staining is visible in root tips (a), lateral root initials (b), developing nodules (c), and vascular bundles of mature nodules (d).

After GUS staining, plants transformed with *ProMA2:uidA* show a blue coloration of the elongation zones of the root, uninfected cells of the nodule N₂ fixation zone, and the cortex and vascular bundles of the nodule (Fig. 26).

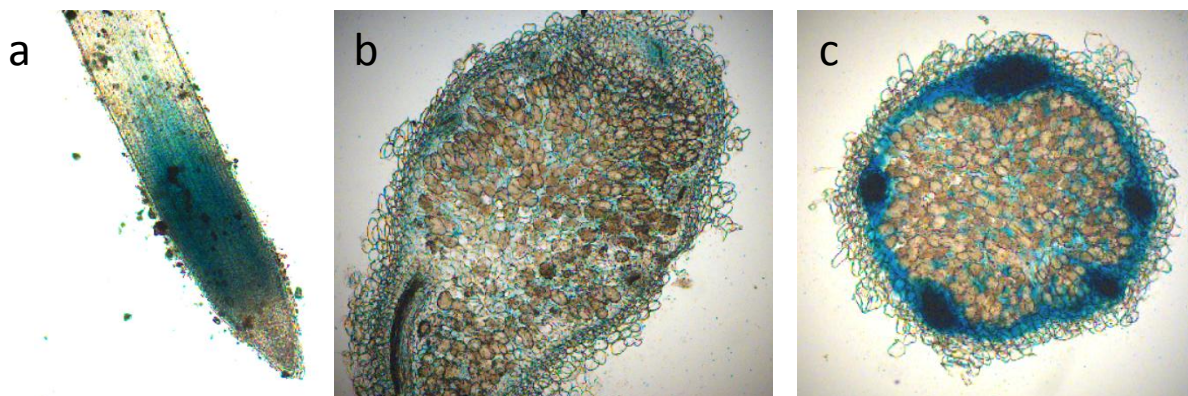


Fig. 26 GUS analysis of MA2 promoter activity.

Blue staining is visible in the elongation zone of roots (a), uninfected cells of the N₂-fixation zone of the nodule (b and c), and the vascular bundles and cortex of the nodule (c).

3. Results

After staining, the vascular bundles of roots and nodules transformed with the *ProMA3:uidA* construct stained blue (Fig. 27 a-c). Blue color was also visible in uninfected cells of the N₂ fixation zone (Fig. 27 d).

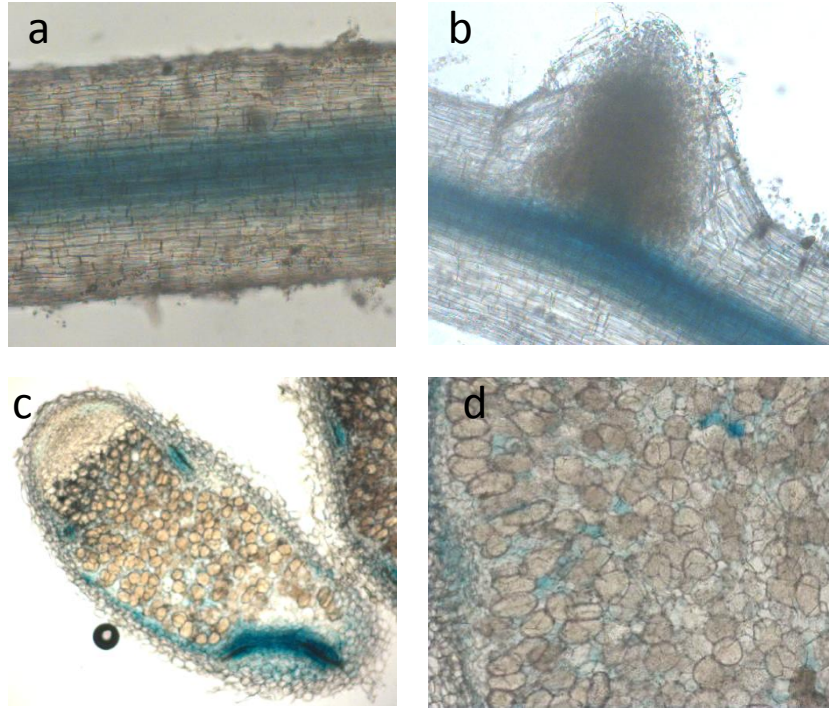


Fig. 27 GUS analysis of MA3 promoter activity.

Blue staining is visible in the vascular bundles of roots (a, b) and nodules (c). Irregular blue color appears in some uninfected cells, interspaced between the infected cells, of the N₂ fixation zone (d).

Nodules transformed with the *ProMA4:uidA* construct showed strong blue coloration in cells of the meristematic zone, the infection zone, and in infected cells of the N₂ fixation zone of the nodule (Fig. 28 b and c). Blue coloration was also visible in developing lateral roots (Fig. 28 a).

3. Results

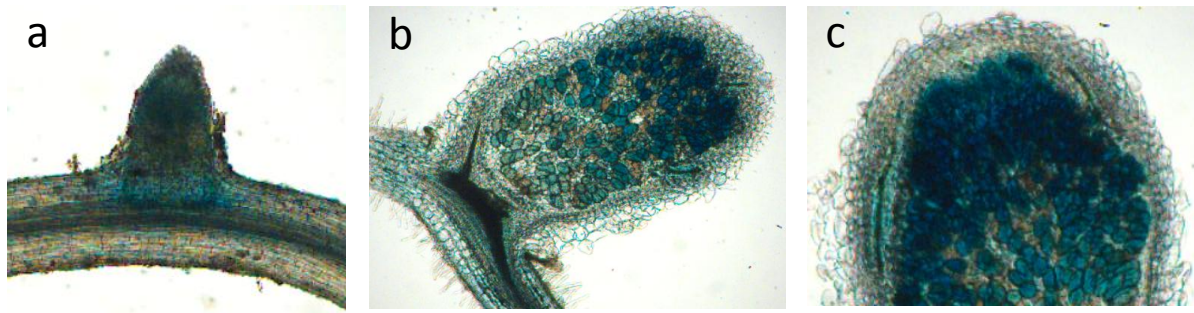


Fig. 28 GUS analysis of MA4 promoter activity.

Developing lateral roots display blue color (a). In nodules blue staining is visible in all tissues, including the meristematic zone, the infection zone, and the N₂ fixation zone (b), where staining is particularly strong in infected cells (c).

For the investigation of MA5 promoter activity three root transformations (à 35 plants) with the *pMA5:uidA* construct were performed according to the standard protocol (2.6). After the first transformation root development was very slow. Nodules were stained 33 dai, but no coloration was visible, neither in nodules nor in roots. Remaining plants, not used for this staining, grew further and were used for another GUS staining at 53 dai. At this time plants were in the generative phase. This time a slight coloration was visible in the infection zone and in the infected cells of the N₂ fixation zone (Fig. 29 c and d). The elongation zone of the root apex and the central cylinder of the root showed an intensive blue coloration (Fig. 29 a and b). After the second transformation the root development was normal and plants were infected 32 days after transformation. Nodules were stained three weeks later, but again no coloration was visible. Remaining plants grew further and underwent another GUS staining four weeks after infection. However, neither roots nor nodules showed GUS activity. Also, no coloration was visible in a further staining performed seven weeks after infection. The root development of plants of the third transformation was also normal, and plants were infected 30 days after transformation. Six weeks after infection, nodules turned completely blue within a few minutes of incubation in the staining solution, even without infiltration and incubation at 37°C (Fig. 29e).

3. Results

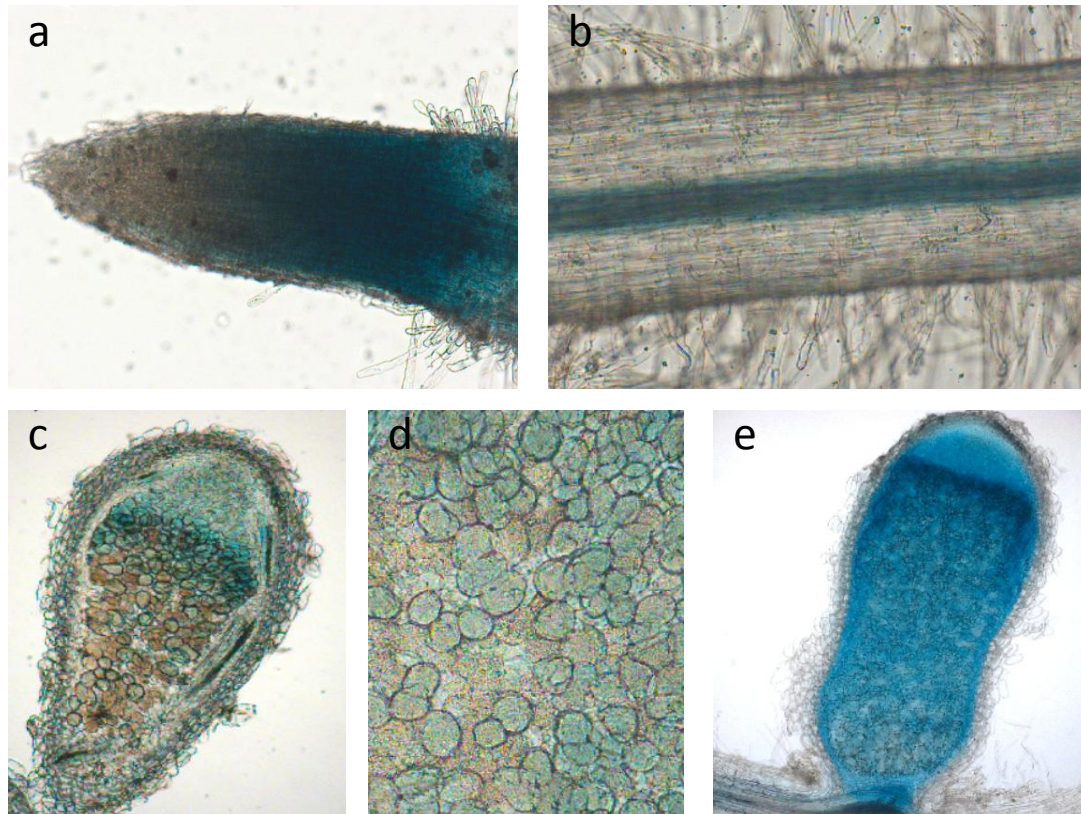


Fig. 29 GUS analysis of MA5 promoter activity.

Blue staining is visible in the root elongation zone (a), the central cylinder of roots (b), nodule infection zone (c), and N₂ fixation zone (d) of mature plants of the first transformation experiment. In vegetative plants of the third transformation experiment, the nodule shows a homogeneous blue staining (e).

3.3.4 Subcellular localization of selected Ca²⁺-ATPases

For subcellular localization, the CDS of the Ca²⁺-ATPases was fused with the gene encoding Enhanced Green Fluorescent Protein (EGFP). Prior to cloning of the CDS of the genes into a vector, the predicted start and stop codons were verified. To this end, the 5' UTR and the first exons as well as the 3'UTR and the last exons were amplified from cDNA and sequenced. To control if the assumed introns and exons were predicted correctly, the sequences were aligned with the predicted sequences. Finally, it was investigated if the amplified sequences contain further ATGs not followed by a stop codon upstream of the predicted start codon. It was also examined if the predicted start codon was followed by a stop codon. All predictions were found to be correct.

3. Results

Furthermore, the predicted localization of the N- and C-termini was investigated using the TMHMM Server 2.0 tool (<http://www.cbs.dtu.dk/services/TMHMM/>). The N-terminus of all Ca²⁺-ATPases is predicted to be localized in the cytosol, while the C-terminus of MA1, MA2, MA4, and MA5 is predicted to lie outside the cytosol (Fig. 30). In case the Ca²⁺-ATPases are localized in the symbiosome membrane, the C-terminus would lie in the acidic symbiosome space. As EGFP is moderately pH-sensitive, it was fused to the N-terminus of the Ca²⁺-ATPases.

3. Results

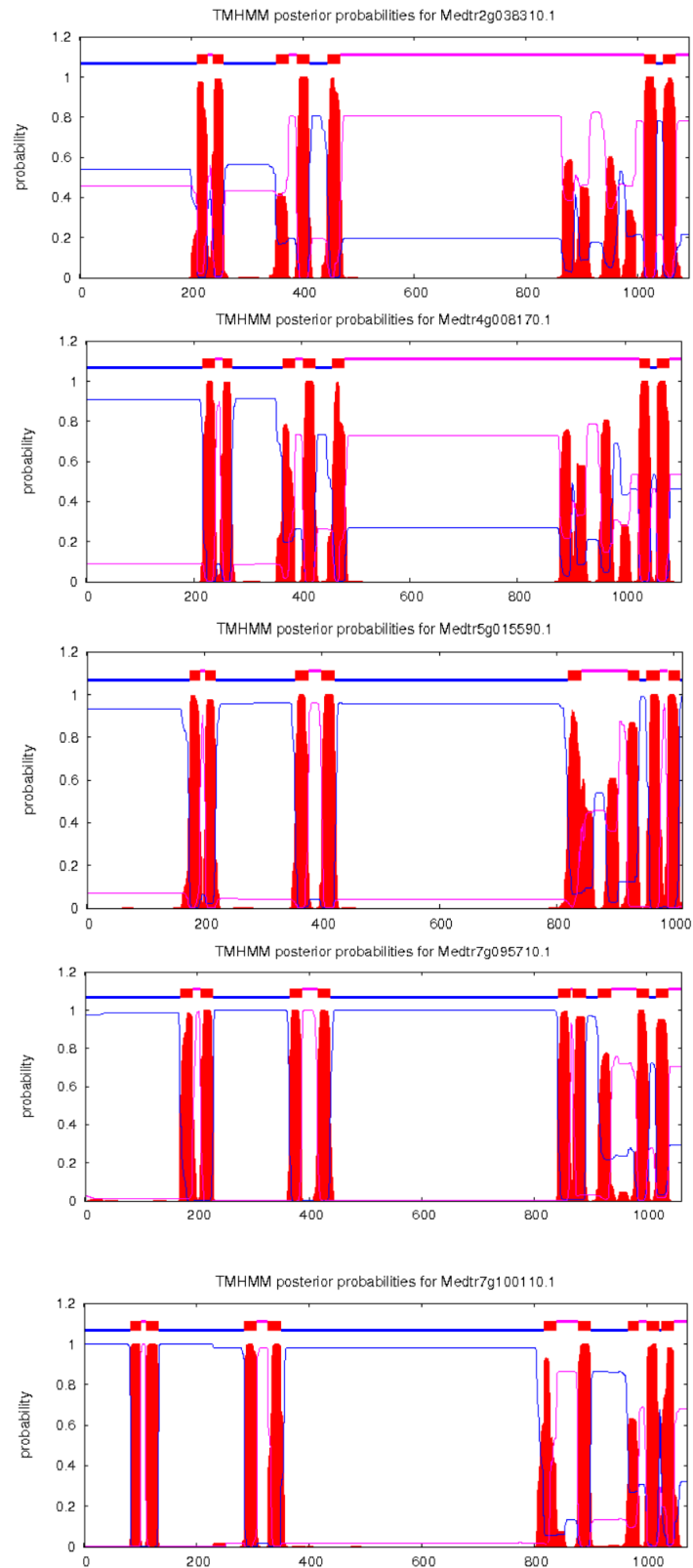


Fig. 30 Predicted topology of the Ca²⁺-ATPases MA1-MA5.

Blue: inside the cytosol, red: transmembrane domain, pink: outside the cytosol. MA1 (Medtr2g038310), MA2 (Medtr4g008170), MA3 (Medtr5g015590), MA4 (Medtr7g095710), and MA5 (Medtr7g100110) are shown starting with the first amino acid (left) to the last amino acid (right) numbered from 1 to >1000.

3. Results

M. truncatula plants were transformed with N-terminal EGFP constructs. Thin sections of nodules and isolated symbiosomes were investigated with a confocal laser-scanning microscope. Nodules transformed with a *EGFP-MA1* construct driven by the constitutive ProCsVMV promoter did not show an EGFP signal in the infected cells. Instead, irregular EGFP signals were detected in uninfected cells (Fig. 31).

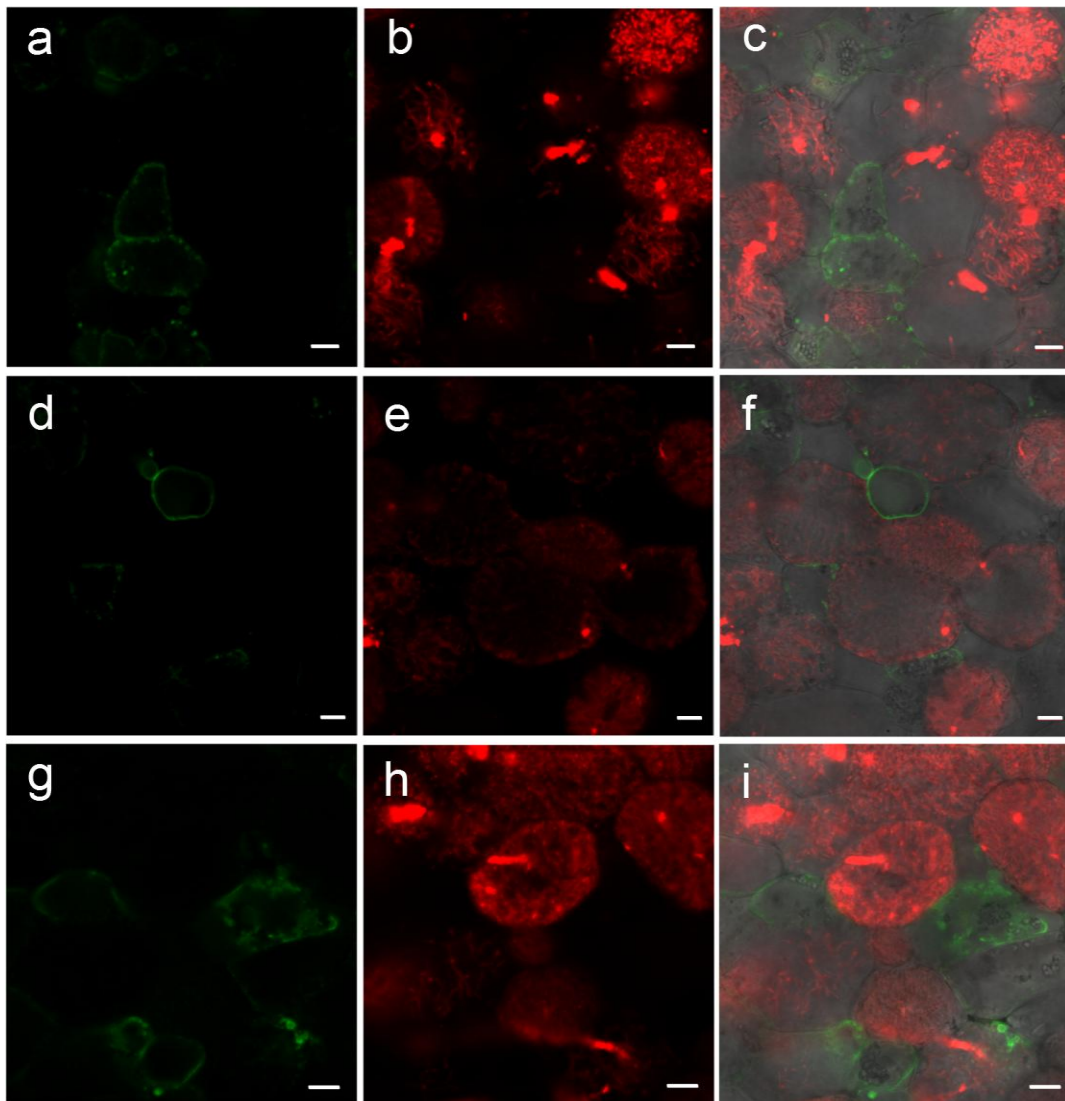


Fig. 31 Confocal microscopic analysis of EGFP-MA1 fusion protein in the N_2 fixation zone of the nodule.

The EGFP signal is present in uninfected cells, but not in infected cells. *S. meliloti* labeled with mRFP indicate infected cells. Pictures show the EGFP signal (a, d, g), the mRFP signal (b, e, h), and merged signals (c, f, i). a-c, d-f, and g-i show sections from three individual nodules. Scale bars 10 μ m.

Nodules expressing the *EGFP-MA2* construct showed an EGFP signal in cortex cells (Fig. 32). Additionally, in some uninfected cells the EGFP signal appeared as small dots.

3. Results

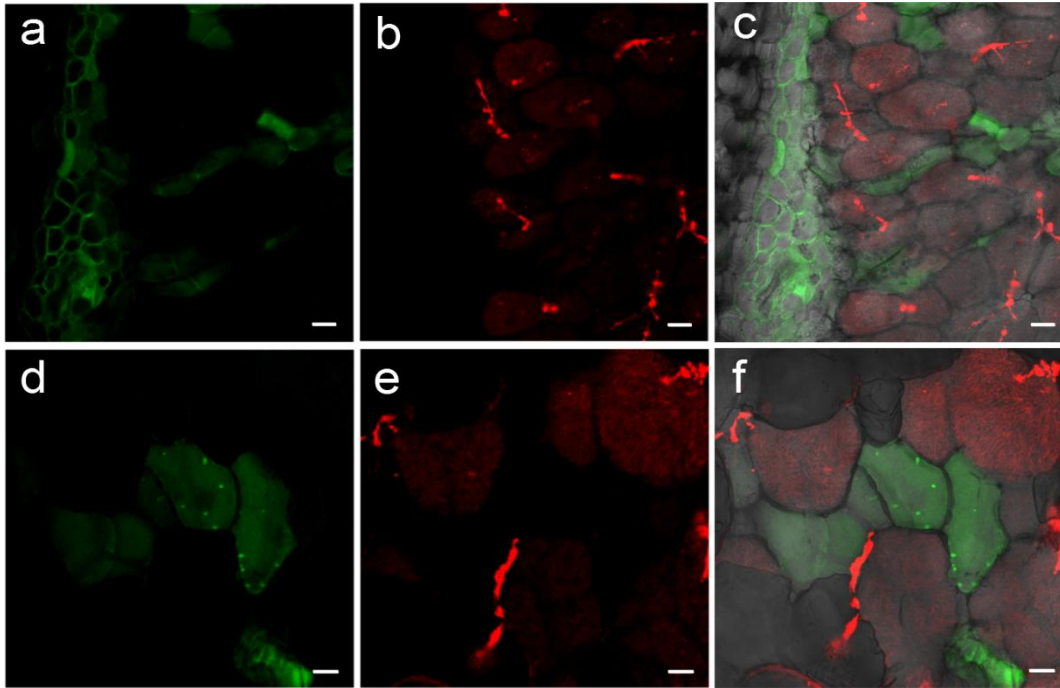


Fig. 32 Confocal microscopic analysis of EGFP-MA2 fusion protein in the nodule.

The EGFP signal is present in cortical cells (a) and uninfected cells (d), but not in infected cells. *S. meliloti* labeled with mRFP indicate infected cells (b, e). Pictures show the EGFP signal (a, d), the mRFP signal (b, e), and merged signals (c, f). a-c and d-f show sections from two individual nodules. Scale bars 20 μm (a-c), 10 μm (d-f).

In contrast to MA1 and MA2, in infected cells of the N_2 fixation zone of nodules transformed with *CsVMV:EGFP-MA3* an EGFP fluorescence was visible (Fig. 33). This signal overlaid perfectly with the mRFP signal of the bacteroids, suggesting that EGFP-MA3 is located in the symbiosome membrane.

3. Results

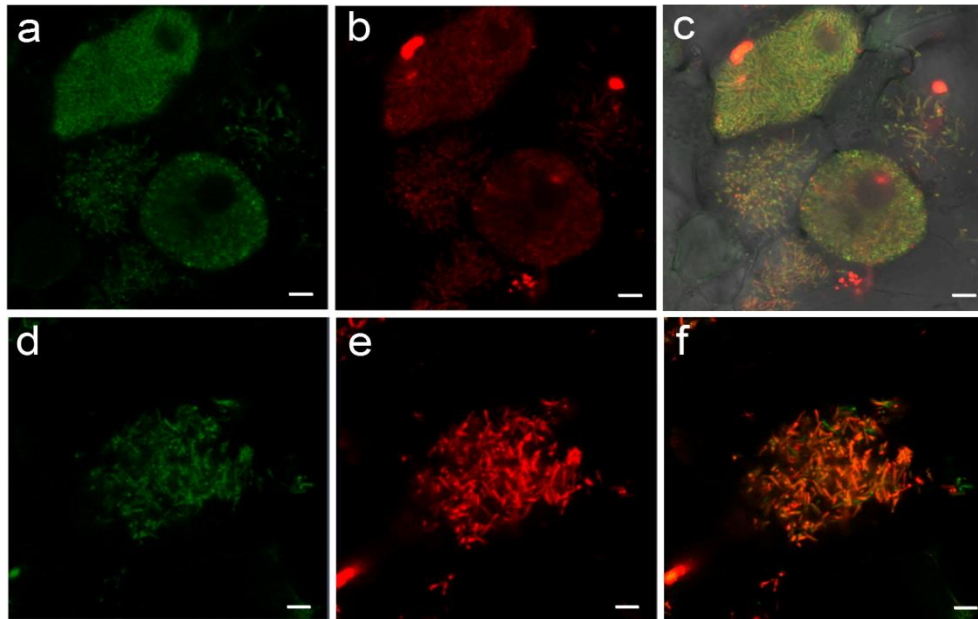


Fig. 33 Confocal microscopic analysis of EGFP-MA3 fusion protein in the N₂ fixation zone of the nodule.

Infected cells of the N₂ fixation zone (a-c) and symbiosomes (d-f) show an overlap of EGFP-MA3 and bacteroid-derived mRFP signals. Pictures show EGFP signal (a, d), mRFP signal (b, e), and merged signals (c, f). Scale bars 10 μ m.

Nodules expressing the *EGFP-MA4* construct also showed an overlap of the EGFP signal and the mRFP signal of the bacteroids (Fig. 34). Furthermore, isolated symbiosomes also show EGFP and mRFP signals, suggesting that also EGFP-MA4 is localized in the symbiosome membrane.

3. Results

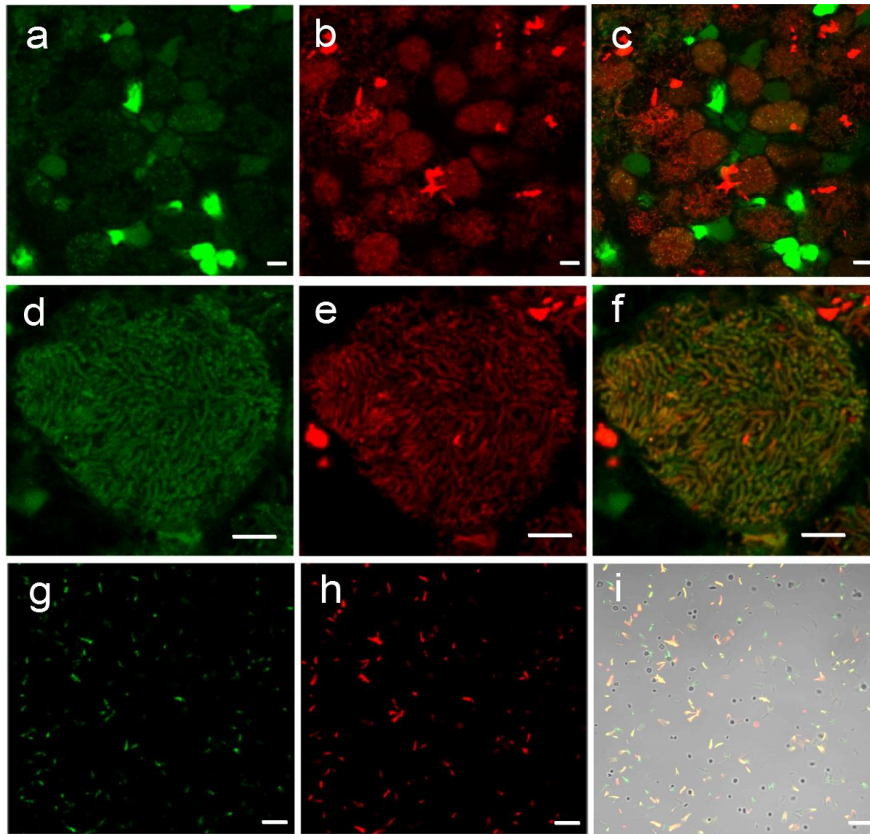


Fig. 34 Confocal microscopic analysis of EGFP-MA4 fusion protein in the N₂ fixation zone of the nodule.

Infected cells of the N₂ fixation zone (a-c, d-f) and isolated symbiosomes (g-i) show an overlap of EGFP-MA4 and bacteroid-derived mRFP signals. Pictures show EGFP signal (a, d, g), mRFP signal (b, e, h), and merged signals (c, f, i). Scale bars 20 μm (a-c and g-i) and 10 μm (d-f).

Roots containing the EGFP-MA5 fusion showed fluorescence in the plasma membrane and the nuclear envelope (Fig. 35 a-c). In nodules EGFP signal was detected in the plasma membrane of uninfected cells and the symbiosome membrane of infected cells in the N₂ fixation zone (Fig. 35 d-f).

3. Results

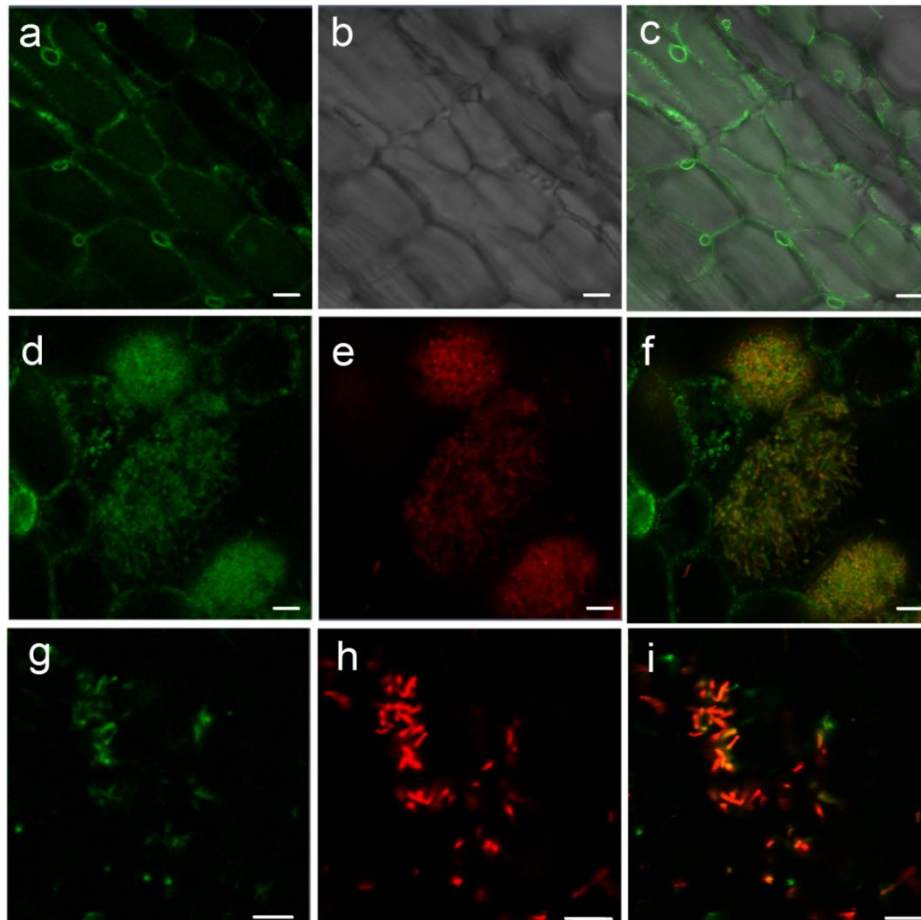


Fig. 35 Confocal microscopic analysis of EGFP-MA5 fusion protein

In root cells (a-c) fluorescence of EGFP-MA5 is present in the plasma membrane and nuclear envelope. In nodules (d-f) EGFP-MA5 signal appears in the plasma membrane of uninfected cells and the symbiosome membrane of infected cells. Isolated symbiosomes (g-i) show an overlap of EGFP-MA5 signal and mRFP signal of *S. meliloti*. Pictures show EGFP signal (a, d, g), mRFP signal (b, e, h), and merged signals (c, f, i). Scale bars 20 μm (a-c), 10 μm (d-i).

3.3.5 Preparations for functional characterization of a candidate gene

According to the GUS analysis of promoter activity and the subcellular localization of the Ca^{2+} -ATPases by EGFP fusion, MA4 was selected as most promising candidate to assess if symbiosome membrane-localized Ca^{2+} -ATPases mediate the inhibition of the ammonium channel and thereby regulate the N_2 fixation. Therefore, two Tnt1 mutant lines (NF11817_high 4 and NF4429-Insertion-3) with insertions in the middle and the end of the CDS, respectively, were ordered from Noble Research Institute. Unfortunately, a PCR screen using gene-specific primers located upstream and downstream of the stated insertion site did not indicate the presence of an insertion in any of the received specimens, as

3. Results

exemplarily shown for some NF4429 plants (Fig. 36). All in all, 21 plants of line NF11817 and 12 plants of line NF4429 were tested.

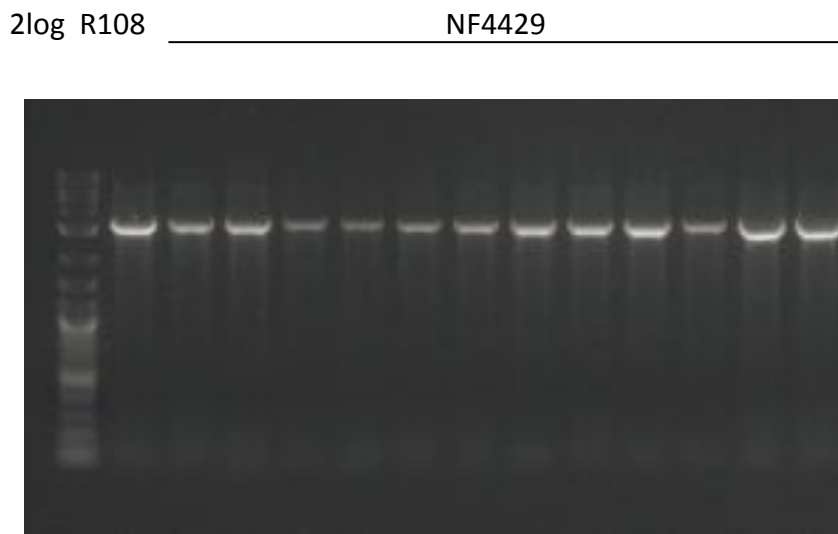


Fig. 36 PCR screen with 12 plants of the NF4429 line.

DNA of the wild type R108 was used as positive control.

Since an insertional knockout mutant was not available, it was decided to generate mutant root systems using a CRISPR/Cas9 approach. The appropriate sgRNAs were designed using CRISPR-P v2.0 and cloned into the shuttle vectors pUC-M1E, pUC-M1 and pUC-M2E, allowing insertion of one or two sgRNAs into the recipient vector. The sgRNAs were inserted between a AtU6 promoter and a scaffold by cloning into the shuttle vectors. The recipient vector contains genes encoding Cas9, GUS, and GFP. For a first test of the recipient vector, a root transformation was performed. It can be assumed that the recipient vector functions in *M. truncatula* because roots turned blue after GUS staining (Fig. 37). Due to the expiration of the project, it was not possible to pursue this approach further. Since in the transient expression system, the Cas9-inflicted mutations will be different in each individual cell, a stable transformation with the CRISPR/Cas9 construct may be more reproducible and effective than the transient root transformation. Furthermore, performing experiments with stably transformed plants would save time because previous root transformation is not necessary, and it may produce more reproducible results because mutant plants are not stressed by root transformation.

3. Results



Fig. 37 *M. truncatula* plants transformed with recipient vector containing *uidA*.

The blue coloration caused by GUS staining shows expression of *uidA* reporter gene and thereby the successful transformation of *M. truncatula* plants with the recipient vector.

3.4 Calcium fertilization experiments with *Vicia faba*

3.4.1 Experiment with quartz sand

The fertilization experiments aimed to assess the effect of elevated Ca^{2+} supply on N provision by symbiotic N_2 fixation. However, with increasing CaCl_2 concentration, plants grown in quartz sand showed necrotic leaves and strongly reduced growth (Fig. 38). Lateral roots also became brown. This approach was not further pursued.



Fig. 38 *Vicia faba* Ca^{2+} fertilization experiment on quartz sand.

Plants were grown in pots filled with quartz sand and supplied with nutrient solution containing 15 mM (left), 35 mM (middle), or 75 mM CaCl_2 (right).

3. Results

3.4.2 Experiment with soil/vermiculite mixture

V. faba plants were grown in a mixture of soil and vermiculite (2:1) under greenhouse conditions for six weeks. While control plants were not Ca^{2+} -fertilized, treated plants were supplied with 3.4 g or 6.8 g CaSO_4 per plant. Plants were harvested six weeks after sowing. At the day of harvest, the chlorophyll content and shoot fresh weight were measured. Compared to control plants, the plants treated with CaSO_4 showed no significant differences with respect to shoot weight, Ca^{2+} concentration, N concentration, and chlorophyll content (Fig. 39).

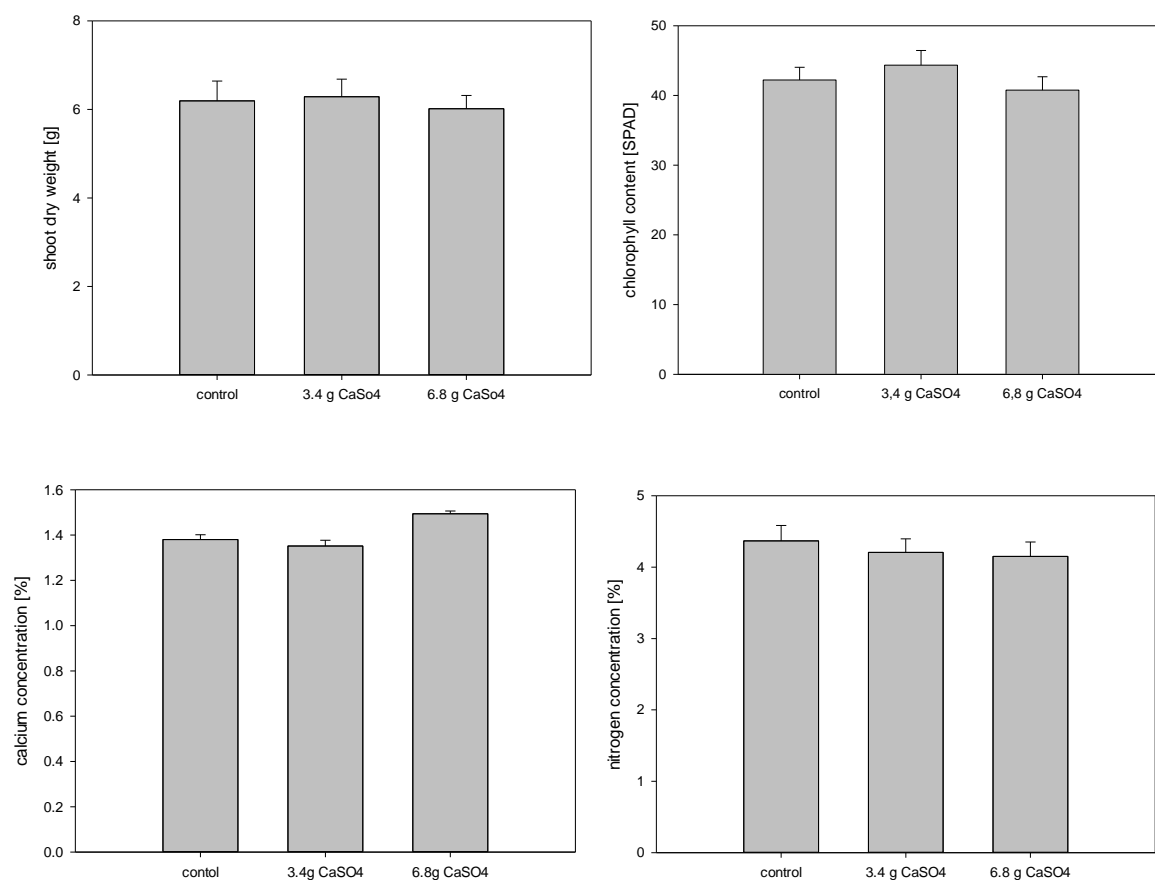


Fig. 39 *Vicia faba* Ca^{2+} fertilization experiment on soil/vermiculite mixture.

Shoot dry weight, chlorophyll content, and Ca^{2+} and N concentration of plants treated with 0, 3.4, and 6.8g CaSO_4 . Control and Ca^{2+} -treated plants show no significant differences (paired t-test, $P > 0.05$). Data are the means \pm SE (N=6).

3.4.3 Experiments with hydroponic culture

Six *V. faba* plants were grown in 50L vessels containing N-free nutrient solution with moderate (1 mM) or enhanced Ca^{2+} concentration (10 mM). After eight weeks of growth

3. Results

plants were harvested and the dry weight, relative chlorophyll content (SPAD value), and Ca^{2+} and N concentration were measured. The experiment was repeated twice. In the third repetition, the Mo concentration of the nutrient solution was increased to ensure a sufficient supply of the bacteria (Loneragan, 1959).

Experiment 1

Although a significant difference in SPAD values between Ca^{2+} -treated plants and control plants was detectable, there was no difference in shoot N concentration. There were also no significant differences in the dry weight of shoots, roots, and nodules. The Ca^{2+} concentration of the shoots of plants treated with 10 mM Ca^{2+} was higher compared to the control plants. Interestingly, the N concentration of nodules was higher in Ca^{2+} -treated plants than in control plants (Fig. 40).

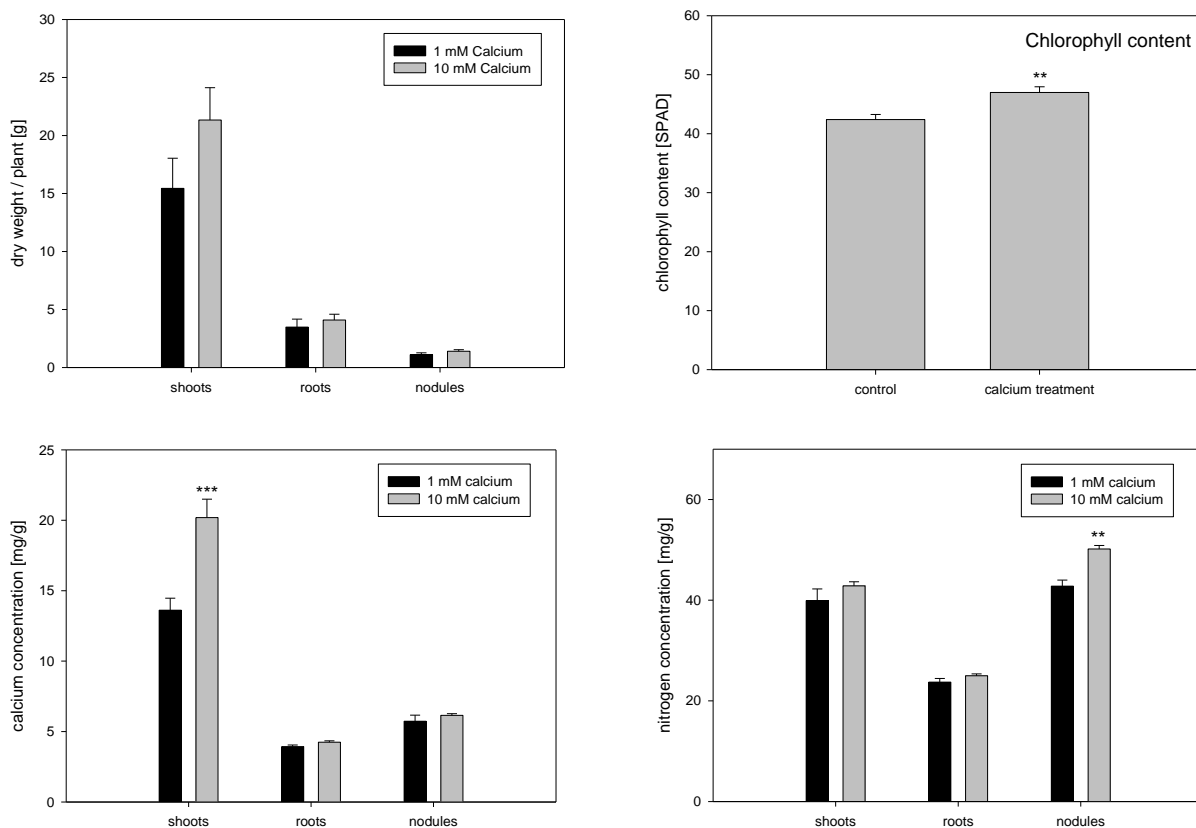


Fig. 40 *Vicia faba* fertilization experiment 1 in hydroponic culture.

Dry weight, relative chlorophyll content, and Ca^{2+} and N concentration of plants treated with 10 mM Ca^{2+} and control plants receiving 1 mM Ca^{2+} . Significant differences between Ca^{2+} -treated plants and control plants were determined for shoot Ca^{2+} concentration and nodule N concentration (**, $P < 0.01$; ***, $P < 0.001$; paired t-test). Data are the means +SE (N=6).

3. Results

Experiment 2

Plants grown in nutrient solution with elevated Ca^{2+} concentration showed increased Ca^{2+} concentration in leaves (Fig. 41). However, this time the N concentration in nodules of Ca^{2+} -treated plants was not enhanced, and SPAD values did not differ.

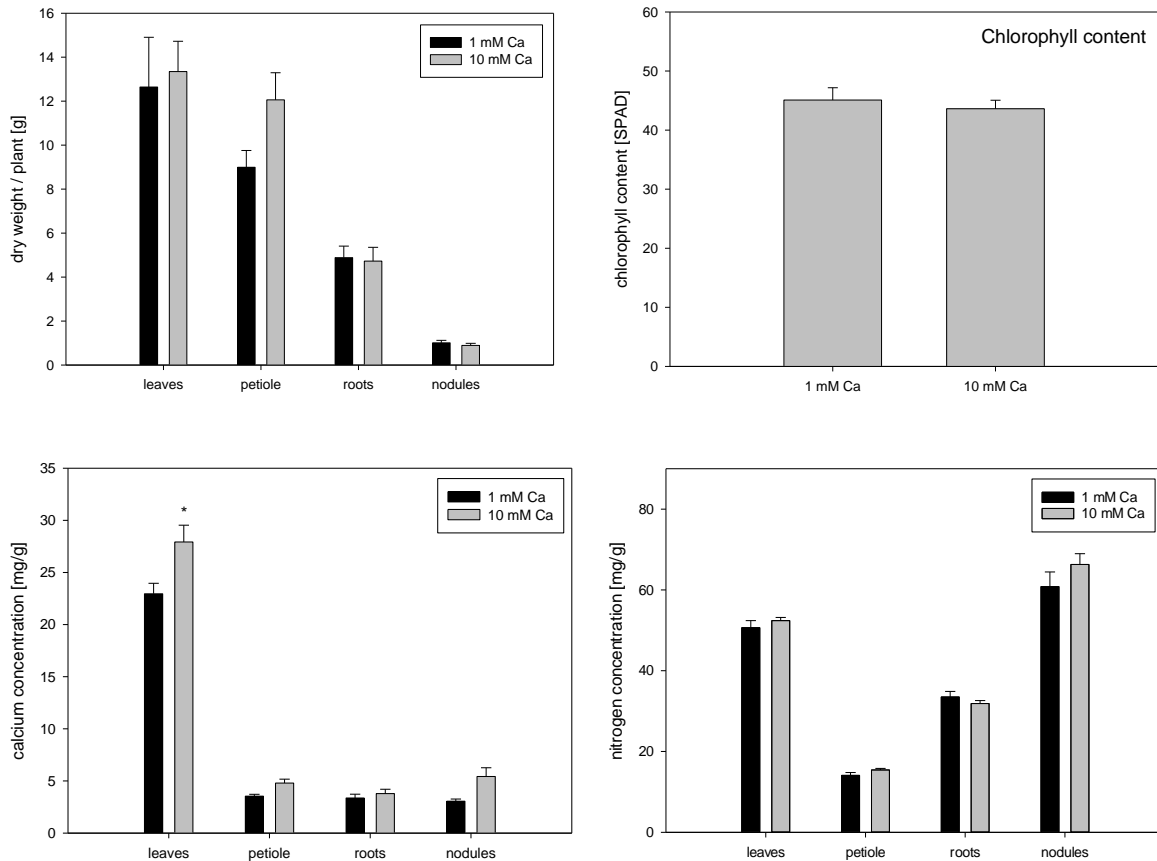


Fig. 41 *Vicia faba* fertilization experiment 2 in hydroponic culture.

Dry weight, relative chlorophyll content, and Ca^{2+} and N concentration of plants treated with 10 mM Ca^{2+} and control plants receiving 1 mM Ca^{2+} . Plants grown in solution with 10 mM Ca^{2+} show significantly higher Ca^{2+} concentration in leaves (*, $P < 0.05$; paired t-test). Data are the means \pm SE ($N=6$).

Experiment 3

In this experiment the Mo concentration was 10 fold higher compared to experiments 1 and 2 to ensure an ample Mo supply for the nitrogenase. The Ca^{2+} concentration and relative chlorophyll content of Ca^{2+} -treated plants was higher compared to the control plants. As before, there were no significant differences between treatments in dry weight and N concentration of shoots, roots, and nodules (Fig. 42).

3. Results

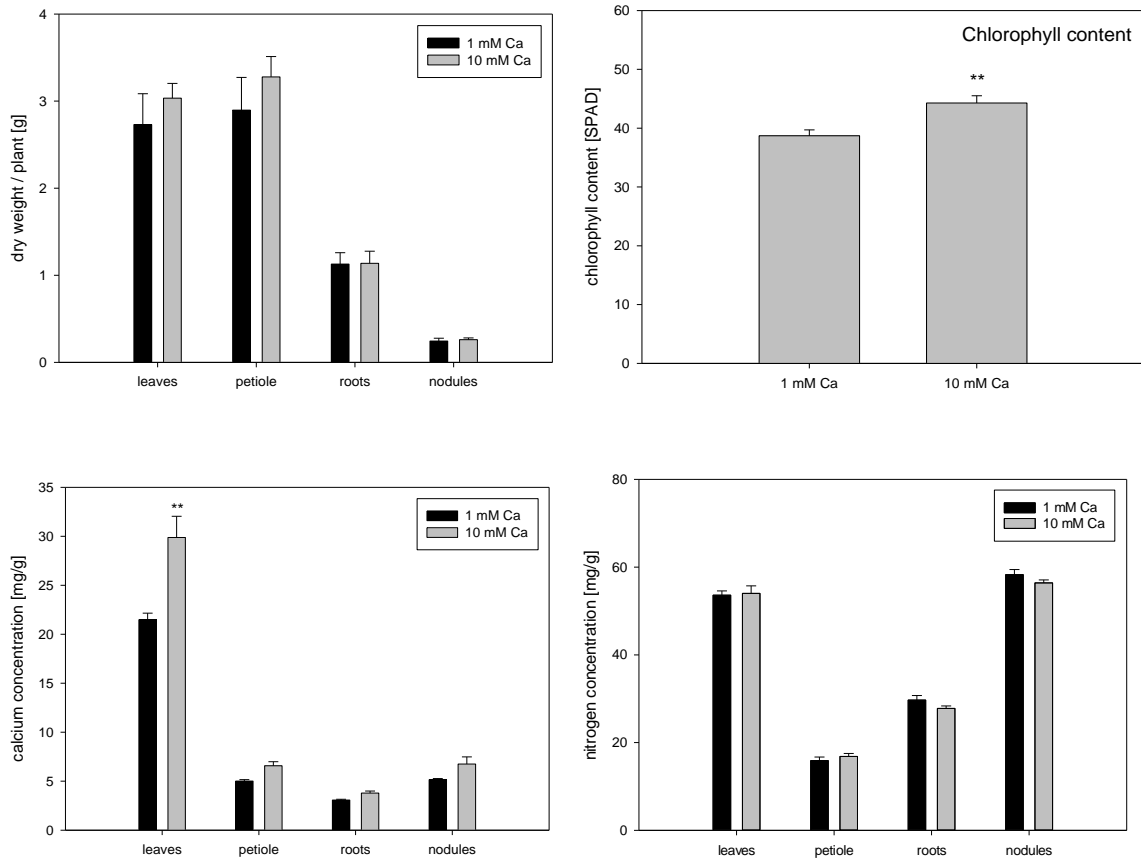


Fig. 42 *Vicia faba* fertilization experiment 3 in hydroponic culture.

Dry weight, relative chlorophyll content, and Ca^{2+} and N concentration of plants treated with 10 mM Ca^{2+} and control plants receiving 1 mM Ca^{2+} in presence of elevated Mo concentration. Ca^{2+} concentration of leaves and relative chlorophyll content differed significantly between Ca^{2+} -treated plants and control plants (**, $P < 0.01$; paired t-test). Data are the means \pm SE (N=6).

4. Discussion

4.1 Measurement of $[Ca^{2+}]_{cyt}$ in nodules of *Medicago truncatula*

The obvious way to investigate if Ca^{2+} is involved in the regulation of N_2 fixation is the measurement of changes in $[Ca^{2+}]_{cyt}$ in nodules of living plants, for example after N supply or removing parts of the shoots. To measure changes in $[Ca^{2+}]_{cyt}$ in living cells, different methods exist. One of them is based on apoaequorin and its cofactor coelenterazine. Together they reconstitute to aequorin, which is able to release a photon after Ca^{2+} binding (Shimomura and Johnson, 1978). In this thesis, *M. truncatula* plants transformed with apoaequorin were treated with cold and NaCl to elicit Ca^{2+} signals. While stimulus-induced luminescence was detectable in roots, no signal was visible in nodules. One reason for this may be the necessity of O_2 for the reconstitution of aequorin, since the O_2 concentration in nodules is very low. The nitrogenase contains cofactors for the exchange of electrons, which are damaged by the strong electron acceptor O_2 , resulting in an inactivation of the nitrogenase. Therefore, the nodule possesses several mechanisms to reduce the O_2 concentration in the infected tissue. Besides an O_2 barrier in the cortex (Iannetta et al., 1993), the nodule contains O_2 -binding leghemoglobin (Lb) in infected cells (Ott et al., 2005). Furthermore, mitochondria in the infected plant cells are adjacent to the plasma membrane (Millar et al., 1995) and respire O_2 with high affinity. As result, the O_2 concentration in infected cells is reduced to 5-60 nM (Kuzma et al., 1993; Layzell et al., 1990). This O_2 concentration is likely too low for the reconstitution of functional aequorin from apoaequorin and coelenterazine.

4.2 Resources to investigate gene expression in root nodules

In this thesis, different methods to investigate the gene expression were employed. *In silico*, the data of several expression studies were collected using the original studies or databases like Genevestigator or eFPBrowser (JCVI). This method was useful to get a first impression of the gene expression in *M. truncatula*, but due to inhomogeneous results, it was not helpful to select genes expressed in the N_2 fixation zone of nodules. For instance, while scatterplot shows moderate expression level of Medtr4g014480 in the proximal infection zone, Roux et

4. Discussion

al. (2014) detected no reads for that gene in proximal infection zone (Fig. 17 and 18). One reason for the differences of the studies may lie in the different growth conditions and treatments of the plants investigated in each study. For instance, Seabra et al. (2012) investigated the transcriptional reprogramming in nodules after inhibition of glutamine synthetase, growing the plants (*M. truncatula* Jemalong A17) in nutrient solution in a 16/8h light cycle at 22/19°C for a herbicide treatment. In contrast, Limpens et al. (2013) investigated untreated plants (*M. truncatula* Jemalong A17) also grown in 16/8h, but at constantly 21°C. Heath et al. (2014) did not use *M. truncatula* Jemalong A17 for their study. They compared the coevolutionary genetic variation of the genotypes *Naut 1* and *Sals 4* and their corresponding rhizobial partners. Besides the variation of investigated plant genotypes and growth conditions, also the methods to investigate the gene expression differ. While in the above mentioned studies (Seabra et al., 2012, Limpens et al., 2013, Heath et al., 2014) gene expression was investigated by using the Affymetrix GeneChip, Roux et al. (2014) used RNA sequencing (RNA-seq). Both methods aim to identify a high number of expressed genes based on extracted RNA. Biotin-labeled cRNA (generated from the extracted RNA) binds to probes arrayed on the Affymetrix GeneChip. After staining with streptavidin-phycoerythrin, arrays are scanned on a Affymetrix GeneChip Scanner. Single genes are often represented by several probe numbers on the GeneChip. Each probe number contains 11 polymers of 25 nt, which are located close to each other in the gene sequence. In this way, each probe number covers a certain part of the gene of 100 bp or more. This part is also named as target sequence. If a gene is represented by several probe numbers the target sequences can be located in exons, which are not present in every splice variant. For instance, two probe numbers of *MA3* (Medtr5g015590.1) are located at the end of the CDS where the splice variants differ strongly (Fig. 43). While Mtr.48837.1.S1_s_at is located in splice variant 1 and 2, probe number Mtr.2046.1.S1_at only binds to splice variant 2. Splice variants 3 and 4 cannot be detected by these probe numbers. Just the probe number Mtr.21285.1.S1_at is located at the beginning of the CDS and therewith represented in every splice variant of *MA3*. Thus, the position of the target sequences can be a reason for the variation of signal values of different probe numbers.

4. Discussion



Fig. 43 Localization of probe numbers in splice variants of MA3.

Splice variants (1-8) are represented by lines (introns: thin black lines, exons: fat grey lines surrounded by red lines). Target sequences of probe numbers ((a) Mtr.2046.1.S1_at, (b) Mtr.21285.1.S1_at, (c) Mtr.48837.1.S1_s_at, (d) Mtr.40540.1.S1_at) are represented by red lines (Mt4.Ov1 Gene Models, JCVI).

For the investigation of gene expression by RNA-seq, RNA is extracted and converted to cDNA. Subsequently, the short cDNA fragments are linked to adapters, and one or both ends are sequenced. In contrast to microarrays, which are only able to detect the expression of genes represented on the chip, every expressed gene is detectable by RNA-seq. Thus, also novel, unannotated genes, alternative splicing and sequence-level alterations, like mutations or gene fusions, can be detected by RNA-seq. Furthermore, the detection of genes with low transcript level is easier with RNA-seq than with microarrays, which have background noise interference.

According to the expression studies a large number of genes encoding Ca^{2+} -permeable transport proteins are expressed in nodules (Fig. A50-A55). For detailed investigations it was necessary to focus one gene family. Therefore, a hypothesis was advanced. As described in the introduction, the NH_4^+ channel is inhibited by the elevation of the Ca^{2+} concentration within the symbiosome space (Tyerman et al., 1995). If the plant regulates the N_2 fixation by increasing the Ca^{2+} concentration in the symbiosome space, Ca^{2+} needs to be translocated from the plant cytosol into the symbiosome space. This transport has to be active against the electrochemical gradient, because the cytosolic Ca^{2+} concentration is much lower than the Ca^{2+} concentration in the symbiosome space. This active transport is an energy-consuming process and likely realized by Ca^{2+} -ATPases (Fig. 44). Therefore, Ca^{2+} -ATPases were focused on in this thesis.

4. Discussion

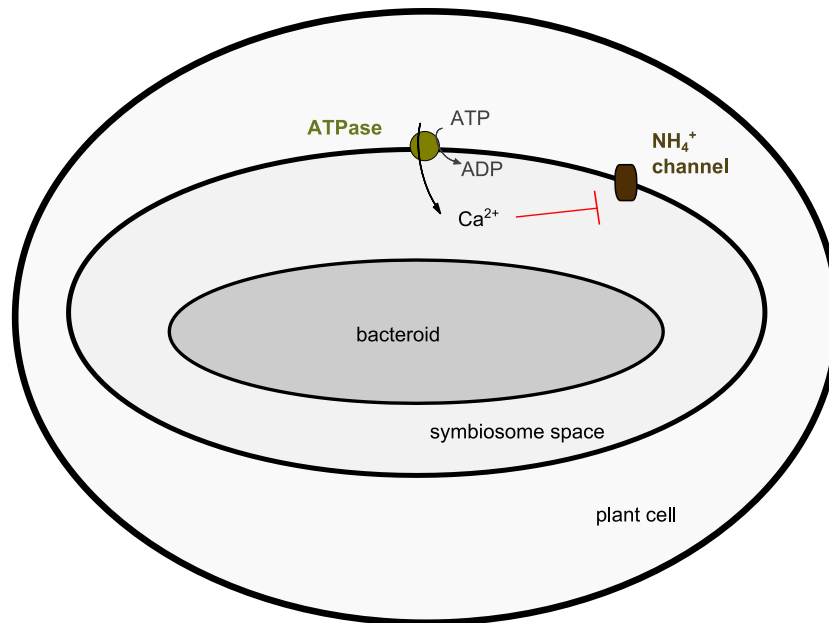


Fig. 44 Hypothesis of the regulation of N_2 fixation by Ca^{2+} -induced inhibition of the symbiosome NH_4^+ channel.

Ca^{2+} -ATPases localized in the symbiosome membrane may increase the Ca^{2+} concentration within the symbiosome space and thereby trigger the inhibition of the NH_4^+ channel.

4.3 Investigation of Ca^{2+} -ATPases

4.3.1 Expression of genes encoding Ca^{2+} -ATPases

4.3.1.1 *In silico* analysis

For the selection of candidate genes encoding Ca^{2+} -ATPases in the symbiosome membrane, genes expressed in the infected cells of the N_2 fixation zone are of interest. Therefore, the expression data of Limpens et al. (2013), who separated the infected cells of the N_2 fixation zone, and the data of Roux et al. (2014), who separated the N_2 fixation zone are discussed in more detail. Limpens et al. (2013) used the Affymetrix GeneChip to investigate the gene expression. For almost each gene encoding a putative Ca^{2+} -ATPase, the signal values of the associated probe numbers show high discrepancies (Fig. 15). One reason for these differences may be non-specific hybridization. For instance, the gene MA2 (Medtr4g008170) is represented by two probe numbers (Mtr.43923.1.S1_at and Mtr.8275.1.S1_at) with different signal intensities (Fig. 15). To test if there is a non-specific hybridization for MA2, the target sequences of both probe numbers were used for a BLAST search. With an identity of 79% the target sequence of the probe number Mtr.43923.1.S1_at matches another gene

4. Discussion

(Medtr2g105690), which is predicted to encode another Ca^{2+} -ATPase and not represented on the GeneChip. Some 25nt-polymers of the target sequence of Mtr.43923.1.S1_at and the sequence of Medtr2g105690 differ in merely five single positioned nucleotides. Thus, a hybridization with these polymers may be possible for RNA of Medtr2g105690. The BLAST result of the target sequence of the probe number Mtr.8275.1.S1_at did not show any similarities with other genes. Therefore, the differences of the signal values for MA2 might be explained by non-specific hybridization.

MA3 (Medtr5g015590) is represented by four probe numbers (Mtr.2046.1.S1_at, Mtr.21285.1.S1_at, Mtr.48837.1.S1_s_at, Mtr.40540.1.S1_at). In contrast to the other numbers, Mtr.40540.1.S1_at shows a high signal value in infected cells of the N_2 fixation zone (Fig. 15). The polymers of this number are located in the 3'UTR, while those of the other three numbers are located in the CDS. Sequences similar to the 3'UTR of *MA3* are also located on chromosome 2. The CDS BLASTn search with the similar sequence on chr 2 does not show a result (Mt4.0v1), but the flanking region (3kb) 467bp show a 100% identity with the gene Medtr2g033980.1. Perhaps, the similar sequence is located in the 5'UTR or 3'UTR of Medtr2g033980. Furthermore, the target sequence of Mtr.2046.1.S1_at contains two polymers with a high similarity to sequence parts of the gene Medtr4g096990. Transcripts of this gene might induce a signal, which assigned wrongly to *MA3*, but this signal would be very low.

MA1 (Medtr2g038310) is represented by four Affymetrix probe numbers (Mtr.31084.1.S1_at, Mtr.30887.1.S1_s_at, Mtr.4152.1.S1_at, Mtr.8909.1.S1_at). Similar to *MA3*, one probe number (Mtr.8909.1.S1_at) shows a much higher signal value than the other three numbers. No other gene can be detected by the polymers. Interestingly, the polymers of the probe number Mtr.8909.1.S1_at are located in the 3'UTR, similar to *MA3* where the polymers of the only number (Mtr.40540.1.S1_at) with high signal value are also located in the 3'UTR.

The strongest difference between the signal values of individual probe numbers shows *MA5*, which is represented by two probe numbers (Mtr.29267.1.S1_at and Mtr.40647.1.S1_at). The signal value of Mtr.40647.1.S1_at is 200 fold higher than that of Mtr.29267.1.S1_at. Just five polymers of the probe number Mtr.40647.1.S1_at are located in the CDS of *MA5*; the residual ones lie in the 3'UTR.

4. Discussion

Compared to the other candidate genes, the signal values of the probe numbers of *MA4* (Mtr.44516.1.S1_at and Mtr.13570.1.S1_at) diverge less. The CDS BLASTn search with the target sequence of Mtr.44516.1.S1_at shows a 100% identity with *MA4*, but not with other genes. In contrast, the identity of the target sequence of Mtr.13570.1.S1_at with *MA4* is 95%. Furthermore, the part of the target sequence, which shows this 95% identity has a length of just 120 bp. However, the target sequence has a full length of 426 bp. Furthermore, the full length target sequence shows a 99% identity with a sequence of chromosome 2. Therefore, this probe number does not reliably report the expression of *MA4*.

Due to the differences of the signal values of different probe numbers for the same gene and the fact that probe numbers showing high signal values may recognize the expression of other genes, the Affymetrix GeneChip data of Limpens et al. (2013) cannot reliably report the expression of the candidate genes in the infected cells of the N₂ fixation zone. Roux et al. (2014) investigated the gene expression in the N₂ fixation zone by RNA-seq. However, because the whole N₂ fixation zone was used for the analysis, the expression data represents genes expressed in infected and/or uninfected cells. Thus, these data are not suitable to extract genes expressed in infected cells of the N₂ fixation zone, which were of interest for this project. Therefore, further approaches were pursued to select genes encoding putative Ca²⁺-ATPases potentially located in the symbiosome membrane. These involved BLAST analyses against Ca²⁺-ATPases of *G. max* suggested to be localized in the symbiosome membrane and a screen for absence of a NLS. Eventually, five putative Ca²⁺-ATPases were chosen for further study.

4.3.1.2 Investigation of gene expression by RT-PCR

The expression of the five candidate genes was investigated by RT-PCR. To avoid changes in gene expression by sample preparation, RNA was extracted from the whole intact nodule. The nodules were harvested by cutting them with a scalpel, transferred into a cooled micro reaction vessel and stored in liquid nitrogen. Around 15 sec passed between the excision and the storage in liquid nitrogen. Within such a short time an alteration of gene expression due to cold or wounding is improbable. Each candidate gene was amplified by RT-PCR and therefore validated to be expressed in nodules. However, because the RT-PCR was

4. Discussion

performed with whole nodules, the expression pattern of the candidate genes remained unknown. For further selection of the candidate genes, a GUS analysis of their promoter activity was performed.

4.3.1.3 Investigation of gene expression by GUS assay

After the expression of the candidate genes was confirmed for the whole nodule, the spatial pattern of promoter activity was investigated by GUS staining of nodule thin sections. In this way, the expression of the candidate genes was assigned to different nodule zones and cell types. Before sectioning, nodules were embedded in low-melting agarose and stored at 4°C for 2h. This cold stimulus and the following wounding caused by the cutting may have influenced the gene expression. For instance, the expression of *AtACA8* and *AtACA10* decreases 2h after cold treatment (5°C) of the whole plant (Schiøtt and Palmgren, 2005). In some studies, nodules were prefixed with paraformaldehyde (Pichon et al., 1992; Tejada-Jiménez et al., 2015; Vernoud et al., 1999), which denatures proteins. In this way, the activity of proteins, such as transcription factors, but also of β -glucuronidase is reduced. For instance, the activity of β -glucuronidase was reduced to approximately 30% in tissues treated with 2% paraformaldehyde for 15 min (Preťová et al., 2003). To exclude changes in expression of the candidate genes by cold, also hand sections of nodules were incubated in GUS staining solution. Nodules prepared by hand sections and thin sections showed the same expression patterns.

Nodules of plants transformed with *ProMA1:uidA* showed a blue coloration specifically in the vascular bundles, indicating it is expressed in this tissue. This result differs strongly from the expression data of Roux et al. (2014), which showed detection of reads of *MA1* in all five nodule zones (Fig. 18).

MA2 appears to be expressed in uninfected cells of the N₂ fixation zone, the vascular bundles and the cortex of the nodule. The expression data of Roux et al. (2014) and Genevestigator showed also an expression of *MA2* in the N₂ fixation zone, but also in other nodule zones (Figs. 17 and 18).

The staining of nodules containing the *ProMA3:uidA* construct indicate an expression of *MA3* in the vascular bundles. An irregular coloration was also visible between the infected cells of the N₂ fixation zone. The irregular manner could be a result of aggregation of the β -

4. Discussion

glucuronidase or the soluble primary product (5-br-4-Cl-3-indolyl) of the enzymatic reaction. The result of staining and the data of the expression studies are contradictory. Roux et al. (2014) detected reads in every nodule zone (Fig. 18). The scatterplot generated by Genevestigator shows high expression level in the infection zone and in the uninfected cells of the N₂ fixation zone (Fig. 17).

Nodules of plants transformed with the *ProMA4:uidA* construct showed a strong staining in the infected cells of the N₂ fixation zone, indicating that *MA4* is expressed in these cells. It appears also to be expressed in the cells of the meristematic zone and the infection zone. This result corresponds to the expression data of Roux et al. (2014).

The staining of nodules transformed with the *ProMA5:uidA* construct indicates the expression of *MA5* in the whole nodule of vegetative plants and in the infection zone of generative plants. A slight blue coloration was also visible in some cells of the N₂ fixation zone in nodules of generative plants. This observation indicates that the expression level of *MA5* decreases in the generative phase, but the results of three independently performed transformations differ for unknown reasons. One explanation for the variability might be that the transformation was not successful for some plants of the first and all plants of the second transformation. During the growth period, plants of the second transformation suffered a heat shock due to a failure of the growth chamber. Gene expression was investigated several days after transfer to an alternative growth room. However, this heat stress may still have severely influenced gene expression.

4.3.1.4 Investigations of gene expression - nodule specific problems

In this thesis, *in silico* data of gene expression estimated by Affymetrix GeneChip and RNA-seq as well as experimental methods (RT-PCR and GUS analysis) were used to investigate the gene expression. As mentioned above, the results of the studies differ for each candidate gene. To investigate the gene expression in nodules, nodules have to be separated from the root. Therefore, roots have to be removed from the growth system (e.g., pots, hydroponic culture or aeroponic caissons), and nodules have to be cut off. This alteration of the root environment and the wounding triggers a response and thereby a change in gene expression. If the gene expression of different nodule zones or cell types shall be investigated, further preparation steps are necessary. The nodules have to be sectioned to

4. Discussion

separate the single zones from each other. These preparation procedures need a long time and may influence the gene expression. For instance, Limpens et al. (2013) fixated the nodules for 30 min in Farmer's fixative under vacuum followed by an overnight incubation at 4°C. Roux et al. (2014), who tested eight different fixation solutions, treated the nodules in a series of methanol and ethanol incubations over several hours. In this case, nodules confronted with environmental changes and wounding were incubated at 4°C for 30 min until the tissues were fixed. It means, that the nodules had more than 30 min to trigger responses to wounding, cold, and other stimuli caused by removing the root out of the growth system (e.g. touch, temperature changes, and light). The expression of every gene involved in the response to these stimuli may have been influenced by the preparation of nodules.

Furthermore, the plants, especially transformed plants, need a long growth time until they develop mature nodules (6-7 weeks). During this time the plants become too tall for growing in petri dishes and have to be transferred to other cultivation systems like aeroponic caissons, hydroponic culture or pots containing substrates like sand, soil or perlite. In these cultivation systems the growth conditions are less constant than in petri dishes, in which plants grow in a sterile atmosphere, buffering temperature differences, air circulation or differences in air humidity. Especially in pots, which are watered manually, plants are exposed to inconstant water supply. These differences may have an effect on the expression of genes involved in responses to environmental changes and therefore, make it more difficult to generate consistent expression data.

4.3.2 Localization of the candidate genes

The CDS of the five candidate genes was fused to the gene encoding an enhanced green fluorescent protein (EGFP) and transformed into *M. truncatula* plants. Nodule sections (100 µm) of transformed plants were investigated by fluorescence microscopy. Infected cells of the N₂ fixation zone were identified by using a *S. meliloti* strain labeled with a red fluorescent protein (mRFP). Tagging proteins with fluorescent proteins (FP) is a common method to identify the subcellular localization of a protein of interest. However, folding, function, and targeting of the protein of interest may be affected by the added FPs (Snapp, 2005). The formation of aggregates is also possible. Furthermore, light exposure affects the

4. Discussion

stability of vacuolar-localized GFP (Tamura et al., 2003). GFP targeted to the vacuolar lumen of *Arabidopsis* cells was stable under dark conditions, but fluorescence in vacuoles disappeared upon exposure to light, while that in ER and Golgi was unaffected.

Fluorescence of EGFP fused to MA1 was detected in an irregular manner in uninfected cells of the N₂ fixation zone (Fig. 31). While the signal appeared as ring structure in some cells, it showed a diffuse manner in other cells, and many uninfected cells did not show an fluorescence signal. These localizations maybe due to the trafficking of MA1 in the membrane of vesicles fusing to targets, such as the plasma membrane or the tonoplast. The precise localization of MA1 should be investigated with appropriate markers for the secretory pathway and possible target membranes, e.g. SNAREs.

Like MA1, signals of EGFP fused to MA2 were detected in uninfected cells (Fig. 32). The signal appeared as small dots and in a homogenous manner over the whole cell. This homogeneous fluorescence may originate from the vacuole lumen, similar to observations on root vacuoles (Fig. 45; Tamura et al., 2003). The dots may represent small organelles, such as the Golgi apparatus.

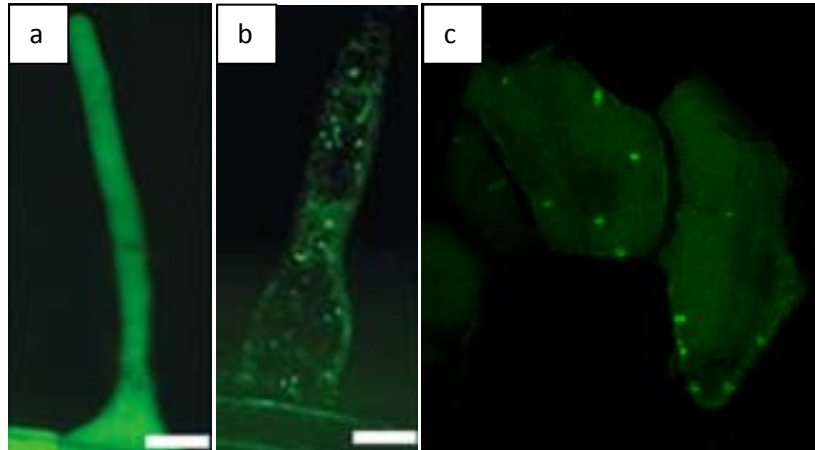


Fig. 45 Comparison of GFP signals localized in vacuoles of *A. thaliana* root hairs and EGFP:MA2 signals detected in *M. truncatula* nodules.

Tamura et al. (2003) detected GFP signal of vacuole-targeted GFP in vacuoles under dark conditions (a) or in endoplasmic reticulum and small granular structures under light conditions (b). The signal of the EGFP:MA2 construct shows similarity to that of vacuole-targeted GFP (c).

The preparation of nodules for fluorescence microscopy was a long procedure. Nodules were embedded in low-melting agarose and cooled in the fridge for 2h. Subsequently, the nodules were cut in thin sections with a vibratome. During this step samples were exposed to light for approximately 30 min. In the experiments of Tamura et al.

4. Discussion

(2003), GFP was degraded within 1h light exposure. ATPases are membrane-bound proteins. Thus, EGFP-MA2 cannot be localized in the vacuole lumen. However, vacuoles are the place of protein degradation during senescence or upon environmental factors. Because the fluorescence pattern of the EGFP:MA2 fusion depicted in Fig. 32c was not visible in all uninfected cells, it is possible that the EGFP:MA2 construct was degraded in the cells showing this specific fluorescence pattern. It is also possible that the prediction of the localization of the N-terminus is wrong. In this case the GFP would be located within the vacuole, if MA2 is integrated in the tonoplast. In cortex cells, MA2 appeared to be localized in the plasma membrane. Clearly, further experiments are required to clarify the localization of MA2.

Nodules transformed with the constructs EGFP:MA3 and EGFP:MA4 showed signals in infected cells surrounding the red-labeled bacteroids, indicating that MA3 and MA4 are located in the symbiosome membrane. Furthermore, symbiosomes isolated from nodules containing the EGFP:MA4 construct showed a GFP signal. This served as additional evidence for the localization of MA4 in the symbiosome membrane. Like MA3 and MA4, MA5 seems to be localized in the symbiosome membrane because fluorescence signals of the EGFP:MA5 fusion were detected around bacteroids in infected cells of the N₂ fixation zone and in isolated symbiosomes. The GFP signal was also visible in the plasma membrane of uninfected nodule cells and root cells. In roots, it was also detected in the nuclear envelope. Capoen et al. (2011) also localized MA5 (there named as MCA8) in the nuclear envelope, where it is involved in the generation of Nod-factor induced Ca²⁺ oscillations.

Although all EGFP-MA constructs were under the control of the constitutive CsVMV promoter, EGFP fluorescence was not apparent in every cell and differed with the fused MA gene. This finding remains unexplainable. The CsVMV promoter is active in each nodule cell of *M. sativa* (Samac et al., 2004). Since Nallu et al. (2013) generated *M. truncatula* RNAi lines with this promoter to investigate genes expressed in nodules, it can be assumed that CsVMV is also active in every nodule cell type of *M. truncatula*.

4.3.3 Possible functions of the investigated Ca²⁺-ATPases

With respect to the yeast complementation assays, in which every candidate gene was able to improve the growth of the mutant K616 on Ca²⁺-deficient medium, it can be assumed that

4. Discussion

the studied ATPases are able to transport Ca^{2+} and thus are involved in the Ca^{2+} homeostasis of cells.

MA1 seems to be expressed in cells of the root cap, in dividing cells (developing lateral roots and nodules), and the vascular bundles of mature nodules. Cells of the root elongation zone and the root cap are involved in root gravitropism. The curvature of roots caused by the gravitropic response is driven by sedimentation of amyloplasts in root cap cells (Kiss et al., 1989). The displacement of amyloplasts triggers a physiological signal. Several models have been suggested for this process (Su et al., 2017; Su et al., 2020). One model proposes that the sedimentation of the amyloplasts triggers the opening of mechano-sensitive ion channels by stretching membranes. It has been proposed that these channels are permeable for Ca^{2+} because roots treated with Ca^{2+} channel inhibitors (verapamil or lanthanum) show reduced curvature (Perdue et al., 1988). Furthermore, treatments of roots with calmodulin inhibitors, like trioperazine (TFP), calmidazolium (CMZ), and N-(6-aminohexyl)-5-chloro-naphthalenesulfonamide (W7), or the Ca^{2+} -ATPase inhibitor thapsigargin is able to alter gravitropism (Sinclair et al., 1996; Urbina et al., 2006), indicating that a Ca^{2+} signal is involved in the root gravitropism. In fern the Ca^{2+} -ATPase CrACA1 was shown to be involved in the gravity response, which polarizes the direction of rhizoid growth (Bushart et al., 2014). However, the responsiveness of *Arabidopsis* roots to thapsigargin rather indicates the involvement of ECAs than ACAs in this plant. As there is currently no evidence for the contribution of ACAs in gravity response, the involvement of *MA1*, which belong to the ACA subfamily, is improbable. The expression of *MA1* in lateral root and nodule meristems may indicate an involvement of *MA1* in cell division, which has been long-known to involve Ca^{2+} -regulated processes (Hepler, 1994). In mature nodules *MA1* seems to be expressed in the vascular bundles indicating a potential role of *MA1* in transport processes between nodules and roots.

MA2 appears to be expressed in uninfected cells of the N_2 fixation zone. The roles of the *MA2* in this cell type are unclear, in particular since its localization needs further analysis. One of the main functions of these uninfected cells has been hypothesized to be the catabolism of sucrose. In contrast to uninfected cells, infected cells are not able to take up sucrose, indicating that sucrose may be converted into malate in uninfected cells and then transported into the infected cells (Peiter and Schubert, 2003). The conversion is realized by sucrose synthase, an enzyme which was shown to be phosphorylated by a Ca^{2+} -dependent

4. Discussion

protein kinase (CDPK) (Zhang and Chollet, 1997). If the sucrose synthase is indeed indirectly regulated by Ca^{2+} , MA2 may be involved in the control of $[\text{Ca}^{2+}]_{\text{cyt}}$ during that process.

MA2 and MA5 are also expressed in the root elongation zone. It has been proposed that Ca^{2+} -ATPases are involved in the symplastic transport of Ca^{2+} through the root endodermis cells of the elongation zone, where the Casparian band blocks the apoplastic pathway, but no suberin lamellae exist (White, 2001). In order to determine whether MA2 and MA5 may be involved in radial transport of Ca^{2+} , their expression in the endodermis needs to be determined.

Albeit the subcellular localization experiments indicated a potential localization of MA3 in the symbiosome membrane, GUS staining indicated that this gene is expressed in the vascular system of roots and nodules. The specific cell type and the membrane localization in this tissue need yet to be determined. If expressed in sieve elements, it may be involved in regulating conformational changes of crystalline P-protein bodies, which plug sieve tubes in response to turgor changes caused by wounding, a process controlled by $[\text{Ca}^{2+}]_{\text{cyt}}$ (Knoblauch et al., 2001). The authors suggested that extracellular Ca^{2+} enters the sieve tube cell, induces the reversible conformational change of crystalline P-protein bodies and is pumped back by Ca^{2+} -ATPases localized in the plasma membrane.

The GUS staining of nodules transformed with the *ProMA4:guiA* construct showed a consistently blue staining of the infected cells of the N_2 fixation zone, indicating the expression of MA4 in these cells. Furthermore, the fluorescence signal of the EGFP:MA4 construct can be assigned to the symbiosome membrane. Located in the symbiosome membrane, MA4 is likely responsible for Ca^{2+} transport into the symbiosome space. The deletion of MA4, as initiated in this project, may therefore serve to test the hypothesis that an elevated Ca^{2+} concentration in the symbiosome space blocks the ammonium channel *in planta*.

Furthermore, Ca^{2+} transport by MA4 into symbiosomes may regulate cellular Ca^{2+} homeostasis. Infected cells of the N_2 fixation zone are enriched with symbiosomes through which the size of vacuoles is strongly reduced. Therefore, symbiosomes are suggested to fulfill the function of vacuoles as internal Ca^{2+} stores. Thus, MA4 may be involved in the maintenance of a low $[\text{Ca}^{2+}]_{\text{cyt}}$ concentration. As Ca^{2+} stores, vacuoles are involved in the generation of Ca^{2+} signals. It is unknown if symbiosomes take over this function of vacuoles. Since symbiosomes are many separated compartments, the generation of a cellular $[\text{Ca}^{2+}]_{\text{cyt}}$

4. Discussion

signal though Ca^{2+} release from symbiosomes would require a simultaneous release of Ca^{2+} ions, implying that each symbiosome of one cell should release Ca^{2+} ions at the same time.

Since the fluorescence signal of the EGFP:MA5 construct can be assigned to the symbiosome membrane, and nodules transformed with the *ProMA5:guiA* construct showed blue coloration of infected cells after GUS staining, also MA5 is likely responsible for Ca^{2+} -transport into the symbiosome space.

4.4 Modulation of N_2 fixation by calcium fertilization

A relationship between N_2 fixation and Ca^{2+} supply of legumes was discovered many years ago. Subterranean clover (*Trifolium subterraneum*) troubled with Ca^{2+} deficiency contained less N compared to plants supplied with adequate Ca^{2+} , and symptoms of N deficiency disappeared by addition of Ca^{2+} (Banath et al., 1966; Loneragan, 1959). This observation indicated that Ca^{2+} is essential for efficient nodule function and raised the question if increased Ca^{2+} supply may elevate nitrogenase activity. Miller and Sirois (1983) indeed measured a reduced nitrogenase activity of Ca^{2+} -deficient alfalfa (*M. sativa*) plants, and the addition of Ca^{2+} to these plants elevated the nitrogenase activity. Streeter (1998) treated soybean plants growing in sand with different Ca^{2+} concentrations in the nutrient solution added to the pots. In one experiment with plants growing for 62 days, nitrogenase activity in plants treated with high Ca^{2+} concentrations (6 and 12 mM) was decreased compared to plant with moderate Ca^{2+} supply (1 mM) and also the N concentration of shoots was less than in control plants. This result indicates a repression of nitrogenase activity by excess Ca^{2+} supply. However, in another experiment, in which plants were harvested earlier (48-52 days after planting) and the nutrient solution was buffered, there were no significant differences between control plants and plants treated with higher Ca^{2+} concentrations regarding the nitrogenase activity, and plants treated with 12 mM Ca^{2+} showed only slightly decreased N concentrations in shoots compared to plants treated with 1 mM Ca^{2+} . In addition, Streeter (1998) determined an inhibitory effect of a decrease in solution pH on nitrogenase activity, which cannot be excluded in the first experiment at high Ca^{2+} . Summarizing, the experiments of Streeter (1998) do not provide clear evidence for an effect of high Ca^{2+} supply on nitrogenase activity.

4. Discussion

In this thesis, experiments were performed with *V. faba* plants grown in hydroponic culture. The pH of the solution was continuously adjusted to 6.5 by a titrator. Control plants grew in a solution containing 1 mM Ca^{2+} , plants grown in solution with increased Ca^{2+} concentration were supplied with 10 mM Ca^{2+} . Similar to Streeter (1998), Ca^{2+} -treated plants contained higher Ca^{2+} concentrations in shoots than control plants. In the first experiment, the nodule N concentration in Ca^{2+} -treated plants was increased compared to control plants, but this effect was not reproducible. The difference of the first experiment may have been caused by positional effects, for example with respect to the position of supplemental lighting. According to the results of the experiments in this thesis, high Ca^{2+} availability has no effect on N_2 fixation. However, this does not mean that Ca^{2+} is not involved in the regulation of N_2 fixation. To generate a Ca^{2+} signal, Ca^{2+} ions move from internal or external stores into the cytosol and are pumped back. For this mechanism, a moderate Ca^{2+} supply is sufficient.

4.5 The pros and cons of current hypotheses on the regulation of N_2 fixation

4.5.1 N feedback

The N feedback hypothesis is supported by experiments in which N remobilization from lower leaves to nodules was observed, when reduction of N_2 fixation rate was induced by leaf darkening (Fischinger et al., 2006). Such experiments implicate that N_2 fixation is regulated by the N shoot status. However, detopping plants also results in a down-regulation of the N_2 fixation. Upon removal of all aboveground parts of *M. sativa* plants, Curioni et al. (1999) measured a down-regulation of the N_2 fixation within the following two hours. This down-regulation cannot be a result of amino acids translocated from the shoot, because the shoot was removed completely. Furthermore, Fischinger et al. (2006) did not measure the nitrogenase activity continuously, instead they calculated the N_2 fixation from the N increment of the whole plant. Hence the time point of the down regulation of the N_2 fixation is unknown. If the nitrogenase activity was down regulated within the first day of the treatment, the remobilization of N could be a result of decreasing N concentration and a decreased N supply of roots and nodules. The down-regulation of N_2 fixation results a drastic decrease in N supply for the entire plant, inducing a N remobilization from older leaves to sinks, such as growing organs, like younger leaves and roots, as demonstrated for N-deficient

4. Discussion

plants (Vouillot and Devienne-Barret, 1999). Indeterminate nodules possess a meristematic zone and consequently, are growing organs with N demand that may be the cause of N retranslocation.

4.5.2 Regulation by oxygen

In nodules, the O₂ concentration is regulated by three mechanisms: a) a diffusion barrier in the cortex, b) O₂-binding leghemoglobin (Lb) in the cytosol of infected nodule cells, and c) the activity of cytochrome c oxidase, including the arrangement of plant mitochondria close to the plasma membrane of infected cells. A current hypothesis suggests the reduction of the O₂ supply for bacterial respiration and consequently a decreased ATP production, resulting in a lower energy supply of nitrogenase. This would mean that one of the above-mentioned mechanisms is changed by the plant to reduce the cytosolic pO₂ of infected nodule cells. For instance, Iannetta et al. (1993) showed correlation between an increased oxygen diffusion resistance and occlusion of intercellular space by glycoprotein in the nodule cortex of *Lupinus albus* plants stressed by low temperature, detopping, darkness, and KNO₃⁻ exposure. The Lb amount is flexible and thus a possible mechanism to regulate N₂ fixation. As mentioned in the introduction, RNAi lines with severely reduced levels of Lb show symptoms of N deficiency under symbiotic conditions (Ott et al., 2005). The authors suggest that Lb is responsible for transport of O₂ to the bacteroids. Slightly decreased Lb abundance may restrict the facilitated diffusion of O₂ in the infected cell, what remains to be tested. An impeded delivery of O₂ to its targets would be expected to cause an increase in cellular pO₂. However, Layzell et al. (1990) measured a decline of pO₂ in infected cells after nitrate treatment, suggesting a decreased O₂ entry due to a more stringent diffusion barrier. This may in turn demand lower amounts of Lb. Accordingly, Cabeza et al. (2014) found a down-regulation of all genes encoding Lb after nitrate treatment. Both studies show that there is a relation between O₂ and nitrogenase activity, but it is unclear if the changes in pO₂ are the cause or the consequence of the regulatory mechanism.

A regulation of nitrogenase activity by high O₂ levels may also be possible. The nitrogenase can be irreversibly damaged if exposed to high O₂ concentrations over a long time period. However, short exposure to O₂ inhibits the nitrogenase activity reversibly, and the enzyme recovers within 40-60 min (Denison et al., 1992; King et al., 1988). It remains to

4. Discussion

be shown, if a fast and short inhibition of the nitrogenase activity is a physiologically relevant response to sudden stimuli, such as wounding of the plant.

4.6 Considerations on the regulation of N₂ fixation

In general, two notions should be taken into consideration: i) different stimuli may trigger different signal transduction pathways and ii) different signal pathways may occur simultaneously. If the whole shoot is removed, a signaling pathway based on shoot-root communication can be excluded. In that case, nitrogenase activity should be decreased by a nodule-internal regulation (e.g. by O₂). A shoot-root interaction is more likely if just some leaves are removed or other stimuli are perceived by the shoot (e.g. darkness). Stimuli first recognized by the root (e.g. nitrate supply) may trigger regulation pathways based on root-nodule interaction or root-shoot-nodule interaction or both. It can hence be assumed that plants induce two or more pathways to decrease the N₂ fixation. Gordon et al. (1997) measured reduced mRNA levels of sucrose synthase and Lbs in nodules of soybean treated with nitrate or exposed to drought and salt stress. Thus, the authors proposed that N₂ fixation is regulated by O₂ barriers and the sucrose metabolism. Interestingly, the extent of the reduction of Lb mRNA levels differed in dependence of the treatment. While salt treatment triggered the greatest reduction of Lb mRNA levels, drought stress induced a lesser reduction and nitrate treatment just a slightly reduction. However, as this analysis was performed six days after the treatments, it could be rather the result of decreased nitrogenase activity than its cause. Cabeza et al. (2014) measured a first decline of nitrogenase activity after 4h and a second decline after 28h of nitrate application. After 4h the expression of genes encoding Lbs was reduced, indicating that Lbs might be involved in the regulation of the second decline and that the first decline might be induced by a different regulatory mechanism. Furthermore, different stimuli may trigger different regulatory pathways. For instance, in contrast to the observations of Cabeza et al. (2014), who found a decline in Lb mRNA levels after nitrate treatment, in experiments of González et al. (1995) on soybean, drought stress did not cause a reduction in Lb protein abundance over eleven days.

To discover regulatory mechanisms of N₂ fixation, nitrogenase activity should be measured continuously before, during, and after the treatment to detect the very first

4. Discussion

decline and possible further declines. The time between the treatment and the decline of nitrogenase activity is the time in which the investigations should be performed. Not just the expression of genes and the abundance of proteins during this time should be investigated. First signals, which happen directly upon or in a very short time after the stimulus, may rather be realized by ion fluxes and the generation of regulatory molecules, such as reactive oxygen species or nitric oxide. Calcium signals in the cytosol and in cellular compartments are likely to play a central role in this respect. Besides a possible regulatory role in the symbiosome space, Ca^{2+} elevations may post translationally regulate nodule proteins, e.g. by phosphorylation. Furthermore, phytohormones should be investigated. For instance, abscisic acid (ABA) was shown to decrease the N_2 fixation rate if supplied exogenously to pea nodules (González et al., 2001). In plants, ABA is involved in the response to drought stress, a stimulus which also induces reduction of N_2 fixation.

Outlook

The investigation of mutant plants is the next logical step in a continuation of this thesis. These mutants may be ordered or created by CRISPR/Cas9. An appropriate plasmid containing the reporter gene encoding EGFP for detection of transformed roots was generated and sgRNAs of *MA4* were designed during this thesis. Mutant plants can be generated with this plasmid by transient root transformation, but a better, yet technically demanding, option to generate mutant nodules would be by stable transformation. In this way a high number of mutant plants could be generated reproducibly. Experiments with these mutants may then be performed without the long transformation procedure required for transient expression.

After the generation of mutants, Ca^{2+} transport activity of *ma4* symbiosomes ought to be analysed to assess whether MA4 operates non-redundantly. If *ma4* symbiosomes still show Ca^{2+} -ATPase activity, a search for other Ca^{2+} -ATPases operating in parallel needs to be pursued and mutants for those genes generated. For an analysis of the dependence of Ca^{2+} signals on MA4, more suitable alternatives to aequorin and R-GECO as Ca^{2+} reporters may be tested once they become available. With respect to the physiological role of MA4, different treatments inducing the down-regulation of N_2 fixation (e.g. drought stress, nitrate treatment, or wounding) could be performed with *ma4* mutant and wild type plants. Subsequently, the nitrogenase activity of *ma4* and wild type should be measured, e.g. by acetylene reduction assay, but more ideally by H_2 evolution. To avoid extensive stress by removing roots from soil or sand, aeroponic or hydroponic growth systems should be preferred. The hydroponic culture for *M. truncatula* was established during this thesis. Experiments allowing a precise estimation of nitrogenase activity after different treatments are necessary. How much time goes by until a decline of nitrogenase activity is measurable? Does this time frame differ dependent on the treatment? Is the down-regulation continuous or stepwise? To answer these questions, the nitrogenase activity should be measured continuously, e.g. by measuring the H_2 evolution. Precise knowledge about the temporal kinetics of the regulation of nitrogenase activity would be helpful to dissect the regulatory mechanisms that induce a down-regulation.

References

- Abd-Alla, M. H., Koyro, H. W., Yan, F., Schubert, S., and Peiter, E. (2000). Functional structure of the indeterminate *Vicia faba* L. root nodule: implications for metabolite transport. *Journal of Plant Physiology* **157**, 335-343.
- Almeida, J. P. F., Hartwig, U. A., Frehner, M., Nösberger, J., and Lüscher, A. (2000). Evidence that P deficiency induces N feedback regulation of symbiotic N₂ fixation in white clover (*Trifolium repens* L.). *Journal of Experimental Botany* **51**, 1289-1297.
- Amberger, A. (1996). Pflanzenernährung (4. Auflage Ausg.). Stuttgart: Ulmer-Verlag.
- Bacanamwo, M., and Harper, J. E. (1996). Regulation of nitrogenase activity in Bradyrhizobium japonicum/soybean symbiosis by plant N status as determined by shoot C: N ratio. *Physiologia Plantarum* **98**, 529-538.
- Bacanamwo, M., and Harper, J. E. (1997). The feedback mechanism of nitrate inhibition of nitrogenase activity in soybean may involve asparagine and/or products of its metabolism. *Physiologia Plantarum* **100**, 371-377.
- Banath, C. L., Greenwood, E., and Loneraga, J. (1966). Effects of calcium deficiency on symbiotic nitrogen fixation. *Plant Physiology* **41**, 760-&.
- Becker, A., Berges, H., Krol, E., Bruand, C., Ruberg, S., Capela, D., Lauber, E., Meilhoc, E., Ampe, F., de Bruijn, F. J., Fourment, J., Francez-Charlot, A., Kahn, D., Kuster, H., Liebe, C., Puhler, A., Weidner, S., and Batut, J. (2004). Global changes in gene expression in *Sinorhizobium meliloti* 1021 under microoxic and symbiotic conditions. *Molecular Plant-Microbe Interactions* **17**, 292-303.
- Benedito, V. A., Torres-Jerez, I., Murray, J. D., Andriankaja, A., Allen, S., Kakar, K., Wandrey, M., Verdier, J., Zuber, H., Ott, T., Moreau, S., Niebel, A., Frickey, T., Weiller, G., He, J., Dai, X., Zhao, P. X., Tang, Y., and Udvardi, M. K. (2008). A gene expression atlas of the model legume *Medicago truncatula*. *Plant Journal* **55**, 504-513.
- Boisson-Dernier, A., Chabaud, M., Garcia, F., Becard, G., Rosenberg, C., and Barker, D. G. (2001). *Agrobacterium rhizogenes*-transformed roots of *Medicago truncatula* for the study of nitrogen-fixing and endomycorrhizal symbiotic associations. *Molecular Plant-Microbe Interactions* **14**, 695-700.
- Buchanan, B. B., Gruissem, W., and Jones, R. L. (2000). "Biochemistry and molecular biology of plants," John Wiley & sons.
- Bushart, T., Cannon, A., Clark, G., and Roux, S. (2014). Structure and function of CrACA1, the major PM-type Ca₂⁺-ATP ase, expressed at the peak of the gravity-directed trans-cell calcium current in spores of the fern *Ceratopteris richardii*. *Plant Biology* **16**, 151-157.
- Cabeza, R., Koester, B., Liese, R., Lingner, A., Baumgarten, V., Dirks, J., Salinas-Riester, G., Pommerenke, C., Dittert, K., and Schulze, J. (2014). An RNA sequencing transcriptome analysis reveals novel insights into molecular aspects of the nitrate impact on the nodule activity of *Medicago truncatula*. *Plant Physiology* **164**, 400-11.
- Cantero, A., Barthakur, S., Bushart, T. J., Chou, S., Morgan, R. O., Fernandez, M. P., Clark, G. B., and Roux, S. J. (2006). Expression profiling of the *Arabidopsis* annexin gene family during germination, de-etiolation and abiotic stress. *Plant Physiology and Biochemistry* **44**, 13-24.
- Capoen, W., Sun, J., Wysham, D., Otegui, M. S., Venkateshwaran, M., Hirsch, S., Miwa, H., Downie, J. A., Morris, R. J., Ane, J.-M., and Oldroyd, G. E. D. (2011). Nuclear membranes control symbiotic calcium signaling of legumes. *Proceedings of the National Academy of Sciences of the United States of America* **108**, 14348-14353.
- Charpentier, M., Sun, J., Martins, T. V., Radhakrishnan, G. V., Findlay, K., Soumpourou, E., Thouin, J., Véry, A.-A., Sanders, D., and Morris, R. J. (2016). Nuclear-localized cyclic nucleotide-gated channels mediate symbiotic calcium oscillations. *Science* **352**, 1102-1105.
- Choi, W.-G., Toyota, M., Kim, S.-H., Hilleary, R., and Gilroy, S. (2014). Salt stress-induced Ca²⁺ waves are associated with rapid, long-distance root-to-shoot signaling in plants. *Proceedings of the National Academy of Sciences* **111**, 6497-6502.

References

- Clarke, V. C., Loughlin, P. C., Day, D. A., and Smith, P. M. (2014). Transport processes of the legume symbiosome membrane. *Frontiers in Plant Science* **5**, 699.
- Clarke, V. C., Loughlin, P. C., Gavrin, A., Chen, C., Brear, E. M., Day, D. A., and Smith, P. M. (2015). Proteomic analysis of the soybean symbiosome identifies new symbiotic proteins. *Molecular & Cellular Proteomics* **14**, 1301-1322.
- Colquhoun, D., and Sivilotti, L. G. (2004). Function and structure in glycine receptors and some of their relatives. *Trends in Neurosciences* **27**, 337-344.
- Cukkemane, A., Seifert, R., and Kaupp, U. B. (2011). Cooperative and uncooperative cyclic-nucleotide-gated ion channels. *Trends in Biochemical Sciences* **36**, 55-64.
- Cullimore, J. V., Ranjeva, R., and Bono, J.-J. (2001). Perception of lipo-chitooligosaccharidic Nod factors in legumes. *Trends in Plant Science* **6**, 24-30.
- Cunningham, K. W., and Fink, G. R. (1994). Calcineurin-dependent growth control in *Saccharomyces cerevisiae* mutants lacking PMC1, a homolog of plasma membrane Ca²⁺ ATPases. *Journal of Cell Biology* **124**, 351-363.
- Curioni, P. M., Hartwig, U. A., Nösberger, J., and Schuller, K. A. (1999). Glycolytic flux is adjusted to nitrogenase activity in nodules of detopped and argon-treated alfalfa plants. *Plant Physiology* **119**, 445-454.
- de Philip, P., Batut, J., and Boistard, P. (1990). *Rhizobium meliloti* FixL is an oxygen sensor and regulates *R. meliloti* nifA and fixK genes differently in *Escherichia coli*. *Journal of Bacteriology* **172**, 4255-4262.
- DeFalco, T. A., Marshall, C. B., Munro, K., Kang, H.-G., Moeder, W., Ikura, M., Snedden, W. A., and Yoshioka, K. (2016). Multiple calmodulin-binding sites positively and negatively regulate *Arabidopsis* cyclic nucleotide-gated channel 12. *The Plant Cell* **28**, 1738-1751.
- Demidchik, V., Shabala, S., Isayenkov, S., Cuin, T. A., and Pottosin, I. (2018). Calcium transport across plant membranes: mechanisms and functions. *New Phytologist* **220**, 49-69.
- Denison, R. F., Witty, J. F., and Minchin, F. R. (1992). Reversible O₂ inhibition of nitrogenase activity in attached soybean nodules. *Plant Physiology* **100**, 1863-1868.
- Dixon, R., and Kahn, D. (2004). Genetic regulation of biological nitrogen fixation. *Nature Reviews Microbiology* **2**, 621-631.
- Ehrhardt, D. W., Wais, R., and Long, S. R. (1996). Calcium spiking in plant root hairs responding to *Rhizobium* nodulation signals. *Cell* **85**, 673-681.
- Elsen, S., Dischert, W., Colbeau, A., and Bauer, C. E. (2000). Expression of uptake hydrogenase and molybdenum nitrogenase in *Rhodobacter capsulatus* is coregulated by the RegB-RegA two-component regulatory system. *Journal of Bacteriology* **182**, 2831-2837.
- Fedorova, E., Thomson, R., Whitehead, L. F., Maudoux, O., Udvardi, M. K., and Day, D. A. (1999). Localization of H⁺-ATPases in soybean root nodules. *Planta* **209**, 25-32.
- Fischinger, S. A., Drevon, J.-J., Claassen, N., and Schulze, J. (2006). Nitrogen from senescing lower leaves of common bean is re-translocated to nodules and might be involved in a N-feedback regulation of nitrogen fixation. *Journal of Plant Physiology* **163**, 987-995.
- Frank, J., Happeck, R., Meier, B., Hoang, M. T. T., Stribny, J., Hause, G., Ding, H., Morsomme, P., Baginsky, S., and Peiter, E. (2019). Chloroplast-localized BICAT proteins shape stromal calcium signals and are required for efficient photosynthesis. *New Phytologist* **221**, 866-880.
- Galon, Y., Nave, R., Boyce, J. M., Nachmias, D., Knight, M. R., and Fromm, H. (2008). Calmodulin-binding transcription activator (CAMTA) 3 mediates biotic defense responses in *Arabidopsis*. *FEBS Letters* **582**, 943-948.
- Geiger, D., Scherzer, S., Mumm, P., Marten, I., Ache, P., Matschi, S., Liese, A., Wellmann, C., Al-Rasheid, K., and Grill, E. (2010). Guard cell anion channel SLAC1 is regulated by CDPK protein kinases with distinct Ca²⁺ affinities. *Proceedings of the National Academy of Sciences* **107**, 8023-8028.
- González, E., Gordon, A., James, C., and Arrese-Lgor, C. (1995). The role of sucrose synthase in the response of soybean nodules to drought. *Journal of Experimental Botany* **46**, 1515-1523.

References

- González, E. M., Gálvez, L., and Arrese-Igor, C. (2001). Abscisic acid induces a decline in nitrogen fixation that involves leghaemoglobin, but is independent of sucrose synthase activity. *Journal of Experimental Botany* **52**, 285-293.
- Gordon, A. J., Minchin, F. R., Skot, L., and James, C. L. (1997). Stress-induced declines in soybean N₂ fixation are related to nodule sucrose synthase activity. *Plant Physiology* **114**, 937-946.
- Gorecka, K. M., Thouverey, C., Buchet, R., and Pikula, S. (2007). Potential role of annexin AnnAt1 from *Arabidopsis thaliana* in pH-mediated cellular response to environmental stimuli. *Plant Cell Physiology* **48**, 792-803.
- Guo, J., Zeng, W., Chen, Q., Lee, C., Chen, L., Yang, Y., Cang, C., Ren, D., and Jiang, Y. (2016). Structure of the voltage-gated two-pore channel TPC1 from *Arabidopsis thaliana*. *Nature* **531**, 196-201.
- Hakoyama, T., Niimi, K., Watanabe, H., Tabata, R., Matsubara, J., Sato, S., Nakamura, Y., Tabata, S., Jichun, L., Matsumoto, T., Tatsumi, K., Nomura, M., Tajima, S., Ishizaka, M., Yano, K., Imaizumi-Anraku, H., Kawaguchi, M., Kouchi, H., and Suganuma, N. (2009). Host plant genome overcomes the lack of a bacterial gene for symbiotic nitrogen fixation. *Nature* **462**, 514.
- Halfter, U., Ishitani, M., and Zhu, J.-K. (2000). The *Arabidopsis* SOS2 protein kinase physically interacts with and is activated by the calcium-binding protein SOS3. *Proceedings of the National Academy of Sciences* **97**, 3735-3740.
- Han, J.-S., and Kim, C. K. (2008). Enhanced accumulation of metals in bottle gourd plants expressing an *Arabidopsis* cation/H exchanger. *Transgenic Plant Journal* **2**, 165-169.
- Hartmann, K., Peiter, E., Koch, K., Schubert, S., and Schreiber, L. (2002). Chemical composition and ultrastructure of broad bean (*Vicia faba* L.) nodule endodermis in comparison to the root endodermis. *Planta* **215**, 14-25.
- Hartwig, U. A., Heim, I., Lüscher, A., and Nösberger, J. (1994). The nitrogen-sink is involved in the regulation of nitrogenase activity in white clover after defoliation. *Physiologia Plantarum* **92**, 375-382.
- Hayashi, T., Banba, M., Shimoda, Y., Kouchi, H., Hayashi, M., and Imaizumi-Anraku, H. (2010). A dominant function of CCaMK in intracellular accommodation of bacterial and fungal endosymbionts. *The Plant Journal* **63**, 141-154.
- He, J., Rössner, N., Hoang, M. T., Alejandro, S., and Peiter, E. (2021). Transport, functions, and interaction of calcium and manganese in plant organellar compartments. *Plant Physiology* **187**, 1940-1972.
- Heath, K. D., Burke, P. V., and Stinchcombe, J. R. (2012). Coevolutionary genetic variation in the legume-rhizobium transcriptome. *Molecular Ecology* **21**, 4735-47.
- Hepler, P. (1994). The role of calcium in cell division. *Cell Calcium* **16**, 322-330.
- Heytler, P. G., and Hardy, R. W. (1984). Calorimetry of nitrogenase-mediated reductions in detached soybean nodules. *Plant Physiology* **75**, 304-310.
- Hill, S., Austin, S., Eydmann, T., Jones, T., and Dixon, R. (1996). *Azotobacter vinelandii* NIFL is a flavoprotein that modulates transcriptional activation of nitrogen-fixation genes via a redox-sensitive switch. *Proceedings of the National Academy of Sciences* **93**, 2143-2148.
- Ho, C.-H., and Frommer, W. B. (2014). Fluorescent sensors for activity and regulation of the nitrate transceptor CHL1/NRT1.1 and oligopeptide transporters. *Elife* **3**, e01917.
- Howitt, S. M., Udvardi, M. K., Day, D. A., and Gresshoff, P. M. (1986). Ammonia transport in free-living and symbiotic *Rhizobium* sp. ANU289. *Microbiology* **132**, 257-261.
- Hwang, J. H., Ellingson, S. R., and Roberts, D. M. (2010). Ammonia permeability of the soybean nodulin 26 channel. *FEBS Letters* **584**, 4339-43.
- Iannetta, P., De Lorenzo, C., James, E., Fernández-Pascual, M., Sprent, J. I., Lucas, M. M., Witty, J., De Felipe, M., and Minchin, F. R. (1993). Oxygen diffusion in lupin nodules: I. Visualization of diffusion barrier operation. *Journal of Experimental Botany* **44**, 1461-1467.
- Jefferson, R. A., Kavanagh, T. A., and Bevan, M. W. (1987). GUS fusions: beta-glucuronidase as a sensitive and versatile gene fusion marker in higher plants. *The EMBO Journal* **6**, 3901-3907.

References

- Johnson, N. A., Liu, F., Weeks, P. D., Hentzen, A. E., Kruse, H. P., Parker, J. J., Laursen, M., Nissen, P., Costa, C. J., and Gatto, C. (2009). A tomato ER-type Ca^{2+} -ATPase, LCA1, has a low thapsigargin-sensitivity and can transport manganese. *Archives of Biochemistry and Biophysics* **481**, 157-168.
- Kiep, V., Vadassery, J., Lattke, J., Maaß, J. P., Boland, W., Peiter, E., and Mithöfer, A. (2015). Systemic cytosolic Ca^{2+} elevation is activated upon wounding and herbivory in *Arabidopsis*. *New Phytologist* **207**, 996-1004.
- King, B. J., Hunt, S., Weagle, G. E., Walsh, K. B., Pottier, R. H., Canvin, D. T., and Layzell, D. B. (1988). Regulation of O_2 concentration in soybean nodules observed by *in situ* spectroscopic measurement of leghemoglobin oxygenation. *Plant Physiology* **87**, 296-299.
- Kiss, J. Z., Hertel, R., and Sack, F. D. (1989). Amyloplasts are necessary for full gravitropic sensitivity in roots of *Arabidopsis thaliana*. *Planta* **177**, 198-206.
- Knoblauch, M., Peters, W. S., Ehlers, K., and van Bel, A. J. (2001). Reversible calcium-regulated stopcocks in legume sieve tubes. *The Plant Cell* **13**, 1221-1230.
- Kovács, I., Ayaydin, F., Oberschall, A., Ipacs, I., Bottka, S., Pongor, S., Dudits, D., and Tóth, É. C. (1998). Immunolocalization of a novel annexin-like protein encoded by a stress and abscisic acid responsive gene in alfalfa. *The Plant Journal* **15**, 185-197.
- Kuzma, M. M., Hunt, S., and Layzell, D. B. (1993). Role of oxygen in the limitation and inhibition of nitrogenase activity and respiration rate in individual soybean nodules. *Plant Physiology* **101**, 161-169.
- Laohavisit, A., Richards, S. L., Shabala, L., Chen, C., Colaço, R. D., Swarbreck, S. M., Shaw, E., Dark, A., Shabala, S., and Shang, Z. (2013). Salinity-induced calcium signaling and root adaptation in *Arabidopsis* require the calcium regulatory protein annexin1. *Plant Physiology* **163**, 253-262.
- Lawn, R., and Brun, W. A. (1974). Symbiotic Nitrogen Fixation in Soybeans. I. Effect of Photosynthetic Source-Sink Manipulations 1. *Crop Science* **14**, 11-16.
- Layzell, D. B., Hunt, S., and Palmer, G. R. (1990). Mechanism of nitrogenase inhibition in soybean nodules: pulse-modulated spectroscopy indicates that nitrogenase activity is limited by O_2 . *Plant Physiology* **92**, 1101-1107.
- Leitão, N., Dangeville, P., Carter, R., and Charpentier, M. (2019). Nuclear calcium signatures are associated with root development. *Nature communications* **10**, 1-9.
- Li, J., Long, Y., Qi, G.-N., Li, J., Xu, Z.-J., Wu, W.-H., and Wang, Y. (2014). The Os-AKT1 channel is critical for K^+ uptake in rice roots and is modulated by the rice CBL1-CIPK23 complex. *The Plant Cell* **26**, 3387-3402.
- Liang, F., Cunningham, K. W., Harper, J. F., and Sze, H. (1997). ECA1 complements yeast mutants defective in Ca^{2+} pumps and encodes an endoplasmic reticulum-type Ca^{2+} -ATPase in *Arabidopsis thaliana*. *Proceedings of the National Academy of Sciences* **94**, 8579-8584.
- Limonta, M., Romanowsky, S., Olivari, C., Bonza, M. C., Luoni, L., Rosenberg, A., Harper, J. F., and De Michelis, M. I. (2014). ACA12 is a deregulated isoform of plasma membrane Ca^{2+} -ATPase of *Arabidopsis thaliana*. *Plant Molecular Biology* **84**, 387-397.
- Limpens, E., Moling, S., Hooiveld, G., Pereira, P. A., Bisseling, T., Becker, J. D., and Kuster, H. (2013). Cell- and tissue-specific transcriptome analyses of *Medicago truncatula* root nodules. *PLoS One* **8**, e64377.
- Loneragan, J. (1959). Calcium in the nitrogen metabolism of subterranean clover. *Australian Journal of Biological Sciences* **12**, 26-39.
- Marino, D., Frendo, P., Ladrera, R., Zabalza, A., Puppo, A., Arrese-Igor, C., and González, E. M. (2007). Nitrogen fixation control under drought stress. Localized or systemic? *Plant Physiology* **143**, 1968-1974.
- McAinsh, M. R., and Pittman, J. K. (2009). Shaping the calcium signature. *New Phytologist* **181**, 275-294.
- Millar, A., Day, D., and Bergersen, F. (1995). Microaerobic respiration and oxidative phosphorylation by soybean nodule mitochondria: implications for nitrogen fixation. *Plant, Cell & Environment* **18**, 715-726.

References

- Miller, R. W., and Sirois, J. C. (1983). Calcium and magnesium effects on symbiotic nitrogen-fixation in the Alfalfa (*Medicago-sativa*) - *Rhizobium-meliloti* system. *Physiologia Plantarum* **58**, 464-470.
- Mills, R. F., Doherty, M. L., Lopez-Marques, R. L., Weimar, T., Dupree, P., Palmgren, M. G., Pittman, J. K., and Williams, L. E. (2008). ECA3, a Golgi-localized P-2A-type ATPase, plays a crucial role in manganese nutrition in *Arabidopsis*. *Plant Physiology* **146**, 116-128.
- Minet, M., Dufour, M. E., and Lacroute, F. (1992). Complementation of *Saccharomyces cerevisiae* auxotrophic mutants by *Arabidopsis thaliana* cDNAs. *The Plant Journal* **2**, 417-422.
- Montanez, A., Danso, S., and Hardarson, G. (1995). The effect of temperature on nodulation and nitrogen fixation by five *Bradyrhizobium japonicum* strains. *Applied Soil Ecology* **2**, 165-174.
- Nallu, S., Silverstein, K. A., Samac, D. A., Bucciarelli, B., Vance, C. P., and VandenBosch, K. A. (2013). Regulatory patterns of a large family of defensin-like genes expressed in nodules of *Medicago truncatula*. *PLoS One* **8**, e60355.
- Niemietz, C. M., and Tyerman, S. D. (2000). Channel-mediated permeation of ammonia gas through the peribacteroid membrane of soybean nodules. *FEBS Letters* **465**, 110-114.
- Nouwen, N., Arrighi, J.-F., Cartieaux, F., Chaintreuil, C., Gully, D., Klopp, C., and Giraud, E. (2017). The role of rhizobial (NifV) and plant (FEN1) homocitrate synthases in *Aeschynomene*/photosynthetic *Bradyrhizobium* symbiosis. *Scientific Reports* **7**, 448.
- Ott, T., van Dongen, J. T., Gunther, C., Krusell, L., Desbrosses, G., Vigeolas, H., Bock, V., Czechowski, T., Geigenberger, P., and Udvardi, M. K. (2005). Symbiotic leghemoglobins are crucial for nitrogen fixation in legume root nodules but not for general plant growth and development. *Current Biology* **15**, 531-5.
- Peiter, E., Maathuis, F. J., Mills, L. N., Knight, H., Pelloux, J., Hetherington, A. M., and Sanders, D. (2005). The vacuolar Ca²⁺-activated channel TPC1 regulates germination and stomatal movement. *Nature* **434**, 404-408.
- Peiter, E., and Schubert, S. (2003). Sugar uptake and proton release by protoplasts from the infected zone of *Vicia faba* L. nodules: evidence against apoplastic sugar supply of infected cells. *Journal of Experimental Botany* **54**, 1691-1700.
- Peiter, E., Yan, F., and Schubert, S. (2004). Amino acid export from infected cells of *Vicia faba* root nodules: Evidence for an apoplastic step in the infected zone. *Physiologia Plantarum* **122**, 107-114.
- Perdue, D. O., LaFavre, A. K., and Leopold, A. C. (1988). Calcium in the regulation of gravitropism by light. *Plant Physiology* **86**, 1276-1280.
- Pichon, M., Journet, E.-P., Dedieu, A., de Billy, F., Truchet, G., and Barker, D. G. (1992). *Rhizobium meliloti* elicits transient expression of the early nodulin gene ENOD12 in the differentiating root epidermis of transgenic alfalfa. *The Plant Cell* **4**, 1199-1211.
- Preťová, A., Obert, B., and Wetzstein, H. (2003). Substrate infiltration and histological fixatives affect the *in situ* localisation of β -Glucuronidase activity in transgenic tissues. *Acta Biotechnologica* **23**, 383-388.
- Qi, Z., Stephens, N. R., and Spalding, E. P. (2006). Calcium entry mediated by GLR3. 3, an *Arabidopsis* glutamate receptor with a broad agonist profile. *Plant Physiology* **142**, 963-971.
- Qiu, Q.-S., Guo, Y., Dietrich, M. A., Schumaker, K. S., and Zhu, J.-K. (2002). Regulation of SOS1, a plasma membrane Na⁺/H⁺ exchanger in *Arabidopsis thaliana*, by SOS2 and SOS3. *Proceedings of the National Academy of Sciences* **99**, 8436-8441.
- Riely, B. K., Lougnon, G., Ane, J. M., and Cook, D. R. (2007). The symbiotic ion channel homolog DMI1 is localized in the nuclear membrane of *Medicago truncatula* roots. *Plant J* **49**, 208-16.
- Rivers, R. L., Dean, R. M., Chandy, G., Hall, J. E., Roberts, D. M., and Zeidel, M. L. (1997). Functional analysis of nodulin 26, an aquaporin in soybean root nodule symbiosomes. *Journal of Biological Chemistry* **272**, 16256-16261.
- Roux, B., Rodde, N., Jardinaud, M. F., Timmers, T., Sauviac, L., Cottret, L., Carrere, S., Sallet, E., Courcelle, E., Moreau, S., Debelle, F., Capela, D., de Carvalho-Niebel, F., Gouzy, J., Bruand, C., and Gamas, P. (2014). An integrated analysis of plant and bacterial gene expression in

References

- symbiotic root nodules using laser-capture microdissection coupled to RNA sequencing. *The Plant Journal* **77**, 817-37.
- Salvador-Recatalà, V. (2016). New roles for the Glutamate Receptor-like 3.3, 3.5, and 3.6 genes as on/off switches of wound-induced systemic electrical signals. *Plant Signaling & Behavior* **11**, e1161879.
- Samac, D. A., Tesfaye, M., Dornbusch, M., Saruul, P., and Temple, S. J. (2004). A comparison of constitutive promoters for expression of transgenes in alfalfa (*Medicago sativa*). *Transgenic Research* **13**, 349-361.
- Schilling, G. (2000). "Pflanzenernährung und Düngung: 164 Tabellen," Ulmer.
- Schindelin, H., Kisker, C., Schlessman, J. L., Howard, J. B., and Rees, D. C. (1997). Structure of ADP- AIF 4⁻-stabilized Nitrogenase Complex and its Implications for Signal Transduction. *Nature* **387**, 370-376.
- Schiøtt, M., and Palmgren, M. G. (2005). Two plant Ca²⁺ pumps expressed in stomatal guard cells show opposite expression patterns during cold stress. *Physiologia Plantarum* **124**, 278-283.
- Schulze, J. (2003). Source-sink manipulations suggest an N-feedback mechanism for the drop in N₂ fixation during pod-filling in pea and broad bean. *Journal of Plant Physiology* **160**, 531-537.
- Schulze, J. (2004). How are nitrogen fixation rates regulated in legumes? *Journal of Plant Nutrition and Soil Science* **167**, 125-137.
- Schwember, A. R., Schulze, J., Del Pozo, A., and Cabeza, R. A. (2019). Regulation of symbiotic nitrogen fixation in legume root nodules. *Plants* **8**, 333.
- Seabra, A. R., Pereira, P. A., Becker, J. D., and Carvalho, H. G. (2012). Inhibition of glutamine synthetase by phosphinothricin leads to transcriptome reprogramming in root nodules of *Medicago truncatula*. *Molecular Plant-Microbe Interactions* **25**, 976-92.
- Seals, D. F., Parrish, M. L., and Randall, S. K. (1994). A 42-kilodalton annexin-like protein is associated with plant vacuoles. *Plant Physiology* **106**, 1403-1412.
- Seigneurin-Berny, D., Rolland, N., Dorne, A.-J., and Joyard, J. (2000). Sulfolipid is a potential candidate for annexin binding to the outer surface of chloroplast. *Biochemical and Biophysical Research Communications* **272**, 519-524.
- Shigaki, T., Rees, I., Nakhleh, L., and Hirschi, K. (2006). Identification of three distinct phylogenetic groups of CAX cation/proton antiporters. *Journal of Molecular Evolution* **63**, 815-825.
- Shimomura, O., and Johnson, F. H. (1978). Peroxidized coelenterazine, the active group in the photoprotein aequorin. *Proceedings of the National Academy of Sciences* **75**, 2611-2615.
- Sinclair, W., Oliver, I., Maher, P., and Trewavas, A. (1996). The role of calmodulin in the gravitropic response of the *Arabidopsis thaliana* agr-3 mutant. *Planta* **199**, 343-351.
- Sinharoy, S., Torres-Jerez, I., Bandyopadhyay, K., Kereszt, A., Pislariu, C. I., Nakashima, J., Benedito, V. A., Kondorosi, E., and Udvardi, M. K. (2013). The C₂H₂ transcription factor regulator of symbiosome differentiation represses transcription of the secretory pathway gene VAMP721a and promotes symbiosome development in *Medicago truncatula*. *Plant Cell* **25**, 3584-601.
- Snapp, E. (2005). Design and use of fluorescent fusion proteins in cell biology. *Current Protocols in Cell Biology* **27**, 21.4. 1-21.4. 13.
- Streeter, J. G. (1985). Nitrate inhibition of legume nodule growth and activity: I. Long term studies with a continuous supply of nitrate. *Plant Physiology* **77**, 321-324.
- Streeter, J. G. (1998). Effect of elevated calcium concentration in infected cells of soybean (*Glycine max* (L.) Merr.) nodules on nitrogenase activity and N input to the plant. *Journal of Experimental Botany* **49**, 997-1003.
- Su, S.-H., Gibbs, N. M., Jancewicz, A. L., and Masson, P. H. (2017). Molecular mechanisms of root gravitropism. *Current Biology* **27**, R964-R972.
- Su, S.-H., Keith, M. A., and Masson, P. H. (2020). Gravity signaling in flowering plant roots. *Plants* **9**, 1290.

References

- Sulieman, S., Fischinger, S. A., Gresshoff, P. M., and Schulze, J. (2010). Asparagine as a major factor in the N-feedback regulation of N₂ fixation in *Medicago truncatula*. *Physiologia Plantarum* **140**, 21-31.
- Swem, L. R., Kraft, B. J., Swem, D. L., Setterdahl, A. T., Masuda, S., Knaff, D. B., Zaleski, J. M., and Bauer, C. E. (2003). Signal transduction by the global regulator RegB is mediated by a redox-active cysteine. *The EMBO Journal* **22**, 4699-4708.
- Tamura, K., Shimada, T., Ono, E., Tanaka, Y., Nagatani, A., Higashi, S. i., Watanabe, M., Nishimura, M., and Hara-Nishimura, I. (2003). Why green fluorescent fusion proteins have not been observed in the vacuoles of higher plants. *The Plant Journal* **35**, 545-555.
- Tapken, D., Anschuetz, U., Liu, L.-H., Huelsken, T., Seeböhm, G., Becker, D., and Hollmann, M. (2013). A Plant Homolog of Animal Glutamate Receptors Is an Ion Channel Gated by Multiple Hydrophobic Amino Acids. *Science Signaling* **6**.
- Tapken, D., and Hollmann, M. (2008). *Arabidopsis thaliana* glutamate receptor ion channel function demonstrated by ion pore transplantation. *Journal of Molecular Biology* **383**, 36-48.
- Taté, R., Riccio, A., Merrick, M., and Patriarca, E. J. (1998). The Rhizobium etli amtB gene coding for an NH₄⁺ transporter is down-regulated early during bacteroid differentiation. *Molecular Plant-Microbe Interactions* **11**, 188-198.
- Tejada-Jiménez, M., Castro-Rodríguez, R., Kryvoruchko, I., Lucas, M. M., Udvardi, M., Imperial, J., and González-Guerrero, M. (2015). *Medicago truncatula* natural resistance-associated macrophage Protein1 is required for iron uptake by rhizobia-infected nodule cells. *Plant Physiology* **168**, 258-272.
- Thonat, C., Mathieu, C., Crevecoeur, M., Penel, C., Gaspar, T., and Boyer, N. (1997). Effects of a mechanical stimulation on localization of annexin-like proteins in *Bryonia dioica* internodes. *Plant Physiology* **114**, 981-988.
- Tidow, H., Poulsen, L. R., Andreeva, A., Knudsen, M., Hein, K. L., Wiuf, C., Palmgren, M. G., and Nissen, P. (2012). A bimodular mechanism of calcium control in eukaryotes. *Nature* **491**, 468-472.
- Timmers, A., Auriac, M.-C., and Truchet, G. (1999). Refined analysis of early symbiotic steps of the Rhizobium-Medicago interaction in relationship with microtubular cytoskeleton rearrangements. *Development* **126**, 3617-3628.
- Tominaga, A., Nagata, M., Futsuki, K., Abe, H., Uchiumi, T., Abe, M., Kucho, K.-i., Hashiguchi, M., Akashi, R., and Hirsch, A. (2010). Effect of abscisic acid on symbiotic nitrogen fixation activity in the root nodules of *Lotus japonicus*. *Plant Signaling & Behavior* **5**, 440-443.
- Toyota, M., Spencer, D., Sawai-Toyota, S., Jiaqi, W., Zhang, T., Koo, A. J., Howe, G. A., and Gilroy, S. (2018). Glutamate triggers long-distance, calcium-based plant defense signaling. *Science* **361**, 1112-1115.
- Tuckerman, J. R., Gonzalez, G., Dioum, E. M., and Gilles-Gonzalez, M.-A. (2002). Ligand and oxidation-state specific regulation of the heme-based oxygen sensor FixL from *Sinorhizobium meliloti*. *Biochemistry* **41**, 6170-6177.
- Tyerman, S. D., Whitehead, L. F., and Day, D. A. (1995). A channel-like transporter for NH₄⁺ on the symbiotic interface of N₂-fixing plants. *Nature* **378**, 629-632.
- Urbina, D. C., Silva, H., and Meisel, L. A. (2006). The Ca²⁺ pump inhibitor, thapsigargin, inhibits root gravitropism in *Arabidopsis thaliana*. *Biological Research* **39**, 289-296.
- Vadez, V., Sinclair, T., and Serraj, R. (2000). Asparagine and ureide accumulation in nodules and shoots as feedback inhibitors of N₂ fixation in soybean. *Physiologia Plantarum* **110**, 215-223.
- Vance, C., and Heichel, G. (1991). Carbon in N₂ fixation: limitation or exquisite adaptation. *Annual Review of Plant Physiology and Plant Molecular Biology* **42**, 373-392.
- VandenBosch, K., and Newcomb, E. (1988). The occurrence of leghemoglobin protein in the uninfected interstitial cells of soybean root nodules. *Planta* **175**, 442-451.
- Vernoud, V., Journet, E.-P., and Barker, D. G. (1999). MtENOD20, a Nod factor-inducible molecular marker for root cortical cell activation. *Molecular Plant-Microbe Interactions* **12**, 604-614.

References

- Vouillot, M., and Devienne-Barret, F. (1999). Accumulation and remobilization of nitrogen in a vegetative winter wheat crop during or following nitrogen deficiency. *Annals of Botany* **83**, 569-575.
- Walsh, K. B., Vessey, J. K., and Layzell, D. B. (1987). Carbohydrate supply and N₂ fixation in soybean: the effect of varied daylength and stem girdling. *Plant Physiology* **85**, 137-144.
- Weaver, C. D., Crombie, B., Stacey, G., and Roberts, D. M. (1991). Calcium-dependent phosphorylation of symbiosome membrane proteins from nitrogen-fixing soybean nodules: evidence for phosphorylation of nodulin-26. *Plant Physiology* **95**, 222-227.
- White, P. J. (2001). The pathways of calcium movement to the xylem. *Journal of Experimental Botany* **52**, 891-899.
- Whitehead, L. F., Tyerman, S. D., and Day, D. A. (2001). Polyamines as potential regulators of nutrient exchange across the peribacteroid membrane in soybean root nodules. *Functional Plant Biology* **28**, 677-683.
- Wu, Z., Liang, F., Hong, B., Young, J. C., Sussman, M. R., Harper, J. F., and Sze, H. (2002). An endoplasmic reticulum-bound Ca²⁺/Mn²⁺ pump, ECA1, supports plant growth and confers tolerance to Mn²⁺ stress. *Plant Physiology* **130**, 128-137.
- Yandulov, D. V., and Schrock, R. R. (2003). Catalytic reduction of dinitrogen to ammonia at a single molybdenum center. *Science* **301**, 76-78.
- Yu, H., Yan, J., Du, X., and Hua, J. (2018). Overlapping and differential roles of plasma membrane calcium ATPases in Arabidopsis growth and environmental responses. *Journal of Experimental Botany* **69**, 2693-2703.
- Zhang, X.-Q., and Chollet, R. (1997). Seryl-phosphorylation of soybean nodule sucrose synthase (nodulin-100) by a Ca²⁺-dependent protein kinase. *FEBS Letters* **410**, 126-130.
- Zipfel, C., and Oldroyd, G. E. (2017). Plant signalling in symbiosis and immunity. *Nature* **543**, 328-336.

List of tables

Tab. 1 List of Organisms used in this work

Tab. 2 Stock solutions of Fahraeus medium

Tab. 3 Nutrient solution of hydroponic culture for *M. truncatula*

Tab. 4 Nutrient solution for *Vicia faba*

Tab. 5 Shuttle vectors for CRISPR/Cas9

Tab. 6 Putative Ca²⁺-permeable channels, transporters, and pumps of *Medicago truncatula*

Tab. 7 Putative *M. truncatula* Ca²⁺-ATPases with high homology to those localized in the symbiosome membrane of *G. max*

Tab. 8 List of candidate genes

Tab. A9 List of chemicals

Tab. A10 List of enzymes

Tab. A11 List of primers for qRT-PCR

Tab. A12 List of primers for amplification of UTRs

Tab. A13 List of primers for EGFP fusion constructs

Tab. A14 List of primers for promoter amplification

Tab. A15 List of primers for yeast complementation

Tab. A16 List of primers for sequencing

Tab. A17 List of sgRNAs for inducing a mutation of *MA4* by CRISPR/Cas9

Tab. A18 List of primers used for R-Geco cloning

List of figures

- Fig. 1 Communication between legumes and rhizobia for initiation of the nodulation.
- Fig. 2 Signal transduction at the beginning of the nodulation process.
- Fig. 3 Entrance of rhizobia into the plant cell by an endocytosis-like process.
- Fig. 4 Structure of an indeterminate nodule.
- Fig. 5 Nitrogen fixation by the enzyme complex nitrogenase.
- Fig. 6 Proposed N-feedback regulation of N₂ fixation by polyamines.
- Fig. 7 Ca²⁺ signatures triggered by different stimuli.
- Fig. 8 Proposed two-step activation mechanism of ACAs.
- Fig. 9 Topology of autoinhibitory Ca²⁺-ATPase (ACA).
- Fig. 10 Detection of [Ca²⁺]_{cyt} in *M. truncatula* roots transformed with *APOAEQUORIN*.
- Fig. 11 Detection of [Ca²⁺]_{cyt} in nodulated roots of *M. truncatula* plants transformed with *APOAEQUORIN*.
- Fig. 12 Phylogenetic tree of GLRs.
- Fig. 13 Phylogenetic tree of Ca²⁺-ATPases in *A. thaliana* (At) and *M. truncatula* (Medtr).
- Fig. 14 Expression of genes encoding putative Ca²⁺-ATPases present on the Affymetrix GeneChip.
- Fig. 15 Expression of genes encoding putative Ca²⁺-ATPases in the infected cells of the N₂ fixation zone.
- Fig. 16 Expression of genes encoding putative Ca²⁺-ATPases in infected cells of the N₂-fixation zone.
- Fig. 17 Scatterplot of expression of genes encoding putative Ca²⁺-ATPases present on the Affymetrix GeneChip.
- Fig. 18 Expression of genes encoding putative Ca²⁺-ATPases based on RNA-seq data.
- Fig. 19 Protein sequences of ATPases containing NLS.
- Fig. 20 Complementation of *S. cerevisiae* K616 by *M. truncatula* MA1.
- Fig. 21 Complementation of *S. cerevisiae* K616 by *M. truncatula* MA2.
- Fig. 22 Complementation of *S. cerevisiae* K616 by *M. truncatula* MA3.
- Fig. 23 Complementation of *S. cerevisiae* K616 by *M. truncatula* MA4 and MA5.
- Fig. 24 Analysis of the expression of the selected genes in root nodules.
- Fig. 25 GUS analysis of MA1 promoter activity.
- Fig. 26 GUS analysis of MA2 promoter activity.
- Fig. 27 GUS analysis of MA3 promoter activity.
- Fig. 28 GUS analysis of MA4 promoter activity.
- Fig. 29 GUS analysis of MA5 promoter activity.
- Fig. 30 Predicted topology of the Ca²⁺-ATPases MA1-MA5.
- Fig. 31 Confocal microscopic analysis of EGFP-MA1 fusion protein in the N₂ fixation zone of the nodule.
- Fig. 32 Confocal microscopic analysis of EGFP-MA2 fusion protein in the nodule.
- Fig. 33 Confocal microscopic analysis of EGFP-MA3 fusion protein in the N₂ fixation zone of the nodule.

List of figures

- Fig. 34 Confocal microscopic analysis of EGFP-MA4 fusion protein in the N₂ fixation zone of the nodule.
- Fig. 35 Confocal microscopic analysis of EGFP-MA5 fusion protein
- Fig. 36 PCR screen with 12 plants of the NF4429 line.
- Fig. 37 *M. truncatula* plants transformed with recipient vector containing *uidA*.
- Fig. 38 *Vicia faba* Ca²⁺ fertilization experiment on quartz sand.
- Fig. 39 *Vicia faba* Ca²⁺ fertilization experiment on soil/vermiculite mixture.
- Fig. 40 *Vicia faba* fertilization experiment 1 in hydroponic culture.
- Fig. 41 *Vicia faba* fertilization experiment 2 in hydroponic culture.
- Fig. 42 *Vicia faba* fertilization experiment 3 in hydroponic culture.
- Fig. 43 Localization of probe numbers in splice variants of MA3.
- Fig. 44 Hypothesis of the regulation of N₂ fixation by Ca²⁺-induced inhibition of the symbiosome NH₄⁺ channel.
- Fig. 45 Comparison of GFP signals localized in vacuoles of *A. thaliana* root hairs and EGFP:MA2 signals detected in *M. truncatula* nodules.
- Fig. A46 Phylogenetic tree of Annexins.
- Fig. A47 Phylogenetic tree of CAXs.
- Fig. A48 Phylogenetic tree of CNGCs.
- Fig. A49 Phylogenetic tree of BICATs.
- Fig. A50 Expression of genes encoding putative ANNEXINs.
- Fig. A51 Expression of genes encoding putative CAXs.
- Fig. A52 Expression of genes encoding putative CNGCs.
- Fig. A53 Expression of genes encoding putative GLRs.
- Fig. A54 Expression of genes encoding putative BICATs.
- Fig. A55 Expression of genes encoding aputative TPC1.

Summary

Legumes living in symbiosis with N₂-fixing rhizobia are able to decrease the N₂ fixation if they are supplied by other N sources or have a reduced N demand. Understanding the mechanism of this regulation process would be helpful in the generation of more efficient nodules. Cultivation of legumes modified in the regulation of N₂ fixation may also increase the N amounts for following crops and thereby decrease the usage of synthetic N fertilizers. The current hypotheses on the regulation of N₂ fixation are controversially debated. In this project, a new hypothesis based on the potential involvement of Ca²⁺ the regulation of nodule function, and in particular of the export of N from the bacteroids was advanced. As signal ion, Ca²⁺ may play a key role in the regulation of N₂ fixation by regulating this N transport step and is likely to have further targets. It was therefore attempted to establish a method to analyse [Ca²⁺]_{cyt} in intact nodules of *Medicago truncatula* based on the luminescent reporter aequorin or the fluorescent reporter R-GECO. Both approaches were unsuccessful. The measurements of [Ca²⁺]_{cyt} by aequorin failed probably due to the low O₂ concentration within nodules, while detection of R-GECO was hampered by heavy autofluorescence. The existence of a nodule-specific machinery to generate Ca²⁺ signals was analyzed. BLAST searches against putative Ca²⁺ transport proteins of Arabidopsis revealed families of putative Ca²⁺-permeable channels (22 CNGCs, 16 GLRs, 10 ANNs, 1 TPC1) transporters (12 CAXs, 3 BICATs) and pumps (20 Ca²⁺-ATPases) in *M. truncatula*. However, none of those genes was nodule-specifically expressed in published transcriptome analyses. Based on their proposed role to actively transport Ca²⁺ from the plant cytosol into the symbiosome space to inhibit an ammonium channel localized in the symbiosome membrane, putative Ca²⁺-ATPases were chosen for further investigation. In order to identify Ca²⁺-ATPases localized in the symbiosome membrane, five candidate genes with high homology to proteins of *Glycine max* previously suggested to be localized in this membrane, were investigated for their function, promoter activity, and subcellular localization by yeast complementation, promoter-GUS analysis, and EGFP fusion, respectively. All selected genes complemented a yeast mutant defective in Ca²⁺ transport. The genes showed different expression patterns and subcellular localizations in roots and nodules. Two of the candidate genes are expressed in infected cells of the N₂ fixation zone and localized in the symbiosome membrane. To obtain mutant plants for one of the genes, insertional mutants were ordered.

Summary

As these were devoid of an insert, vectors for CRISPR/Cas9-based genome editing were constructed, which are functional and will serve the further functional analysis of the function of this gene. In a further approach, it was examined whether elevated Ca^{2+} supply has an effect on N_2 fixation by *Vicia faba*. Plants supplied with excess Ca^{2+} concentration did not show altered growth and higher N concentration and thus, no altered N_2 fixation. However, moderate Ca^{2+} supply will be sufficient for Ca^{2+} to act as signal ion in regulating the N_2 fixation.

Appendix

Tab. A9 List of chemicals

Substance	Structure	Company	Cat. No.
2-propanol	C_3H_8O	Carl Roth	T910.1
3',5'-Dimethoxy-4'-hydroxyacetophenon (Acetosyringon)	$C_{10}H_{12}O_4$	Sigma-Aldrich	D134406
(4-(2-hydroxyethyl)-1-piperazineethanesulfonic acid)HEPES	$C_8H_{18}N_2O_4S$	Sigma-Aldrich	H3375
5-Brom-4-chlor-3-indolyl- β -D glucuronic acid (x-Gluc)	$C_{14}H_{13}BrClNO_7$	xGluc direct	P5264044
Ammonium molybdate	$(NH_4)_6Mo_7O_{24} \cdot 4 H_2O$	Fluka	09880
Ammonium nitrate	NH_4NO_3	Merck	1.01188.1000
Ampicillin sodium	$C_{16}H_{18}N_3OSNa_4$	Duchefa	A0104.0005
Ascorbat	$C_6H_8O_6$	Carl Roth	3525.1
Biozym Plaque agarose	-	Biozym Scientific	840101
Boric acid	H_3BO_3	Carl Roth	6943.1
Bovine serum albumin (BSA)	-	Carl Roth	T844.2
Calcium chloride dihydrate	$CaCl_2 \cdot 2H_2O$	Carl Roth	5239.1
Cobalt chloride	$CoCl_2 \cdot 6H_2O$	Riedel-deHaen	12914
Coelenterazine	$C_{26}H_{21}N_3O_3$	Carl Roth	4094.4
Complete Supplement Mixture (CSM) Drop-Out: -URA	-	Formedium™	DCS0169
Complete Supplement Mixture (CSM) -TRP/HIS/LEU/ADE	-	Formedium™	DCS1221
Copper sulfate	$CuSO_4 \cdot 5H_2O$	Fluka	61240
Dimethylsulfoxide (DMSO)	C_2H_6OS	Carl Roth	7029.1
Dipotassium hydrogenphosphate	$K_2HPO_4 \cdot 3 H_2O$	Merck	CAS 7758-11-4
Disodium hydrogen phosphate	$Na_2HPO_4 \cdot 2H_2O$	Fluka	0052689
Disodium molybdate	$Na_2MoO_4 \cdot 2H_2O$	Riedel-de Haen	31439
Dithiothreitol (DTT)	$C_4H_{10}O_2S_2$	Carl Roth	6908.3
Ethanol (molBio)	C_2H_6O	Carl Roth	9065.2
Ethylene glycol tetraacetic acid(EGTA)	$C_{14}H_{24}N_2O_{10}$	Carl Roth	3054.2
Ethylenediamine tetraacetic acid ferric(III)-sodium salt (EDTA)	$C_{10}H_{12}FeN_2NaO_8$	Duchefa	006835.05
Ferric citrate	$C_6H_5O_7Fe \cdot x H_2O$	Carl Roth	CAS 3522-50-7
Glucose	$C_6H_{12}O_6$	Carl Roth	HN06.2
Glycerol	$C_3H_8O_3$	Carl Roth	3783.2

Appendix

Hydrogen peroxide	H ₂ O ₂	Carl Roth	8070.1
Hygromycin B-Lösung 50 mg/L	C ₂₀ H ₃₇ N ₃ O ₁₃	Carl Roth	CP12.2
Iron-sodium EDTA	FeNaEDTA	Duchefa	E0509.1000
Kanamycin monosulfate	C ₁₈ H ₃₆ N ₄ O ₁₁ x H ₂ SO ₄	Carl Roth	T832.1
Magnesium sulfate	MgSO ₄ x 7 H ₂ O	Normapur	25165.292
Magnesium chloride	MgCl ₂	Fluka	63063
Manganese chloride	MnCl ₂ x 4H ₂ O	Carl Roth	T881.1
Manganese sulfate	MnSO ₄ x H ₂ O	Fluka	M7634
Mannitol	C ₆ H ₁₄ O ₆	Sigma-Aldrich	M1902
MES	C ₆ H ₁₃ NO ₄ S	Sigma-Aldrich	M2933
Nitric acid	HNO ₃	Carl Roth	X943.1
Percoll	-	Sigma-Aldrich	P1644
Phytigel	-	Sigma -Aldrich	71010-52-1
Potassium chloride	KCl	Duchefa	P0515.1000
Potassium dihydrogen phosphate	KH ₂ PO ₄	Fluka	60220
Potassium hexacyanoferrate	K ₃ [Fe ₂ (CN) ₆] (III)	Fluka	60300
Potassium hexacyanoferrate-II-Trihydrat	K ₄ [Fe ₂ (CN) ₆] (II) x 3 H ₂ O	neoLab	9570.0500
Potassium hydroxide	KOH	Fluka	60375
Potassium nitrate	KNO ₃	Sigma-Aldrich	P8291
potassium sulfate	K ₂ SO ₄	Normapur	26997.293
Polyvinylpyrrolidone (40kDa) (PVP40)	(C ₆ H ₉ NO) _n	Sigma -Aldrich	EC201-800-4
Sodium chloride	NaCl	Carl Roth	3957.1
Sodium Dodecyl sulfate (SDS)	NaC ₁₂ H ₂₅ SO ₄	Carl Roth	CN30.2
Tetracycline Hydrochloride	C ₂₂ H ₂₄ N ₂ O ₈ x HCl	Sigma -Aldrich	T7660
Tris(hydroxymethyl)aminomethane (Tris)	C ₄ H ₁₁ NO ₃	Carl Roth	AE15.2
Triton™ X-100	t-Oct-C ₆ H ₄ - (OCH ₂ CH ₂) _x OH, x= 9-10	Fluka	93426
Tryptone	-	Formedium™	TRP02
Tween20	-	Carl Roth	9127.1
YeastExtract	-	Formedium™	YEM02
Yeast Nitrogen Base without Amino Acids & Calcium Chloride	-	Formedium™	CYN2501
Zinc chloride	ZnCl ₂	AppliChem GmbH	A6285
Zinc sulfate heptahydrate	ZnSO ₄ x 7H ₂ O	Merck	1.08883.0500

Appendix

Tab. A10 List of enzymes

Enzymes	Company	Cat. No.
Bpil	Thermo Fisher Scientific	ER1011
Bsal-HF	New England Biolabs (NEB)	R3733S
POWER SYBR Green PCR mastermix	Thermo Fisher Scientific	4367659
Go Taq	Promega	M784B
HindIII-HF	New England Biolabs (NEB)	R5104S
M-MLV reverse Transcriptase	Promega	M1708
Nt.BbvCI	New England Biolabs (NEB)	R0632S
Pacl	New England Biolabs (NEB)	R0547S
Phusion HF DNA Polymerase	New England Biolabs (NEB)	M0530S
Phusion U	Thermo Fisher Scientific	F-555S
Protoscript II	New England Biolabs (NEB)	M0368
PvuI	Thermo Fisher Scientific	ER035
RNase	Applichem	A3832
SmaI	New England Biolabs (NEB)	R0141S
T4DNA Ligase	New England Biolabs (NEB)	M0202S
USER enzym mix	New England Biolabs (NEB)	M5505S
XbaI	New England Biolabs (NEB)	R0145S

Lists of primers

Tab. A11 List of primers for qRT-PCR

Gene	Name	Sequence (5'→3')
Medtr2g038310	MA1_qRT_f	ACATTCCGAGCCTTGTCAGA
	MA1_qRT_r	CAACATGGCCCTTCCTCCTT
Medtr4g008170	MA2_qRT_f	GAAAGGGAACAGGTTGCGAAG
	MA2_qRT_r	CACGTCACCTCCTTTACGCA
Medtr5g015590	MA3_qRT_f_2	GGTTTCCAAAGCAGCATTTC
	MA3_qRT_r_2	CCAGCAAATCAGCATCATTG
Medtr7g095710	MA4_qRT_f_2	CTTCGATTGGAAAGGTTGGA
	MA4_qRT_r_2	CCGCAACGATACTCACAACA
Medtr7g100110	MA5_qRT_f_2	TTGGCTTGGTATGATGGTGA
	MA5_qRT_r_2	AAAGCCTCAAAGCCTTCTC

Tab. A12 List of primers for amplification of UTRs

Gene	Name	Sequence (5'→3')
Medtr2g038310	MA1_5'UTR_f_2	AGCACGTCACACCGACTTGT
	MA1_5'UTR_r_2	CACCAGTAGAGGTTGGAGGAG
	MA1_3'UTR_f	CTTCGACGACATAGGCAACC
	MA1_3'UTR_r	CAGAGAGTAAGGGTCAATCCCA
Medtr4g008170	MA2_5'UTR_f	GCGATCCAAATCTCCTTCAG
	MA2_5'UTR_r	CATACCATCCGTCACCTCAA
	MA2_3'UTR_f_neu	ACGATTGAGGAGGTCTCGTTC
	MA2_3'UTR_r_neu	CATGCCAATGCTTTCCTTTC
Medtr5g015590	10xUni_A_long	CTAATACGACTCACTATAGGGCAAGCAGTGGTATCAACGCAGAGT
	MA3_5'RACE_R	TCAACTTCTTCACATCATGGCCTTCAAC
	MA3_3'UTR_F	CATTGGACTTGCCATGGGTAT
	MA3_3'UTR_R	CGAGTTGTTCCAGCAACAAG
Medtr7g095710	MA4_5'UTR_F	TTCTAGGAAGTTACATGGAACTATT
	MA4_5'UTR_R	TGTCCTTAACCATATCAGCAAGT
	MA4_3'UTR_F	GAATTCAACTCAAGAAGCATGG
	MA4_3'UTR_R	AGCAACACACCAAAGATTACAAT
Medtr7g100110	MA5_5'UTR_f	GCGTGAGACCCCTTCTAAAT
	MA5_5'UTR_r	GCCTTCTCCGCATTACTTTC
	MA5_3'UTR_f	GTGGGTCTGCAAGAAGATCA
	MA5_3'UTR_r_neu	TCGGCATGTTACGGCTTT

Tab. A13 List of primers for EGFP fusion constructs

Gene/Fragment	Name	Sequence (5'→3')
CsVMV	CsVMV_F	GGCTTAAUCCAGAAGGTAATTATCCAAGAT
	CsVMV_R	AGCCTCCTUAGCAGCTGCCTCTGCTACAAACTTACAAATTTCTCTGA
Nos	Nos_F	ACCTAAUAGCACCTCCAATCCCGATCGTTCAAAC
	Nos_R	GGTTTAAUCCCGATCTAGTAACATAGAT
eGFP	U_eGFP_II_for	AAGGAGGCUGCAGCTAAGGCTATGGTGAAGCAAGGGC
	U_eGFP_III_rev	ACCGCTGCCGCUACCTGCCTGTACAGCTCG
Medtr2g038310	U_MA1_III_for	AGCGGCAGCGGUAGCATGAGTTTCATGAACGGTTCATC
	U_MA1_IV_rev	ATTTAGGUTCAGGAGCTGGTTTCTATTGAGAAGGCTCAGGTTG
Medtr4g008170	U_MA2_III_for	AGCGGCAGCGGUAGCATGGCTTCCAACGGCAACG
	U_MA2_IV_rev	ATTTAGGUTCAGGAGCTGGTTTCTATTGCGAAGAACGAGACC
Medtr5g015590	U_MA3_III_for	AGCGGCAGCGGUAGCATGGAGAATTATTTGCAAGAGAA
	U_MA3_IV_rev	ATTTAGGUTCAGGAGCTGGTTTTAGACGGGGATCTTCTTTAA
Medtr7g095710	MA4_linkerII_f	AGCGGCAGCGGUAGCATGTCTAATAATCATAATCTACAATATG
	MA4_linkerIII_r	AGGCTTAGGUTCAGGAGCTGGTTTTAAAAAGCATTCTTAATCTTGAAG
Medtr7g100110	U_MA5_III_for	AGCGGCAGCGGUAGCATGGGGAAGGAGGCGCAAAA
	U_MA5_IV_rev	ATTTAGGUTCAGGAGCTGGTTTCTAATCTGATTTTTGCTTTGATC

Tab. A14 List of primers for promoter amplification

Gene	Name	Sequence (5'→3')
Medtr2g038310	pMA1_XbaI_F	AAAAAATCTAGAGGTTCTTACCGATCTAGATTTACCC
	pMA1_SmaI_R	AAAAAACC CGGGCGTGAAAATAACTGTGCGCAGG
Medtr4g008170	MA2_Promoter_USER_F	GGCTTAAUGGTATAACTTCACCACAAACACCA
	MA2_Promoter_USER_overlap_R	AGATTTGGAUCGCATATCAGTTGAGATGAGACA
	MA2_5'UTR_USER_overlap_F	ATCCAAATCUCCTCAGATAGATTTGTGTCTCTGT
	MA2_5'UTR_USER_R	GGTTTAAUTGTTATTGCCGCAAATTTGA
Medtr5g015590	pMA3_XbaI_F	AAAAAATCTAGACAATTATGTTTATGAAGCTGCAAT
	pMA3_SmaI_R	AAAAAACC CGGG CGTCTCAATTTTGTGCTATTTAT
Medtr7g095710	pMA4_XbaI_F	AAAAAATCTAGACCCAGGACACTGGTTAAGAACT
	pMA4_SmaI_R	AAAAAACC CGGGGTGGAATTTTACTAAAGGTTTAGA
Medtr7g100110	pMA5_XbaI_F	AAAAAATCTAGACAATGCAATAATGAAATGGCTT
	pMA5_SmaI_R	AAAAAACC CGGGTGAGATCCAATTAATTAACCTAGAG

Tab. A15 List of primers for yeast complementation

Gene	Name	Sequence (5'→3')
Medtr2g038310	MA1_USER_F_trun	GGCTTAAUATG TTCAAGGCAGCTGGA
	MA1_USER_R	GGTTTAAUCTATTGAGAAGGCTCAGGTTG
Medtr4g008170	MA2_USER_F_trun	GGCTTAAUATG TTTAGATTGGCCGGTGAACGT
	MA2_USER_R	GGTTTAAUCTATTGCGAAGAACGAGACCTCCTCA
Medtr5g015590	MA3_USER_F_trun	GGCTTAAUATG AGCGATTACAAAGTGCC
	MA3_USER_R	GGTTTAAUTCAGACGGGGATCTTCTTTAAG
Medtr7g095710	MA4for_User	GGCTTAAUATGTCTAATAATCATAATCTACAATATGATGG
	MA4rev_User	GGTTTAAUTAAAAAGCATTCTTAATCTTGAAG
Medtr7g100110	MA5for_User	GGCTTAAUATGGGGAAGGAGGCGCAA
	MA5rev_User	GGTTTAAUCTAATCTGATTTTTGCTTTGATC

Tab. A16 List of primers for sequencing

Gene/Plasmid	Name	Sequence (5'→3')
pCAMBIA2300u	M13_long_R	CCAGGCTTTACACTTTATGCTTC
pBI101.3	pBI101.3_F pBI101.3_R	GCGGATAACAATTTACACAGGA CGGGTTGGGGTTTCTACAGG
pFL61	pFL61_F2 pFL61_R2	TCAAGTCTTAGATGCTTTCTTTT GCGTAAAGGATGGGGAAAGAG
Medtr2g038310	MA1_Seq_F2 MA1_Seq_F3 MA1_Seq_F4 MA1_Seq_F5 MA1_Seq_F6 MA1_Seq_F7 MA1_Seq_F8 MA1_Seq_F9 MA1_Seq_F10 MA1_Seq_R1 MA1_Seq_F11 MA1_Seq_F12	GCTCAAGCCATCAGAGCAGCA TAGCGGCAGCAGCTTCATTG TGGCAGATGGCAGTGGGACT GGCTCCCACTTGCACTCACTCT GGATGAATTTTGTGACTGCTCGG GGATCCTTGTGACCTGGTGTC TGCAATGGGTATTGCTGGTACAG GGAGGAATTTGCTGATACAGGCA GGTTGGCCTCTTGTGTGGTT GCACTTGCCGTGCCCTTGT GATGTTGATGACGACGGTGATG CAAGGGAGCATGATACTGCTTCT
Medtr4g008170	MA2_CDS_1_F MA2_CDS_2_F MA2_CDS_3_F MA2_CDS_4_F MA2_CDS_5_F MA2_CDS_6_F MA2_CDS_7_F MA2_CDS_8_F MA2_CDS_9_F	CAATGCGTCCAGGCGTTTTAG TGGAATAATACATATCCTCGGAAAA CCCCTTAAAATAGGAGATCAGTTTC TAGTGCTTGCACTCCTTGGG ATATGTTGGGAAGAGCAAATAAATC CCAATATCTTGATTCAAATAGTCACCTG AGTGTGGGATACTGGCTTCAAATG GGGCCGCTCTGTATATGCAA AAGCCCATGACTATCAAGTGAAGAA
Medtr5g015590	MA3_Seq2_F MA3_Seq3_F MA3_Seq4_F MA3_Seq5_F MA3_Seq6_F MA3_Seq7_F MA3_Seq8_F MA3_Seq9_F MA3_Seq10_F MA3_Seq11_F	CGCGAAACCAAGCGATTAC GGAAGCACTTCAAGACATGACTC CCTGGTGATATAGTGCATCTTGC CTTGTGCAAGGACTTGTGAGCCTT CAACCAATCACATGACTGTTGTG GTGGTGGAGCTCCCTAGTGG CCGGTGTTAAGGAGTCTGTAGCT CTTCATGAAGCAGACATTGGACT CAGCTTACGGTTAATATCGTTGC CAATGCATTTGTATTCTGCCAG
Medtr7g095710	MA4_Seq_F MA4_Seq_F2 MA4_Seq_F3 MA4_Seq_F4 MA4_Seq_F5 MA4_Seq_F6 MA4_Seq_F7 MA4_Seq_F8 MA4_Seq_F9	CGAATTCAACTCAAGAAGCATGGAG CTTCAAGTTCCACCACTACTCTTGAT GTGCTGGTCTTCCCTTGGTT CATGACAGGTGAGAGCGACC GAATTCTGTTGTGAGTATCGTTGC CTACAATCCTCCATCTGTTCTGA TGCTCACACGGAGATTTAGAT AGTCGATAATATCCGAGTAATGGC GCAGCAGTTTCTTCTGGTGATG
Medtr7g100110	MA5_Seq1_F	GTCACGATGAGGTTGAGAATCG

Appendix

	MA5_Seq2_F	GAGATTCAATCGGAGCAAGCT
	MA5_Seq3_F	AGATACATGAGGCGTCGCAG
	MA5_Seq4_F	CCTGGTTAGGAAGCTACCAAGTG
	MA5_Seq5_F	TGTTGTGAATGGTGGAAACGAA
	MA5_Seq6_F	ATGGGAACGAGGATCATCCA
	MA5_Seq7_F	AGCTTGACAGACATTGGTATTGC
	MA5_Seq8_F	GACCTCAGCAGCGATGGAC

Tab. A17 List of sgRNAs for inducing a mutation of *MA4* by CRISPR/Cas9

sgRNA	Oligo	Sequence (5'→3')
sgRNA1	Oligo 1	ATTGAGAGGCGCGGTACGACCTAT
	Oligo 2	AAACATAGGTCGTACCGGCCTCT
sgRNA2	Oligo 1	ATTGTTAAAGGCTCAATCTCTACA
	Oligo 2	AAACTGTAGAGATTGAGCCTTTAA

Tab. A18 List of primers used for R-Geco cloning

Promoter/Gene/ Terminator	Name	Sequence (5'→3')
CsVMV	USERforpCsVMVLinker	GGCTTAAU CCAGAAGGTAATTATCCAAGAT
	USERrevpCsVMVLinker	AGCCTCTU AGCAGCTGCCTCTGCTACAAACTTACAAATTTCTCTGA
R-Geco	USERforRGECOLinker	AAGGAGGCU G CAGCTAAGGCTATGGTCGACTCTTCAGTCG
	USERrevRGECOLinker	ATTTAGGUTCAGGAGCTGGTTTCTACTTCGCTGCATCATTTGT
Nos	USERforptermNOSLinker	ACCTAAU G CACCTCCAATTC CCGATCGTTCAAAC
	USERrevptermNOSLinker	GGTTTAAU C CCGATCTAGTAACATAGAT

Phylogenetic trees

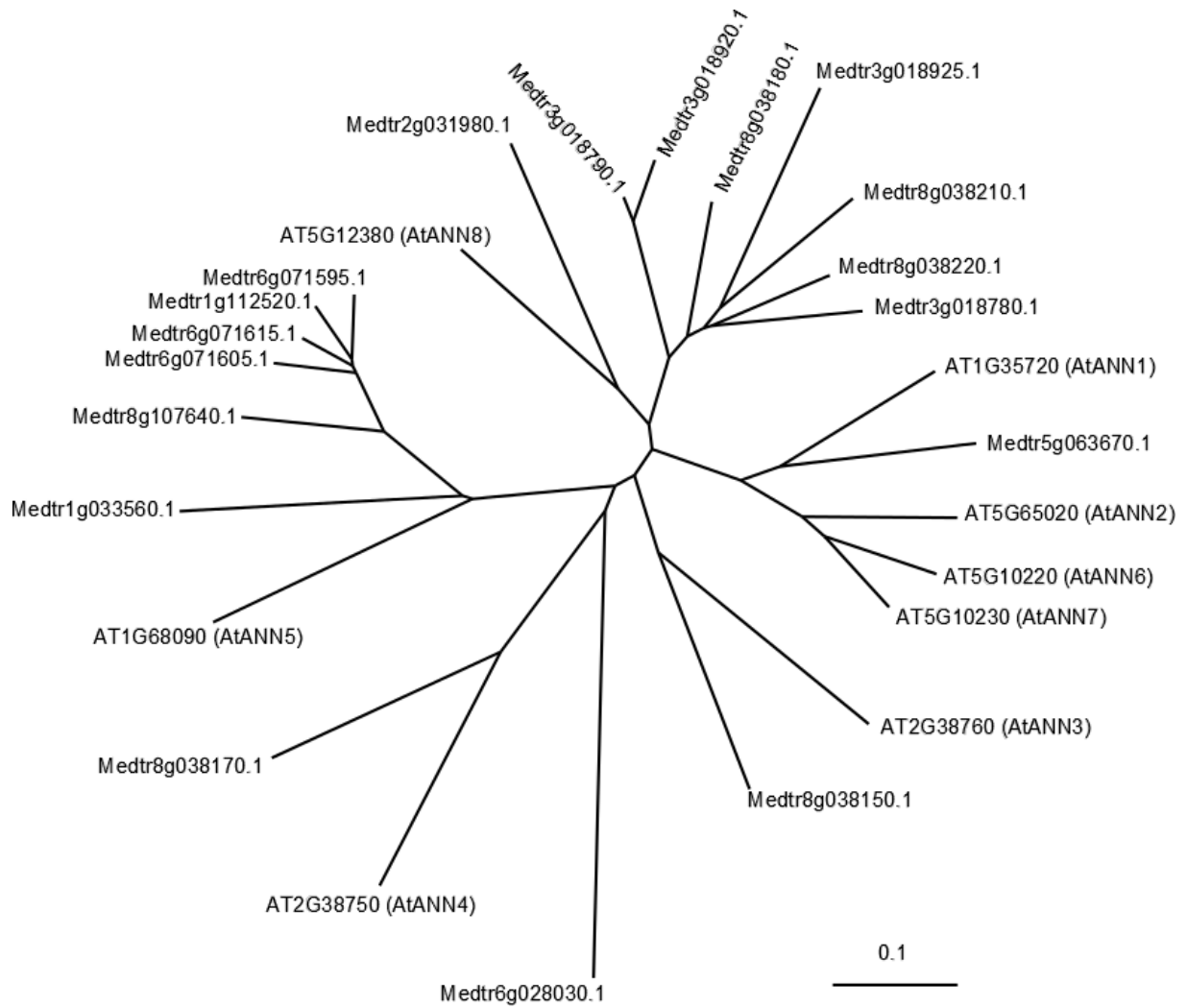


Fig. A46 Phylogenetic tree of Annexins.

Unrooted tree of annexin proteins of *A. thaliana* (AT) and *M. truncatula* (Medtr).

Appendix

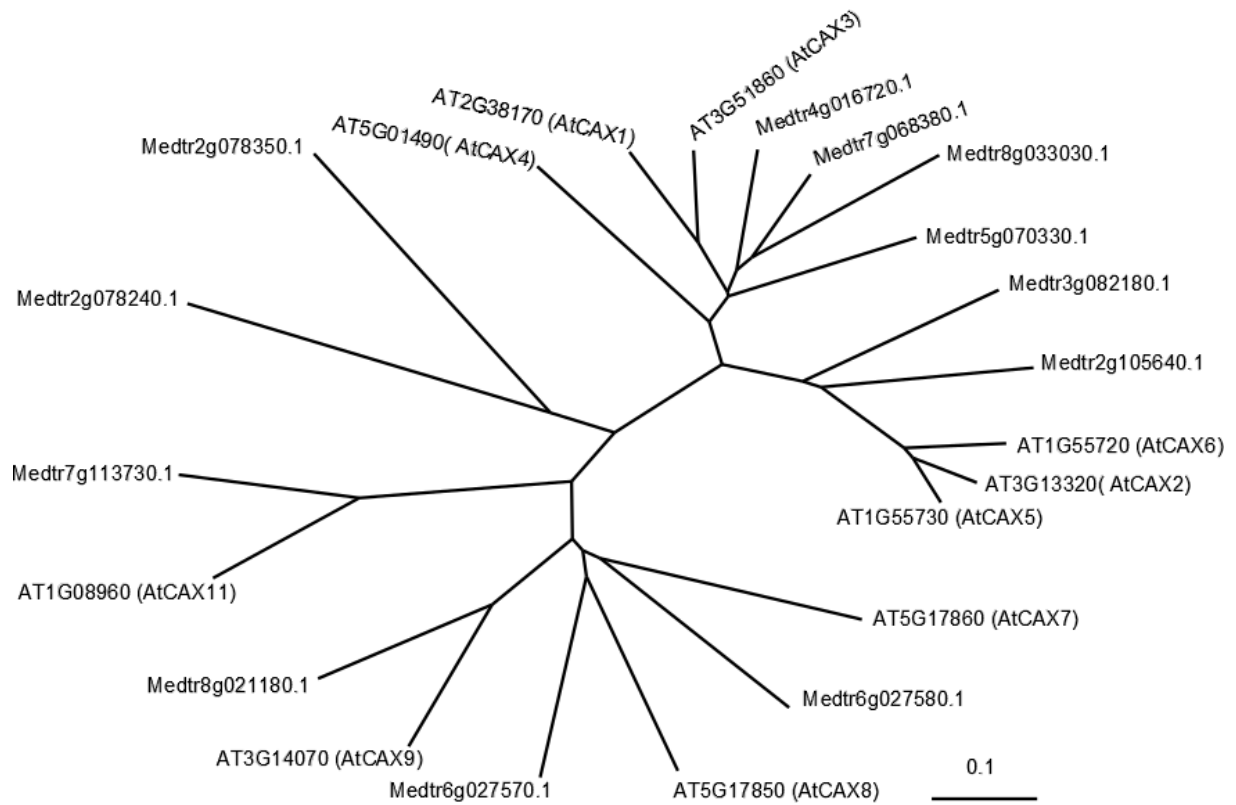


Fig. A47 Phylogenetic tree of CAXs.

Unrooted tree of CAX proteins of *A. thaliana* (AT) and *M. truncatula* (Medtr).

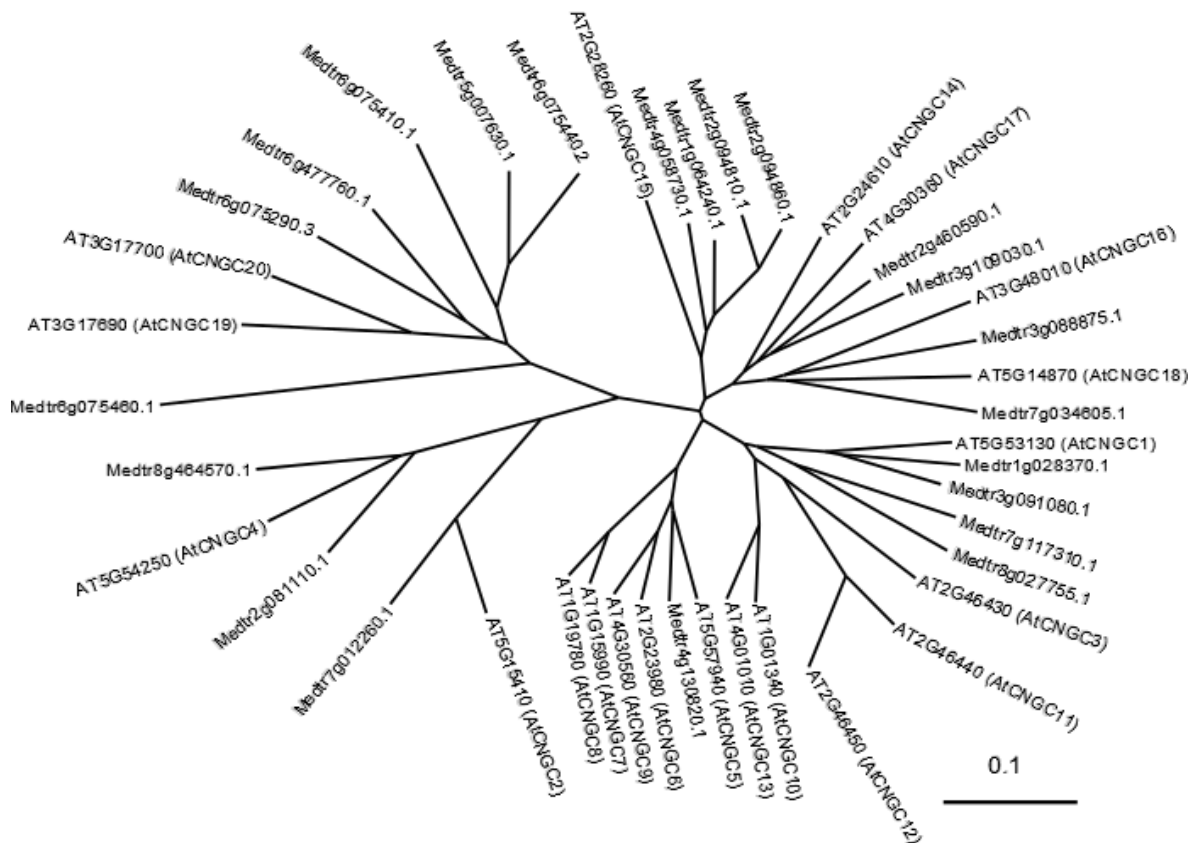


Fig. A48 Phylogenetic tree of CNGCs.

Unrooted tree of CNGC proteins of *A. thaliana* (AT) and *M. truncatula* (Medtr).

Appendix

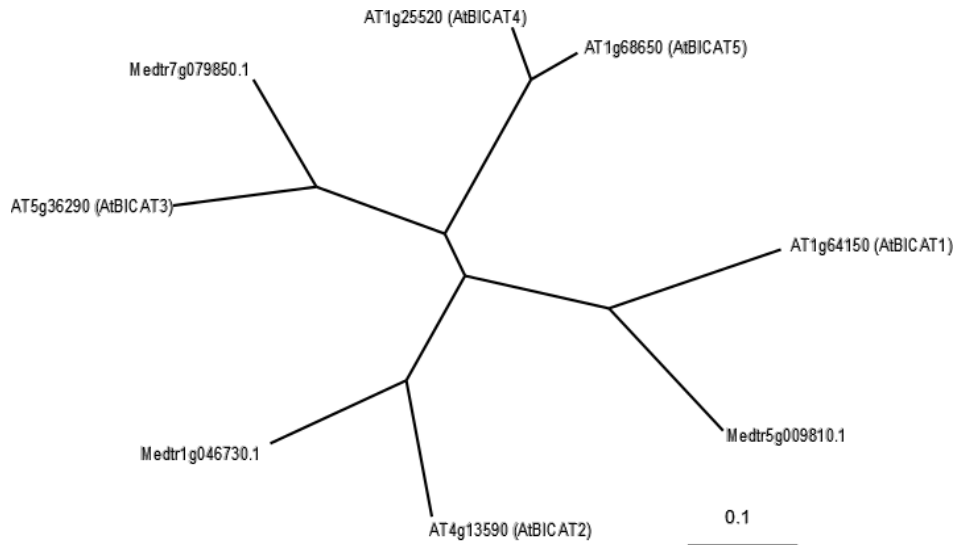


Fig. A49 Phylogenetic tree of BICATs.

Unrooted tree of BICAT proteins of *A. thaliana* (AT) and *M. truncatula* (Medtr).

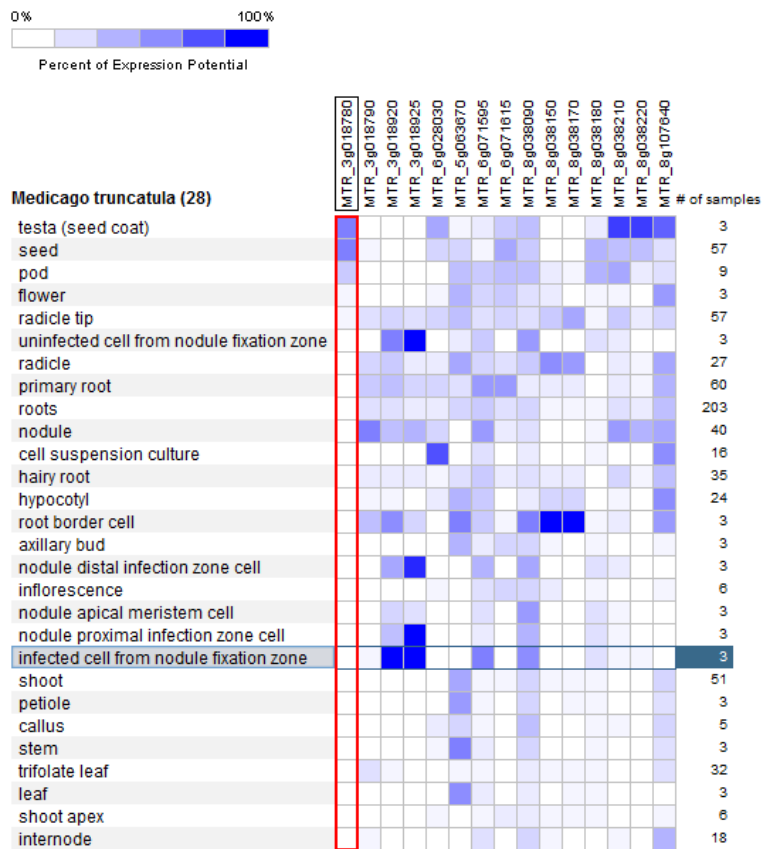


Fig. A50 Expression of genes encoding putative ANNEXINs.

Linear heat map combining the expression data of 691 samples using the Affymetrix GeneChip (Genevestigator).

Appendix

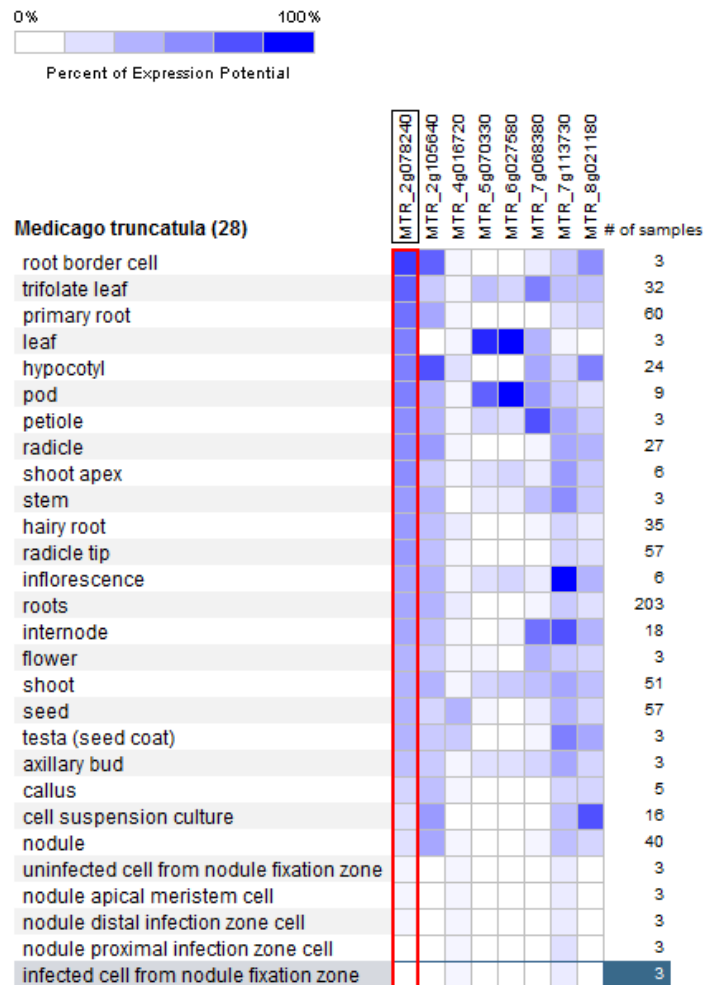


Fig. A51 Expression of genes encoding putative CAXs.

Linear heat map combining the expression data of 691 samples using the Affymetrix GeneChip (Genevestigator).

Appendix

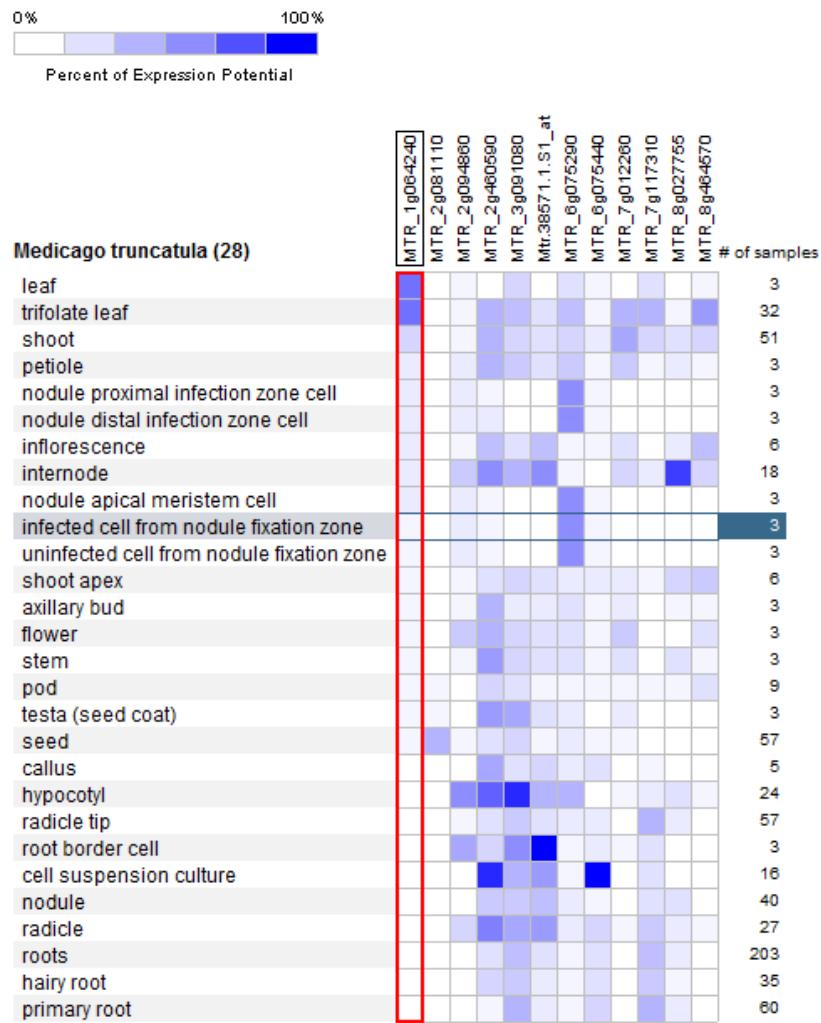


Fig. A52 Expression of genes encoding putative CNGCs.

Linear heat map combining the expression data of 691 samples using the Affymetrix GeneChip (Genevestigator). Mtr.38571.1.S1_at = Medtr4g130820.1

Appendix

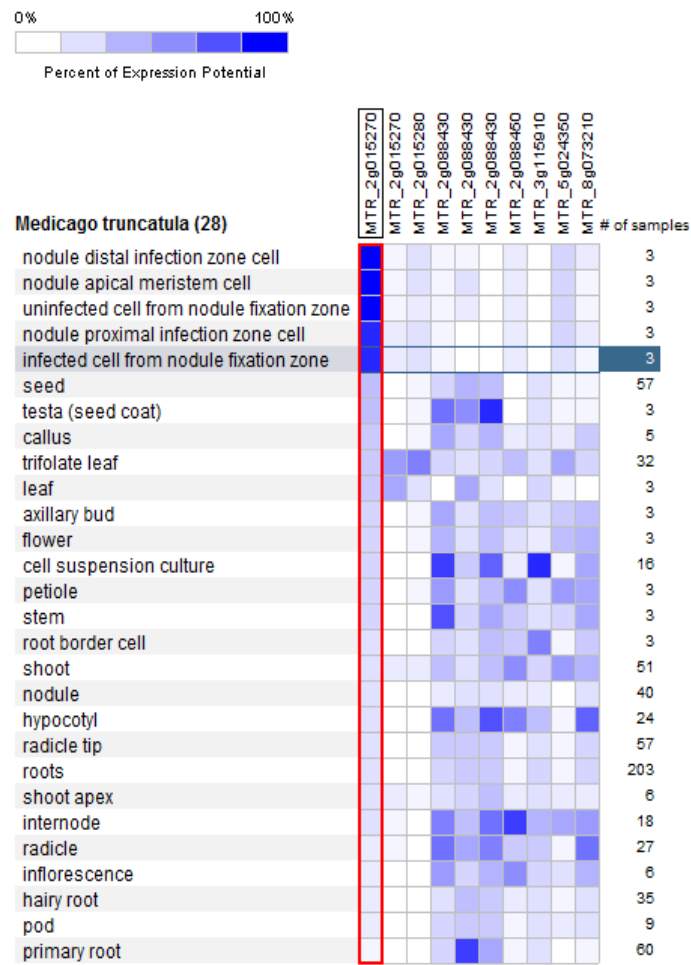


Fig. A53 Expression of genes encoding putative GLRs.

Linear heat map combining the expression data of 691 samples using the Affymetrix GeneChip (Genevestigator).

Appendix

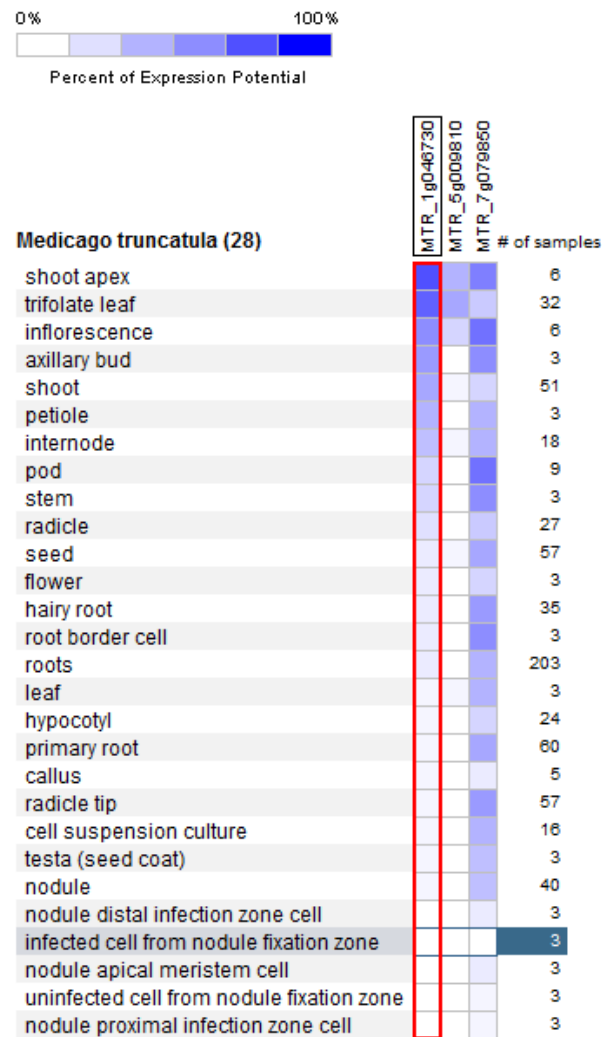


Fig. A54 Expression of genes encoding putative BICATs.

Linear heat map combining the expression data of 691 samples using the Affymetrix GeneChip (Genevestigator).

Appendix

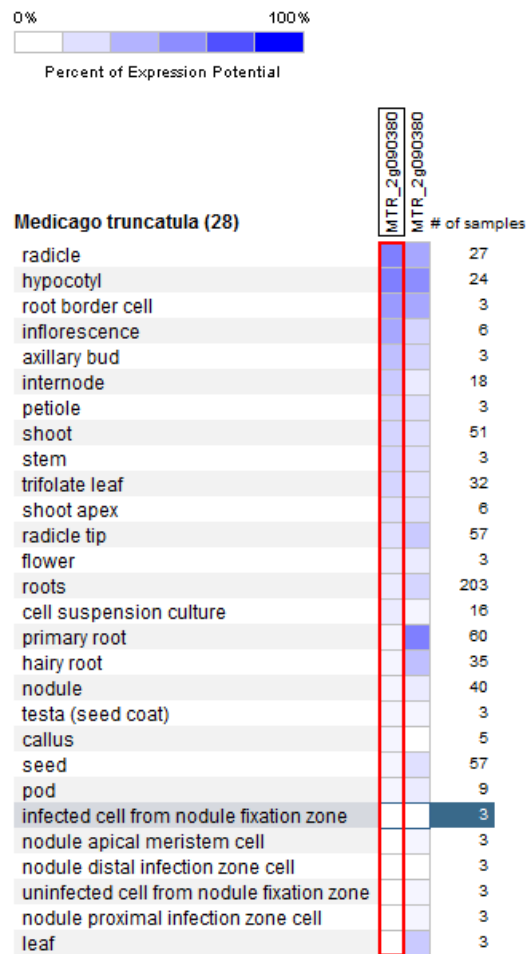


Fig. A55 Expression of genes encoding a putative TPC1.

Linear heat map combining the expression data of 691 samples using the Affymetrix GeneChip (Genevestigator).

Amino acid sequences of the five candidate proteins

>Medtr2g038310.1 (MA1)

MSFMNGSSPHRNPPPPENDIEAGPLSRNSDVDDGDVFDIARTKHA SIDRLRRWRQAALVLNASRRFRYTLDL
 KKEEEKKQILRKIRAHQAIRAAYLFKAAGRGQGHGQVQGVQVGTDTIKPPPTSTGEFFPIGPEQLASISREHDTA
 SLQQYGGVAGVSNLLKTDLEKGINGDDADLLRRRNFAGSNNYPRKKGRSFFMFMWDACKDLTLVILMVAAAASLA
 LGIKSEGIKEGWYDGGSI AFAVILVIVVTAVSDYKQSLQFRDLNEEKRNIHLEVIRGGRRVEISYIDL VVGDVIP
 LNIGNQVPADGVVITGHSLSIDESSMTGESKIVHKDSKDPFMMMSGCKVADGSGTMLVTVGVINTEWGLLMASISE
 DTGEETPLQVRLNGVATFIGIVGLSVAVLVLLARYFSGHTRNSDGTKQFIAGKTKAGHAIDGAIKIITVAVT
 IVVVAVPEGLPLAVTTLTAYSMRKMMADKALVRRLSACETMGSATTICSDKTGTLTMNQMTVVEVYAGGSKVDP
 HELERSPKLRTLLIEGVAQNTNGSVYVPEGANDIEVSGSPTEKAILNWGLQVGMNFVTARSESSILHVFPFNSEK
 KRGGVAIQTADSDVHIHWKGAAEIVLACCTGYIDANDQLVEIDEEKMTFFKKAIEDMASDSLRCVAIAYRPEYE
 KVPDNEEQADWLSLPEEELVLLAIVGIKDPKPCRPVGVKNSVQLCQKAGVKVVMVTDGNVKTAKAIALECGILSS
 LADVTERSVIEGKTFRALSDSREEIAESISVMGRSSPNDKLLLVQALRRKGHVAVTGDGTNDAPALHEADIGLAMG
 IAGTEVAKESSDIIILDDNFASVVKVVRWGRSVYANIQKFIQFQLTVNVAALVINVVAAVSSGDVPLNAVQLLWV
 NLIMDTLGALALATEPPTDHLMDRSPVGRREPLITNIMWRNLLIQAMYQVSVLLVLFNFRGISILGLEHQPT
 EHAIKVKNTLIFNAFVICQIFNEFNARKPDEYNIKGVTRNYLFMGI VGVFTVVLQVIVIVEFLGKFTTTTRLN
 NWKQWLISVAIGFIGWPLAVVGKLI PVPATPINNVFTKLLRHRQPEPSQ

> Medtr4g008170.1 (MA2)

MASNGNGNGHFSVTIGTGHNDDDDNNHHPSDNNRRNDNDNNGDNDDEDEQIDPDDPFDAQTKNASHETLRR
 WRQAALVLNASRRFRYTLDFKGEEEKQKSLIRAHQVIRAALLFRLAGERELVISPAATPSPQHSVGFDFVGL
 EQLASMSKDQNISALQQYGGVKGSLSSLLKASPKGISGDDADLLKRKNAGTNTYPRKKGRSFWRFWEAWQDLT
 LIILIVA AVVSLVLGKIKTEGWSGWDGGSIAFAVLLVIVVTAVSDYRQSLQFQNLNAEKQNIQLEVMRSGRTIK
 ISIFDIVGDV IPLKIGDQVPADGVLITGHSLIDESSMTGESKIVHKDQKAPFFMSGCKVADGVGMVMTAVGI
 NTEWGLLMASISEDTGEETPLQVRLNGVATFVIGVGLSVAVLVAVLLGRYFSGHTYDAKGNPQFVAGKTEISIV
 VDGVIKIFTIAVTIVVVAVPEGLPLAVTTLTAYSMRKMMADKALVRRLSACETMGSATTICSDKTGTLTLNQMTV
 VEAYVGKSKLNPPDDSSKFHPEALSLINESIAQNTTGNVVFVSKDGGELEVSGSPTEKAILSWAVKLG MNFV
 DIRSNSTVLHVFPFNSEKRRGGVALKLVDSGVHIHWKGAAEIVLGACTQYLDNSHLSQIEQEKDFLKEAIDDMAARSL
 RCVAIAYRSYELDKIPSNEEDLAQWSLPEDELVLLAIVGIKDPKPCRPVGVKDAVRICTDAGVKVRMVTGDNLQTA
 KAI ALECGILASNEEA VDPCEIEGKVFRELSKEREQVAKKITVMGRSSPNDKLLLVQALRKG G DVVAVTGDGT
 NDAPALHEADIGLSMGIQGTVEAKESSDIIILDDNFASVVKVVRWGRSVYANIQKFIQFQLTVNVAALVINV
 VAAISSGDVPLNAVQLLWVNLIMDTLGALALATEPPTDHLMHRSPVGRREPLITNIMWRNLI VQALYQVSV
 LLLFLNFCGESILPKQDTKAHDYQVKNTLIFNAFVMCQIFNEFNARKPDEMNVFPVGTNRLFMGIIGITFILQ
 IVIIEFLGKFAS TVRLDWKLWLVSLIIGLVSWPLA IAGKFI PVPKTPLSRTFMKPIRRLRRSRSSQ

> Medtr5g015590.1 (MA3)

MENYLQENFGGVKSKNSSEEALRRWRDVC GFVKNPKRRFRFTANLDRGEAAAMRRTNQEKLRVAVLVSKAAFQF
 IQGAKPSDYKVP EEVKDAGFQICGDELGSIVEGH DVKLLKYHGKIDGIAEKLSTSA TEGISNDADLLDKRQQIYG
 INKFTESQAKSFWVFW EALQDMTLMILGVCALVSLIVGIATEGWPKGAHDGLGIVASILLVVFVTATSDYRQSL
 QFKDL DKEKKKISIQVTRNGYRQKMSIYELLPGDIVHLAIGDQVPADGLFVSGFSLIIDESSLTGESEPVVNT
 E NPFLLSGTKVQDGSCKMLVTTVGMRTQWGKLMATLSEGGDDETPLOVKLNGVATIIGKIGLFFAIVTF
 FAVLVQGLVSLKLQQENFWNWNGDDALEMLEYFAIAVTIVVVAVPEGLPLAVTSLAFAMKMMNDKALVRN
 LAACETMGSATTICSDKTGTLTTHMTVVKTCICMKSKEVSNKTSSELPE SVVKLLQOSIFNNTGGEVV
 VNKQKGHEILGTPETAILEFGLSLGGDFQGERQACKLVKVEPFNSTKKRMGAVVELPSGGLRAHCKGASE
 IVLAACDKVLNSNGEVVPLDEESTNHLTNTINQFANEALRTLCLAYMELENGFSAEDTIPVTGYTCIGV
 VGIKDPVRPGVKESVALCRSAGITVRMVTGDNINTAKAIARECGILTDDGIAIEGPEFREKSLEELLE
 LIPKIQVMARSSPLDKHTLVRHLRTTFGEVAVTGDGTNDAPALHEADIGLAMGIAGTEVAKESADVI
 ILDDNFSTIVTVAKWGRSVYINIQKFVQFQLTVNIVALIVNFTSACLTGTAPLTA VQLLWV
 NMIMDTLGALALATEPNDLMDKRAPVGRKGNFISNMWRNILLGQSLYQFMV IWFLQSKGKTIFSLD
 GPNSDLVNLTLIFNAFVFCQVFNEINSREMEKINVFKGILDNYVFGVISATIFFQIIIV EYLGTFAN
 TPLTLVQWFFCLFVGFMGMPIAARLKKIPV

Appendix

>Medtr7g095710.1 (MA4)

MSNNHNLQYDGTFSFIIDITNTLAKVTSKYTNAKRRWRFAFYTAIYSRRVMLSLAKEVISRKNSNPYTKLFHTESSS
STTTLDIIEPLITQHNGTNHYSLVSDVVDKTKLADMVKDKNLKSLSEFGGVEGVGHVLTGTFPTKGIIGSDDDIS
RRLELFGSNTYKKPPPGLLHFVLEAFNDTTIIILLVCAGLSLGFGIKEHGPGEWYEGGSI FLAVFLVVVVSAL
SNFRQERQFHKLSKISNNIKVEVVRNGRPQQISIFDVLVGDIVSLKIGDQIPADGVFLSGYSLQVDESSMTGESD
HVEIEPLRAPFLLSGAKVVDGYAQLVTSVGKNTSWGQMMSSISRDTNERTPLQARLDKLTSSIGKVGLAVAFV
LLVLLIRYFTGNSHDEKGNKEFRGSKTDINDVMNSVVSIVAAAVTIVVVAIPEGLPLAVTLTLAYSMKRMMADHA
MVRKLSACETMGSATVICDTKTGTLTLNQMRVTKFCLGPENI IENFSNAMTPKVLELFHQGVGLNTTGSVYNPPS
GSEPEISGSPTEKAILMWAVL DLGMDMDEMCKQKHKVLHVETFNSEKRSVVAIRKENDDNSVHVHWKGAEMILA
MCTNYIDSNGARKSLDEEERSKIERIIQVMAASSLRCAIAFAHTEISDSEDI DYMIKREKKSHQMLREDGLTLLGI
VGLKDCRPNTKKAVETCKAAGVEIKMITGDNI FTAKAIAIECGILDSNSDHAKAGEVVEGVEFRSYTEEERMEK
VDNIRVMARSSPMDKLLMVQCLRKKGHVAVTGDGTNDAPALKEADIGLSMGIQGTVEVAKESSDIVILDDNFNSV
ATVLRWGRVCVYNNIQKFIQFQLTVNVAALVINFI AAVSSGDVPLTTVQLLWVNLIMDTLGALALATERPTKELMK
KKPIGR TAPLITNIMWRNLLAQASYQIAVLLIMQFYGKSI FNVSKEVKDTLIFNTFVLCQVFNEFNSRSMEKLYV
FEGILKNHFLGLIIGITIVLQILMVELLRK FADTERLTWEQWGCIGIAVVS WPLACLVKLIPVSDKPSFSYTKW
VKLLVFKIKNAF

>Medtr7g100110.1 (MA5)

MGKGGENYGRKENTSSDNSDGEIFKAWSKDVRECEEHFVSVKVTGLSHDEVENRRKIYGFNELEKHDGQSIWKLV
LEQFNDDLVRILLAAAIISFVLAWYDGDDEGGEMEITAFVEPLVIFLILIVNAIVGVWQESNAEKALEALKEIQSE
QASVIRNNEKIPSLPAKDLVPGDIVELKVGDKVPADMRVVELISSTLRLEQGS LTGESEAVNKTNKPAVEDADIQ
GKKCIVFAGTTVVNGHCFCLVTQTGMDEIGKVHNQIHEASQSEEDT PLKKKLNEFGERLTMMIGLICILVWLIN
VKYFLTWDYVDDGWPTNFKFSFEKCTYYFEIAVALAVAAIPEGLPAVITTC LALGTRKMAQKNALVRKLP SVET
LGCTTVICSDKTGTLTTNQMAVSKLVAIGTNVDALRAFKVEGTTYNPN DGQIENWPAGQLDANLQTMAKIAAVCN
DAGISQSEHKFVAHGMPTEAALKARYIFSCSLACVLVEKMGLPEGSKNVQSGSKSTILRCCEWWNEHRR IATLE
FDRDRKSMGVIVDSGVGKKKSLLVKGAENVLDRSSKVQLRDG SVVKLDNNAKNLILQALHEMST SALRCLGFAY
KDEL TNFENYNGNEDHPAHQLLLDPNNYSSIEDELI FVGLVGLRDP PREEVYQAIEDCRAAGIRVMVITGDNKNT
AEAICREIGVFAPNENISSKSLTGKDFMELRDKKAYLRQTGGLLFSRAEPRHKQDIVRLLKEDGEV VAMTGDGVN
DAPALKLADIGIAMGIAGTEVAKEASDMVLADDNFSSIVAAVGEGRS IYNNMKAFIRYMISSNIGEVASIFLTAA
LGIPEGLIPVQLLWVNLVTDGPPATALGFNPPDKDIMKPPRRSDDSLINLWILFRYLVI GIVYVGLATVGVFI IW
YTHGSFMGIDLSSDGHTLV TYSQLANWGCSSWNNFTAAPFTAGSRIISFDADPCDYFTTGKVKAMTLSLSVLVA
IEMFNLSNALSEDGSLT MPPWVNPWLLLAMSVSFGLHFLILYV PFLAKVFGIVPLSFNEWLLVLAVALPVILID
EVLK FVGRCTSGSARRSKQSD

Acknowledgements

First of all I would like to thank Prof. Dr. Edgar Peiter, who enabled me the research on legume plants by creating this project and introducing me to scientists working on legumes. Especially, I would like to thank Prof. Dr. Bettina Hause, Ulrike Huth and Dr. Heena Yadav (Department of metabolic and cell biology, Leibniz Institute of Plant Biochemistry), who taught me the root transformation and supplied me with *M. truncatula* seeds. Further thanks go to Dr. Joachim Schulze (Department of Crop Sciences, Georg August University of Göttingen) and Prof. Dr. Helge Küster (Institute of Plant Genetics, Leibniz University Hannover), who supported me with good advice and provided *S. meliloti* strains 102F51 and 2011-mRFP, respectively. I would also like to thank many other scientists supporting me with further organisms, plasmids or helpful tips. Thanks to Prof. Dr. Kyle W. Cunningham and Dr. Nathan Snyder (Department of Biology, Johns Hopkins University), who sent me the yeast strains K601 and K616, to Prof. Dr. Debora A. Samac (USDA-ARS Plant Science Research Unit) for sending a plasmid with the CsVMV promoter to me and thanks to Prof. Dr. Hussam H. Nour-Eldin (Department of Plant and Environmental Science, University of Copenhagen), who provided the USER plasmid. Many thanks to Dr. Johannes Stuttmann (Institute of Biology, MLU) for the design and providing of plasmids used for CRISPR/Cas9. Special thanks goes to Dr. Martin Bachmann (Professur of Animal Nutrition, MLU), who supported me a lot with the establishment of the acetylene reduction assay. Furthermore, I would like to thank Christine Krenkewitz and Alexandra Boritzki (Professur of Soil Science, MLU) for ICP analysis. However, the warmest thanks goes to the lab members of the Professur of Plant Nutrition and the students, who supported me in this project. Special thanks to Liane Freitag, Tina Peiter-Volk, Anja Janssen, Dr. Bastian Meier, Dr. Stefanie Höller, Dr. Wolfgang Gans, Dr. Heidrun Beschow, Dr. Mario Lange, Nico Rössner, Elisabeth Bönisch and Elisabeth Hahn.

Publications

Poster presentations

Bischoff L, Peiter E (2018). Regulation der symbiontischen Stickstofffixierung durch Calcium? Jahrestagung der Deutschen Gesellschaft für Pflanzenernährung, 13 - 14 September 2018, Osnabrück.

Bischoff L, Schlindwein C, Hause B, Schulze J, Peiter E (2016). Calcium as regulator of the N₂-fixing legume nodule. Resource efficiency - from model plants to crops and crop systems: International Conference of the German Society of Plant Nutrition, 28 - 30 September 2016, Hohenheim.

Bischoff L, Schlindwein C, Hause B, Schulze J, Peiter E (2016). Calcium as regulator of the N₂-fixing legume nodule. International Conference The Role of Soil Microorganisms in Crop Nutrition, 18-19 November 2016, Bernburg.

Schlindwein C, **Bischoff L**, Schulze J, Peiter E (2016). Genome-wide identification of the *CPK* gene family in *Medicago truncatula* and its expression in nodules. Resource efficiency - from model plants to crops and crop systems: International Conference of the German Society of Plant Nutrition, 28 - 30 September 2016, Hohenheim.

Schlindwein C, **Bischoff L**, Schulze J, Peiter E (2016). Genome-wide identification of the *CPK* gene family in *Medicago truncatula* and its expression in nodules. International Conference The Role of Soil Microorganisms in Crop Nutrition, 18-19 November 2016, Bernburg.

Oral presentations

Bischoff, L (2017). Calcium – Übermittler der Reaktion von Pflanzen auf Umwelteinflüsse. ProGrow-Tagung, 27 November 2017, Steinkirchen.

Bischoff, L (2016). Calcium - a key regulator of root nodule function? 14. Mitteldeutsche Pflanzenphysiologie-Tagung, 1- 2 April 2016, Jena.

Curriculum vitae

Name: M.Sc. Lisa Bischoff
Date/Place of Birth: 31 December 1983, Berlin (Germany)
Nationality: German

Education

Sept. 2004 - March 2008

Undergraduate studies in Agriculture, University of Applied Sciences Neubrandenburg,
Degree: Bachelor of Science

Oct. 2012 - April 2015

Graduate Studies in Crop Science, Martin Luther University Halle-Wittenberg,
Degree: Master of Science

Experience

Sept. 2015 - Dec. 2017

Scientific Employee, Martin Luther University Halle-Wittenberg, Faculty of Natural
Sciences III, Institute of Agricultural and Nutritional Sciences

Jan. 2018 - Dec. 2019

Biological technician, Martin Luther University Halle-Wittenberg, Faculty of Natural
Sciences III, Institute of Agricultural and Nutritional Sciences

Declaration under Oath

Eidesstattliche Erklärung / Declaration under Oath¹

Ich erkläre an Eidesstatt, dass ich die Arbeit selbstständig und ohne fremde Hilfe verfasst, keine anderen als die von mir angegebenen Quellen und Hilfsmittel benutzt und die den benutzten Werken wörtlich oder inhaltlich entnommenen Stellen als solche kenntlich gemacht habe.

I declare under penalty of perjury that this thesis is my own work entirely and has been written without any help from other people. I used only the sources mentioned and included all the citations correctly both in word or content.

Datum / Date

Unterschrift des Antragstellers / Signature of the applicant

¹Origin: <http://www.natfak3.uni-halle.de/ordnungen/Eidesstattliche-Erklaerung.pdf> vom 22.03.2013